Stony Brook University

Exploring the Role of Interferons in Adenovirus Replication and Establishment of Persistent Infection in Normal Human Cells

A Dissertation Presented

by

Yueting Zheng

to

The Graduate School

In Partial Fulfillment of the

Requirements

for the Degree of

Doctor of Philosophy

in

Molecular Genetics and Microbiology

Stony Brook University

December 2015

Stony Brook University

The Graduate School

Yueting Zheng

We, the dissertation committee for the above candidate for the

Doctor of Philosophy degree, hereby recommend

acceptance of this dissertation.

Dr. Patrick Hearing, Ph.D – Dissertation Advisor
Professor, Department of Molecular Genetics and Microbiology

Dr. Laurie T. Krug, Ph.D – Chairperson of Defense
Assistant Professor, Department of Molecular Genetics & Microbiology

Dr. Nancy C. Reich Marshall, Ph.D
Professor, Department of Molecular Genetics & Microbiology

Dr. Michael J. Hayman, Ph.D
Professor, Department of Molecular Genetics & Microbiology

Dr. Ed Luk, Ph.D
Assistant Professor, Department of Biochemistry & Cell Biology

This dissertation is accepted by the Graduate School

Charles Taber
Dean of the Graduate School

Abstract of the Dissertation

Exploring the Role of Interferons in Adenovirus Replication and Establishment of Persistent Infection in Normal Human Cells

By

Yueting Zheng

Doctor of Philosophy in

Molecular Genetics and Microbiology

Stony brook University

2015

Adenoviruses (Ad) are ubiquitous pathogens that infect a wide range of vertebrates and have been recognized in recent years as significant pathogens in immunocompromised patients. Interferons (IFNs) are cytokines that have pleiotropic effects and play important roles in innate and adaptive immunity. IFNs have broad antiviral properties and function by different mechanisms. IFNs fail to inhibit wild-type Ad replication in established cancer cell lines. In this study, I analyzed the effects of IFNs on Ad replication in normal human cells. The results demonstrated that both IFNα and IFNγ blocked wild-type Ad5 replication in primary human bronchial epithelial cells (NHBEC) and TERT-immortalized normal human diploid fibroblasts (HDF-TERT). IFNs inhibited the replication of divergent adenoviruses. The inhibition of Ad5 replication by IFNα and IFNγ is the consequence of repression of transcription of the E1A immediate early gene product. Both IFNα and IFNγ impede the association of the transactivator GABP with the E1A enhancer region during the early phase of infection. The repression of E1A expression by IFNs requires a conserved E2F binding site in the E1A enhancer, and IFNs increased the enrichment of the E2F-associated pocket proteins, Rb and p107, at

the E1A enhancer *in vivo*. PD0332991 (Pabociclib), a specific CDK4/6 inhibitor, dephosphorylates pocket proteins to promote their interaction with E2Fs and inhibited wild-type Ad5 replication dependent on the conserved E2F binding site. Consistent with this result, expression of the small E1A oncoprotein, which abrogates E2F/pocket protein interactions, restored Ad replication in the presence of IFNα or IFNγ.

Ads establish latent infections in T lymphocytes in tonsil and adenoid tissues yet the molecular mechanisms by which Ads establish and maintain the latent state are completely unknown. Here, I established a persistent Ad infection model *in vitro* and demonstrated that IFNγ suppresses productive Ad replication in a manner dependent on the E2F binding site in the E1A enhancer. These results reveal a novel mechanism by which adenoviruses utilize IFN signaling to suppress lytic virus replication and promote persistent infection.

Table of Contents

List of Abbreviations

Ad	Adenovirus
AIM2	Absent in melanoma 2
CAR	Coxsackie virus and adenovirus receptor
CDK	Cyclin-dependent kinase
cGAS	Cyclin GMP-AMP synthase
Daxx	Death domain-associated protein 6
DBP	DNA binding protein
DDX41	DEAS (Asp-Glu-Ala-Asp) box polypeptide 41
DSBR	Double-strand break repair
GABP	GA-binding protein
GAF	Gamma-interferon activation factor
GAS	Interferon-gamma activated site
HCMV	Human cytomegalovirus
HSV-1	Herpes simplex virus 1
IFI16	Interferon gamma-inducible protein 16
IFN	Interferon
ISGF3	Interferon-stimulate gene factor 3
ISRE	Interferon-stimulated response element
ITR	Inverted terminal repeat
kDa	kilodalton
KSHV	Kaposi’s sarcoma-associated herpesvirus
MNase	Micrococcal nuclease
MRN	Mre11-Rad50-Nbs1
Mx1	IFN-induced GTP-binding protein
NPC	Nuclear pore comple
nt	Nucleotide
OAS	2’-5’-oligoadenylate synthase
ORF	Open reading frame
PKR	Protein kinase R
PML	Promyelocytic leukemia protein

PML-NBs	PML nuclear bodies
Sp100	Nuclear autoantigen Sp100
STAT	Signal transducer and activator of transcription
STING	Stimulator of interferon genes
SUMO	Small ubiquitin-like modifier
TBP	TATA box binding protein
TC	Tetracysteine
TLR	Toll-like receptor
TP	Terminal protein
WT	Wild-type

List of Figures

List of Tables

Acknowledgments

The first person I would like to thank is Dr. Patrick Hearing. I am very grateful to him for his mentorship during the past six years. Pat has always been very supportive to my ideas, even to the crazy ones, he would not say no but instead encourage me to explore, which I really appreciate. In many cases it was Pat's suggestions that made those proposals into something real. Without his help, encouragement and trust, this challenging thesis project could not be accomplished.

I would also like to thank my dissertation committee, Dr. Laurie T. Krug, Dr. Nancy Reich Marshall, Dr. Michael Heyman and Dr. Ed Luk. I really enjoyed the scientific discussions in every committee meeting; all the suggestions and help they provided are invaluable to me.

I want to thank all the members in our lab for creating such a friendly and creative work environment. It is a great pleasure to get to know each of you, Mena, Suk-young, Becc, Steve, and past memebers, Hsin-Chieh, Kai, Kasey, Liz, Versha, and Ilana. Thank you all, not only for a lot fun in the office but also for all the scientific and technical discussions that pushed me towards graduation everyday. I also want to give my special thanks to Dr. Janet Hearing, for her inspiring idea of exploring adenovirus persistent infection, which ultimately drove me to a new and exciting area.

The Molecular Genetics & Microbiology Department has been a wonderful place. I would like to thank all the faculty, staff and students I am privileged to know and work with. I am also grateful to the neighboring labs, Krug's lab, Reich's lab, Zong's lab, Mackow's lab, Carpino's lab and Center of infectious Center, for sharing reagents and equipment, as well as all the scientific advises.

The past six years at Stony Brook University will always be one of the most memorable times of my life. I was lucky enough to know quite a few friends that inspire me, motivate me, encourage me and most importantly make my life much happier. Thank you and wish you all the best for the new journeys, or soon to be new journeys of your life.

The last and most important thanks are dedicated to my family, my parents and my husband, Ding. I want to thank them for the love, and belief in me. I would not be where I am today without your support.

Chapter 1 General Background

Adenovirus (Ad), a DNA virus, was first isolated and characterized in the 1950's as a pathogen causing acute respiratory infections (1, 2). So far there are more than 50 different serotypes of human Ad identified, and they are further categorized into six different subgroups, A, B, C, D, E and F on the basis of their neutralization properties with specific antisera. Ad is a ubiquitous pathogen. It primarily infects the respiratory tract causing mild flu-like symptoms and is normally cleared within two weeks by the immune system. Ad infection is only involved in rare cases of acute respiratory morbidity in the general population and approximately 10% of respiratory illnesses in children. However, important exceptions exist. Infection of conjunctiva by Ad can also cause conjunctivitis and pharyngeal conjunctival fever; especially subgroup D Ad is responsible for epidemic keratoconjunctivitis (EKC) worldwide. Ad serotypes 4 (Ad4) and 7 (Ad7), both belonging to subgroup E, are the cause of acute respiratory diseases (ARD) syndrome in military recruits. Ad also causes significant morbidity and mortality among immunosuppressed individuals, including the recipients of both solid organs and stem cell transplantation, and patients with immunodeficiency diseases.

Ad was the first DNA tumor virus discovered. It was found that Ad12 and Ad9 were able to cause malignant tumors after inoculation of rodents (3). Ad encodes multiple oncogenes to transform cultured cells. However, no evidence indicates that Ad is associated with malignant disease in humans (4, 5).

Ad is a well-characterized oncolytic viruse. Almost every individual gene of Ad has been studied for their functions, and oncolytic viruses can be easily engineered to exhibit tumor targeting, as well as tumor clearance though virus-induced cell lysis and/on

enhanced immune response by viral-delivered cytokines. A recombinant Ad that expresses the wild-type p53 gene product has been approved by the Chinese State Food and Drug Administration for use in combination with chemotherapy to treat head and neck cancer. Many ongoing clinical trials use Ad-based therapy to target both localized cancers and metastatic cancers.

1.1 Ad virion structure and genome organization

Ad has a non-enveloped, icosahedral particle approximately 70-100 nm in diameter. It contains a linear double-stranded viral DNA genome (~36kb) (6) surrounded by a protein-based capsid. Hexon is the most abundant protein in the capsid. Each triangular facet of the icosahedron contains 12 hexon trimers and 3 penton bases at the vertexes (7, 8). Fiber protein projects from each penton base outwards. Inside the capsid, the Ad genome is associated with more than 800 copies of core protein VII (9), and the 5'-ends of the genome are covalently attached to the terminal protein (TP). Core protein VII is a histone-like protein, and it can wrap and condense Ad DNA to form a beads-on-string structure. Core protein V forms a shell tethering VII-DNA core to the interior of the capsid (10, 11).

The Ad genome encodes more than 40 viral proteins; they are roughly divided into the early or late class based on their expression kinetics. There are five early transcription units (E1A, E1B, E2, E3, and E4) and one late transcription unit that expresses a large pre-mRNA that is further processed to generate five different families of late mRNAs (L1, L2, L3, L4, and L5). Two inverted terminal repeats (ITRs) are located at very ends of the Ad genome and are involved in the initiation of bi-directional Ad replication. The packaging sequence was mapped to the left-end of the genome adjacent to the left ITR.

1.2 Ad lytic life cycle

1.2.1 Virus Entry

The attachment of Ad to the host cell is initiated by the fiber protein. The C-terminal knob domain of the fiber protein binds to coxsackie B virus and adenovirus receptor (CAR) on the cell surface (12-15), followed by Ad penton base interaction with the cellular integrins, αvβ3 and αvβ5 (16-18). The penton-integrin interaction results in the detachment of fiber proteins from the capsid and stimulates viral entry through endocytosis (19, 20). Cell surface protein CD46 is also used as the receptor for subgroup B Ad infection, while Ad37 from subgroup D uses sialic acid as the receptor (21). Following the internalization, virion-containing vesicles mature into the endosome, where the viral particle is further disassembled by the low pH environment. Viral protease processing cleaves protein VI that bridges the interaction between V and hexon, releasing the virion into the cytosol (22). Viral particles are transported to the nuclear pore complex (NPC) on microtubules (23-26). At the NPC, the uncoating process is accomplished, the Ad core enters the nucleus, including the viral genome along with proteins VII, TP, and a small portion of hexon and μ proteins (27).

1.2.2 The Early Stage of Infection

Protein VII protects the input genome from a DNA damage response at the early stage of infection (28). Cellular histone proteins replace protein VII to form a chromatin-like structure (29, 30). However, the role of protein VII in regulating transcription of early genes still controversial. It has been shown that VII represses transcription (31, 32). The association of VII to the parent genome is negatively correlated with the onset of E1A transcription (32). The opposite observation is also described (30). Evidence suggested that a chromatin remodeling protein, template activating factor I (TAF-I), interacts with

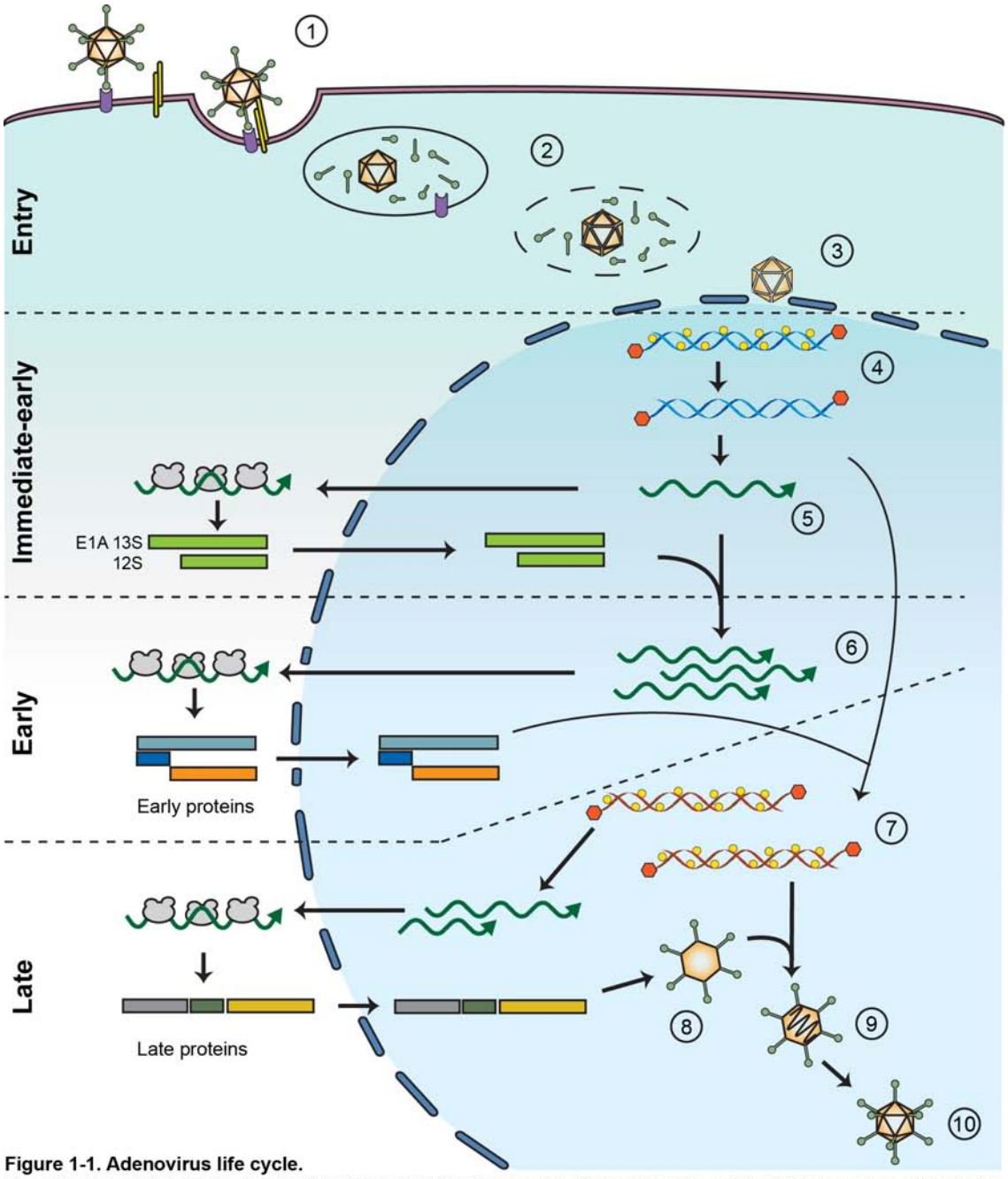

Figure 1-1. Adenovirus life cycle.
The attachment of Ad to the host cell is initiated by the fiber protein interacting with cellular CAR receptor, followed by the interaction between Ad penton base and cellular integrin. Ad enters the cell through endocytosis pathway. Viral particle is partially degraded in the endosome, and then released into cytosol in a low pH dependent manner. Viral particle is completely disassembled at the nuclear pore complex. In the nucleus, Cellular histone proteins replace protein VII to form a chromatin-like structure. The E1A is the first viral protein expressed during Ad infection and induced the expression of other early genes that facilitate viral replication. After replication occurs, major late promoter is activated to produce late proteins late proteins are produced and formed empty procapsids. Following the encapsidation of viral genome, viral encoded protease proteolyzes multiple viral proteins inside the virus particle to generate a mature virion that is released from the infected cell.

protein VII (33-35). In the absence of VII, both TAF-I and acetylated histone H3 fail to accumulate on the viral genome (30).

There are three major functions of early Ad proteins. The first is to induce the cell to enter S phase, providing the optimal environment for viral replication. The second is antagonizing and escaping from various antiviral responses. The third is to synthesize viral proteins required for viral DNA replication. E1A is the first transcription unit activated during Ad infection (36). E1A transcription is controlled by a constitutively active enhancer region localized at Ad nt 194-350. The E1A protein is a transcription factor that is critical and indispensable for Ad replication. It is responsible for activating transcription of both early and late genes. However, E1A does not directly bind to DNA, rather it influences transcription by binding to a variety of cellular transcription factors and cofactors. E1A can also regulate IFN signaling, as well as alter the cell cycle progression and promote the G1/S phase transition. In cooperation with the E1B55k protein, E1A is known to induce the transformation of primary cells. More details of E1A functions, as well as the regulation of E1A transcription, can be found in Chapter 3. The E1B region encodes two proteins, E1B19k and E1B55k. The former one is homologous to cellular Bcl-2 proteins and exhibits anti-apoptosis property (37, 38), while E1B55k is involved in both inactivation of p53 protein and p53 protein degradation as part of an E3 ubiquitin ligase (39-42). The E2 region encodes three viral proteins, ssDNA binding protein (DBP), precursor terminal protein (pTP) and Ad DNA polymerase (Adpol). They are all directly involved in viral DNA replication. Viral proteins from the E3 region are immune response modulators, but deletion of E3 region has no effect on Ad replication in cell culture. The E4 region products E4ORF1 and E4ORF4 cooperatively activate the protein kinase mammalian target of rapamycin (mTOR), leading to enhanced translation. E4ORF3 and E4ORF6 are functionally redundant for the inactivation of a cellular DNA damage response (43-45). E4ORF3 has also been shown to counteract a promyelocytic

leukemia nuclear bodies (PML-NBs)-mediated, IFN-induced antiviral response in cancer cell lines (46, 47).

1.2.3 DNA Replication

As E2 proteins accumulate, the stage is set for viral DNA replication. The ITRs serve as the replication origins. Adpol and pTP form a complex and bind to the first 20 nt of the Ad genome (48). Cellular nuclear factor I (NFI) and nuclear factor III (NFIII, also known as Oct-1) bind to Ad nt 25-48. They also interact with Adpol and pTP, respectively, to stabilize the entire replication initiation complex (49-52). The priming reaction begins with the transfer of a deoxycytidine monophosphate (dCMP) to pTP at serine 580 (53) by Adpol. Then the pTP-dCMP complex is used as a protein primer for the synthesis of the nascent strand. After adding the first three or four nucleotides, the Adpol leaves pTP and continues to precede through the entire viral genome, with the help of DBP and cellular topoisomerase I(54).

1.2.4 The Late Stage of Infection

Once viral replication is initiated, E1A activates the major late promoter (MLP) to express viral structure proteins. All Ad late genes are transcribed from the MLP as a single large transcript, and randomly terminated at one of 5 different polyadenylation sites to generate 5 late families of transcripts (L1 to L5). All of these late mRNAs have an identical 201 nt untranslated 5'-end, the tripartite leader (TPL), generated from the splicing of three short exons to a longer exon containing the coding regions. Each pre-mRNA gives rise to multiple mRNAs by alternatively splicing.

The current model of Ad packaging is described as the formation of an empty procapsid which serves as the substrate for viral DNA encapsidation. Before being packaged into the capsid, newly synthesized viral DNA is coated by core protein VII and then inserted into the procapsid driven by a protein motor, Ad IVa2 (55, 56). Within the

virion, the L3-encoded protease is activated, and it proteolyzes the precursors of proteins VI, VII, VII, u, and TP to complete the maturation of the virion. At the end of the infection, Ad protease disrupts the cellular cytoskeleton, and the Ad death protein (ADP) induces cell death (57, 58). As a result, progeny virions are released to infect adjacent cells. Free fiber proteins that are released from the infected cells also bind to CAR at the tight junctions of epithelial cells. This interaction prevents oligomerization of CAR, and facilitates the release of progeny virions to the airway lumen (59).

1.3 IFN signaling pathway

Interferons (IFNs) are widely expressed cytokines that have pleiotropic effects on cells. IFNs play important roles in both innate and adaptive immunity (60). There are three types of IFNs: I, II and III classified basing on the cell surface receptors they are engaged. Briefly, they bind to the cell surface receptors, triggering the JAK-STAT pathway and ultimately inducing the expression of IFN-stimulated genes (ISGs)(61).

Type I IFNs (α, β, ε, κ and ω) are produced by multiple cell types following the activation of pathogen pattern recognitions receptors (PRRs) and function in both an autocrine and paracrine manner. They bind to the IFNα receptor (IFNAR) complex, a heterodimer of IFNAR1 and IFNAR2, and induce the autophosphorylation of receptor-associated Janus kinase 1 (JAK1) and tyrosine kinase 2 (TYK2) (62). These kinases phosphorylate and activate signal transducer and activator of transcription (STAT) proteins, including STAT1, STAT2, STAT3 and STAT5. The heterodimer of STAT1 and STAT2 associates with IFN-regulatory factor 9 (IRF9) to form a transcription factor complex, IFN-stimulated gene factor 3 (ISGF3), which translocates into the nucleus and active ISG expression from ISREs (IFN-stimulated response elements) (63). Type II IFN (IFNγ) is only produced by Th1, Tc and NK cells. It has broad antimicrobial activity primarily acting through regulation of adaptive immunity. The dimer of IFNγ binds to a

tetrameric receptor which consists of two IFNGR1 and IFNGR2 proteins, leading to the autophosphorylation of JAK1 and JAK2 (64), and the formation of a STAT1 homodimer (also known as IFNγ-activating factor, GAF) (63, 65). GAF binds to the IFNγ-activating sequence (GAS) and induces downstream gene expression. Type III IFNs (λs) play an important role in mucosal cell immunity. They bind to a distinct receptor, a dimer of IL-28 receptor α (IL-28Rα, or IFNLR1) and IL-10 receptor 2 (IL-10Rβ), but trigger a type-I IFN-like response (66). This class of IFN signaling is less well understood. For this reason, I did not include type III IFNs in the study.

Type I IFN signaling is the first line of defense against the invading virus. Many ISGs induced by type I IFNs have been shown directly target viral components by controlling translation, regulation of RNA stability and editing, as well as protein transport and turnover (67). For example, 2', 5'-oligoadenylate synthetase (OAS) and ribonuclease L (RNaseL) mediate RNA degradation in response to viral infection. Viral dsRNA can activates monomeric OAS to forms a tetramer that can synthesize 2', 5'-linked oligoadenylates (2-5A) (68). In turn, this unique 2'-to-5' linked oligoadenylate binds to and activate RNaseL by inducing dimerization. Activated RNaseL cleaves both cellular and viral RNAs. Moreover, the cleavage product of dsRNA by RNaseL can also be recognized by pattern recognition receptors (PRRs), retinoic acid-inducible gene-I (RIG-1 or DDX58) and melanoma differentiation associated gene-5 (MDA5 or IFIH1), leading to the induction of IFNβ and amplification of antiviral innate immunity (69). Similar to OAS, protein kinase R (PKR) is also activated by viral dsRNA. As a serine/threonine kinase, PKR phosphorylates eukaryotic translation initiation factor 2A, a subunit of the translation initiation complex(70, 71). PKR results in a global shutdown of protein synthesis. Lastly, IFN stimulated gene 15 (ISG15) is an ubiquitin-like protein that is conjugated to target proteins and regulates protein function. It can also be secreted by monocytes and lymphocytes and function as a cytokine.

Divergence from the canonical IFN signaling pathways can occur. Type I IFNs also induce the formation of STAT homodimers, leading to expression of GAS-driven ISGs. JAK and TYK can phosphorylate signaling molecules involved in other pathways. It is well known that IFN signaling has extensive crosstalk with MAPK and PI3K signaling pathways (61). In addition to antiviral activities, IFNs also have antitumor properties. IFNα, β and γ are used for treatment of various cancers in clinical settings, such as chronic myeloid leukemia, hairy-cell leukemia, malignant melanoma, and severe malignant osteoporosis (72).

1.4 Induction of IFN by Ad infection

When a virus invades a host cell, it is sensed by various PRRs, leading to the induction of type I IFN, proinflammatory cytokines, and chemokines. These molecules recruit the immune cells of innate and adaptive immunity to the site of infection, aiming for clearance of the virus. So far there are at least five different types of dsDNA sensors identified for their ability to detect the intracellular viral DNA and trigger innate immune response. Toll-like receptors 9 (TLR9) was the first DNA virus sensor identified. It recognizes CpG DNA in the endosome and activates transcription factor IRF7 and NF-κB through adaptor protein MyD88 (73). Ultimately, this signaling cascade leads to IFN expression and inflammation response (74). In 2007, the first cytosolic DNA sensor was identified, DNA-dependent activator of IFN-regulatory factor (DAI, also known as ZBP1 and DLM-1) (75). It has been shown that DAI recognizes human cytomegalovirus (HCMV) and herpes simplex virus type I (HSV-1) and induces the expression of type I IFNs through the STING/TBK1/IRF3 cascade. PYHIN/HIN-200 family proteins, a class of IFN-inducible proteins, were known for their abilities to control myeloid differentiation, activate the inflammasome and induce type I IFN expression in response to cytosolic dsDNA (76). Four human HIN-200 proteins have been identified, IFI16, AIM2, IFIX and

MNDA (77). It is known that AIM2 binds to cytosolic vaccinia virus and induces activation of caspase-1, leading to the activation of IL1β (78, 79). In contrast, the function of IFI16 in regulating innate immune responses during virus infection is case-dependent. Cytoplasmic IFI16 protein recognizes HSV-1 viral DNA resulting in the induction of IFNs (80). IFI16 detects kaposi sarcoma associated herpresvirus (KSHV) in the nucleus and traffics to the cytoplasm where it induces inflammasome formation (81). Moreover, IFI16 also represses HSV-1 gene expression through modulating histone modifications (82, 83). More recently, DEAD box polypeptide 41 (DDX41) and cyclin GMP-AMP synthase (cGAS) were found to induce IFN expression in response to a variety of DNA virus infections (84-86). IFI16, DDX41 and cGAS all signal through the STING/TBK1/IRF3 cascade to elicit innate immunity, but it is not clear whether they target STING independently. It is possible that IFI16 and DDX41 feed the cytosolic DNA to cGAS, and cGAMP produced by cGAS functions as a second messenger to trigger downstream signaling.

Ad infection can induce type I IFN expression in both a TLR9-dependent and TLR9-independent manner. Ad triggers TLR9/MyD88 signaling in plasmacytoid dendritic cells (pDCs), but not in conventional DCs and macrophages (87, 88). Loss-of-function studies suggests that cGAS, DDX41 and AIM2 sense Ad DNA in RAW264.7 macrphage-like cells and induce phosphorylation of IRF3 (89, 90). However, in non-antigen presenting cells, including the murine endothelial cell line MS1 and the hepatocyte cell line FL83B, the stimulation of IFN expression is severely dampened or completely lost, implying that the signaling cascade might be disrupted in both cell lines (91). In addition to dsDNA sensors, OAS protein is also activated by adenovirus-associated type I RNA (VAI RNA), a late viral product, presumably leading to IFN expression (92).

Chapter 2 Materials and Methods

2.1 Cells

Normal human bronchial epithelial cells (NHBEC) were purchased from Lonza and maintained in Bronchial Epithelial Cell Growth Medium containing BulletKits™ (Lonza) according to manufacturer's instructions. HDF-TERT cells (93) were kindly provided by Dr. Kathleen Rundell (Northwestern University, Chicago, IL) and maintained in Dulbecco's Modified Eagle's Medium (DMEM) containing 10% fetal bovine serum (HyClone Laboratories). A549 cells (ATCC) were grown in DMEM containing 10% bovine calf serum. 293FT cells (Life Technologies) were used for the generation of lentivirus stocks and were maintained in DMEM containing 10% fetal bovine serum, 2 mM L-Glutamine, 0.1 mM MEM non-essential amino acids and 1 mM MEM sodium pyruvate. 293-TP cells (Schaack et al., 1995) were used to propagate mutant virus ΔTP-GFP and were maintained in DMEM containing 10% fetal bovine serum and 400 µg/ml G418. N52Cre cells were kindly gifted by G. Schiedner and S. Kochanek, University of Ulm, Germany, and maintained in DMEM containing 10% Fetalclone III serum (HyClone). Lymphocytes Jurkat (lymphoblastoid cell line derived from an acute T cell leukemia) and BJAB (human burkitt lymphoma B cell line) were obtained from ATCC, and maintained in RPMI/1640 medium containing 10% FBS. PM1, a cutaneous T lymphocyte derived from HUT 78, was obtained from the NIH AIDS reagent program, and also maintained in RPMI/1640 medium containing 10% FBS. All cell growth media were supplemented with 100 U/ml penicillin and 100 µg/ml streptomycin.

2.2 Antibodies and Reagents

For detection of viral proteins, the following antibodies were used: anti-E1A (sc-430, Santa Cruz Biotechnology), anti-DBP (clone B6-8 or A1-6, Arnold Levin, Princeton Univeristy)(94), anti-E4ORF3 (clone 6A11)(95), anti-E1B55K (clone 2A6)(96)(Sarnow et al., 1982), anti-IVa2 (Gustin, K. E., 1996), anti-pVII (gift of Daniel Engel, University of Virginia), anti-Hexon (sc-58085, Santa Cruz Biotechnology, and 65H6, Abnova), anti-Penton (gift of Dr. Carl Anderson, Brookhaven National Laboratory, Upton, NY). For detection of PML-NB components, anti-PML (H-238, Santa Cruz Biotechnology), anti-Daxx (25C12, Cell Signaling Technology) and anti-Sp100 (AB1380, Chemicon International) antibodies were used. Anti-STAT1 (Cat. No. #9172), anti phospho-STAT1 (Cat. No. #9171) anti anti-phospho-STAT6 (Cat. No. 9364) were purchased from Cell Signaling Technology. Anti-STAT1 and anti-STAT6 serum were kindly provided by Dr. Nancy Reich, Stony Brook University. Anti-γ-Tubulin (T5192) and anti-α-Tubulin (T5168) were obtained from Sigma-Aldrich. For EMSA antibody supershift reactions, anti-E2F-3 (C-20), anti-E2F-4 (C-20 and C-108), anti-E2F-5 (C-20), anti-Rb (C-15), anti-p107 (C-18 and SD9X), anti-p130 (C-20X) and anti-DP-1 (K-20) were from Santa Cruz Biotechnology and anti-E2F-1 (KH95) was from Lab Vision/NeoMarkers. For immunoprecipitation and chromatin immunoprecipitation reactions, anti-GABPα (H-180), anti-GABPβ (E-7), anti-Rb (C-15), and anti-p107 (C-18) were from Santa Cruz Biotechnology; anti-HA were from Rockland. Anti-Histone H3 (Cat No. ab1791) and anti-Histone H3 K9me3 (Cat No. ab8898) were purchased from Abcam; anti-H3K4me3 (Cat No. 39915) and anti-Histone H3K27me3 (Cat No. 39155) was purchased from Active Motif. Anti-Histone H3.3 (17-10245) and anti-Sp1 (17-601) were from Millipore.

Human IFNα (universal type I interferon 11200-2) and human IFNγ (11500-2) were from PBL Assay Science, dissolved in phosphate-buffered saline (PBS) containing 0.1% BSA according to the manufacturer's instructions. Human IL4 and mouse IFNγ

were provided by Dr. Nancy Reich, Stony Brook University. PD 0332991 (Palbociclib) was from APExBIO and dissolved in DMSO.

2.3 Viruses

The replication defective adenovirus, ΔTP-GFP, was generously provided by Dr. Jerry Schaack (University of Colorado, Denver, CO; unpublished data). With ΔTP-GFP, the Ad5 terminal protein coding region is disrupted by the GFP gene. It was propagated in 293-TP complementing cell lines. Mutant viruses, *in*340, *in*340-A5, *in*340-B1, *dl*309-21, *dl*309-3 and *dl*309-317/358, were previously described (97, 98). *In*340-Δ2-CMV, *dl*309-273/371, and pTG3602 mutants 1 through 5 (Ad5-mut1 to -mut5) were generated by PCR and recombination using parent viruses *in*340 (98), *dl*309 (99), and pTG3602 (100).Virus particle concentration was determined by measuring the optical density at 260 nm, and multiplied by 1 X 10^{12} particles per milliliter.

2.4 Replication Assay

HDF-TERT cells were incubated with 500 U/ml IFNα, 1000 U/ml IFNγ or left untreated for 24 hr, followed by Ad infection at 37 °C for 1 hr at the multiplicities of infection indicated in the text and figure legends. The infection mixture was removed and medium with or without IFNs was added to the culture. Nuclear DNA and total cell DNA were purified at 6 and 48 hr post-infection, respectively, using a QIAGEN DNeasy Blood & Tissue Kit. Both viral and cellular genome copy numbers were determined by qPCR using primer pairs that recognize either the Ad5 genome or cellular glyceraldehyde-3-phosphate dehydrogenase (GAPDH) gene with DyNAmo HS SYBR Green qPCR Kit (F-410XL, Thermo). The relative viral copy numbers of each time point were normalized to GAPDH. The fold-increase of viral copy number was calculated by normalizing to input viral DNA at 6 hr post-infection samples. Relative viral replication efficiency in IFN-treated cells was presented as the relative value compared to untreated cells. In the

case of infection in A549 and NHBEC cells, nuclear and total DNA was harvested at 2 and 24 hr post-infection, respectively.

2.5 Isolation of Nuclear DNA

At 6 hr post-infection, HDF-TERT cells were washed with ice-cold PBS twice, then scraped and transferred into a cleaned 1.7 ml microfuge tubes. Cells were pelleted by centrifugation at 1,000 X g for 7.5 min. The supernatant was aspired, and cell pellets were resuspended in 1 ml isotonic buffer (150 mM NaCl, 10 mM Tris pH7.4, 1.5 mM MgCl2) containing 0.6 % NP-40. The samples were incubated on ice for 10 min, followed by centrifugation at 2,000 X g for 7.5 min to pellet nuclei. The nuclear pellet was subject to a QIAGEN DNeasy Blood & Tissue Kit for DNA isolation.

2.6 RT-qPCR

At 48 hr post-infection, total RNA from infected cells was isolated using a QIAGEN RNeasy kit. Equal amounts of RNA from each sample were used to synthesize the first strand of cDNA using SuperScript® II Reverse Transcriptase. Then equal amounts of cDNA were subjected to qPCR using primer pairs that recognize different Ad5 early mRNAs or cellular GAPDH mRNA. The Pfaffl method of relative quantification was used to convert the resulting threshold cycle data for each sample to relative fold change information (101). Viral mRNA levels were normalized to internal control, GAPDH mRNA.

2.7 Immunoprecipitation (IP)

HDF-TERT cells were treated with 500U/ml IFNα, 1000U/ml IFNγ or left untreated for 24 hr, then infected with *dl*309 at 200 particles/cell or left uninfected for additional 18 hr. Cell pellets were resuspended in 1 ml lysis buffer (50 mM Tris pH7.5, 150 mM NaCl, 0.5% NP-40, 1 µg/ml aprotinin, 1 µg/ml pepstatin A, 1 mM Leupeptin, 1

mM sodium orthovanadate [Na3VO4], 1 mM sodium fluoride [NaF], 1 mM phenylmethanesulfonyl fluoride [PMSF]) each 10 cm plate, incubated on ice for 10 min, and sonicated by brief pulses five times. After centrifugation at 16,100 X g for 10 min, the supernatant was precleared with protein A-agarose beads (Roche) for 1 hr and then incubated with 2 µg of anti-GABPα (H-180) overnight. Immunocomplexes were pulled down by the addition of protein A-agarose for 1 hr. They beads were washed five times with lysis buffer and analyzed by western blot.

2.8 Chromatin Immunoprecipitation (ChIP)

ChIP was performed as described previously (102) with modification. HDF-TERT cells were pre-treated with 500 U/ml IFNα, 1,000 U/ml IFNγ or left untreated for 24 hr, followed by Ad infection at 37 °C for 1 hr at 200 virus particles/cell. At 18 hr post-infection, cells were cross-linked by adding serum-free DMEM containing 1% formaldehyde and incubated at 37 °C for 10 min. Cross-linking was quenched by the addition of glycine to a final concentration of 125 mM. Cells were harvested and cell pellets were resuspended in 1 ml SDS lysis buffer (50 mM Tris-HCl, (pH 8.0), 10 mM EDTA, 1% SDS, 1 µg/ml aprotinin, 1 µg/ml pepstatin, 1 mM PMSF) per 10^7 cells, followed by incubation on ice for 10 min. Lysed cells were sonicated to yield chromatin fragments of 200-1,000 bp. Cellular debris was removed by high speed centrifugation. Cell lysates containing 100 µg chromatin were diluted 10-fold using dilution buffer (16.7 mM Tris-HCl [pH 8.0], 167 mM NaCl, 1.2 mM EDTA, 0.01% SDS, 1.1% Triton X-100, plus protease inhibitors) and pre-cleared by incubation with protein A agarose/salmon sperm DNA slurry (Millipore) for 1 hr at 4°C with rotation. Samples were clarified by centrifugation and pre-cleared lysates incubated with 10 µg of polyclonal antibodies overnight at 4°C. Immune complexes were captured using protein A agarose/salmon sperm DNA for 2 hr at 4°C with rotation and pelleted by centrifugation.

Immunoprecipitates were washed once with low-salt wash buffer (20 mM Tris-HCl [pH 8.0], 150 mM NaCl, 2 mM EDTA, 0.1% SDS, 1% Triton X-100, plus protease inhibitors), once with high salt wash buffer (20 mM Tris-HCl [pH 8.0], 500 mM NaCl, 2 mM EDTA, 0.1% SDS, 1% Triton X-100, protease inhibitors), once with LiCl wash buffer (10 mM Tris-HCl [pH 8.0], 0.25 M LiCl, 1 mM EDTA, 1% SDS, 0.5% Triton X-100, 1% sodium deoxycholate, plus protease inhibitors), and twice with TE buffer (10 mM Tris-HCl [pH 8.0], 1 mM EDTA, plus protease inhibitors). Immune complexes were eluted using 100 mM $NaHCO_3$, 1 % SDS at room temperature. Formaldehyde cross-links were reversed with 50 mM Tris-HCl (pH 7.5), 200 mM NaCl, 10 mM EDTA, and 0.5 mg/ml proteinase K at 65°C overnight. DNA was recovered by standard phenol/chloroform extraction and ethanol precipitation and resuspended in 50 µl 10 mM Tris-HCl (pH 7.5), 1 mM EDTA. 2 µl of DNA sample was subjected to qPCR. One µg pre-cleared chromatin was used to measure DNA input levels. The fold-enrichment of specific DNA target was presented as a percentage of input DNA.

2.9 Immunofluorescence Assays

HDF-TERT cells were seeded on glass coverslips and infected as described above. At appropriate time points, the cells were fixed with ice-cold methanol and processed for immunofluorescence as described (28). Images were captured and analyzed using a Zeiss Axiovert 200M digital deconvolution microscope with AxioVision 4.8.2 SP3 software. More details may be found in the Supplemental Information.

2.10 Electrophoretic Mobility Shift Assays (EMSA)

Nuclear extract was used in the EMSA binding reactions. HDF-TERT cells were incubated with 500 U/ml IFNα, 1000 U/ml IFNγ or left untreated for 24 hr, and nuclear extracts were prepared as described previously. Briefly, cells were washed with PBS, resuspended in 4 pellet volumes of buffer A (10 mM HEPES pH7.9, 10 mM KCl, 1.5 mM

$MgCl_2$, 5 mM dithiothreitol [DTT] and protease inhibitors), and incubated on ice for 30 min. The cells were further disrupted by passing through 20-gauge needle twenty times. The nuclei were pelleted at 16,100 X g for 30 min at 4 °C, and the supernatant was the cytoplasmic fraction. The nuclei were extracted with 3 pellet volumes of buffer C (20 mM HEPES pH7.9, 420 mM NaCl, 1.5 mM $MgCl_2$, 0.2 mM EDTA, 20% Glycerol, 5mM DTT and protease inhibitor) and incubated on ice for 30 min. The nuclear fraction was cleared by centrifugation at 16,100 X g for 30 min, and stored at -80 °C. EMSA binding reactions were performed in a total volume of 15 µl containing 20 mM HEPES (pH 7.9), 5 mM $MgCl_2$, 50 mM KCl, 1 mM DTT, and 6% glycerol. 4 µg of each nuclear extract was incubated with 250 ng sonicated salmon sperm DNA or poly (dI:dC), with or without 0.2 µg specific antibody, for 15 min at room temperature. 80,000-150,000 cpm of ^{32}P-labeled probe was added to each reaction and incubated for an additional 30 min at room temperature. DNA-protein complexes were resolved in a 4.5% polyacrylamide gel in 0.5 X Tris-borate-EDTA buffer for 4-5 hr at 150 V. The gels were dried and autoradiographed. For the peptide competition assay, 0.2 µg antibodies were incubated with 0.5 µg corresponding peptide at 4 °C overnight prior to EMSA binding reaction. The E1A-ENH probe, 5'- GGTTCCATTTTCGCGGGAAAACTGCCGC-3', corresponds to Ad5 nt 271-288. The GABP probe, 5'-AGTCATAAGAGGAAGTGAAATCTGCCGC-3', corresponds to Ad5 nt 292-311. The STAT6 probe is 5'- GTATTTCCCAGAAAAGGAAC-3'. The GAS/IRES probe is 5'-AAGTACTTTCAGTTTCATATTACTCTA-3'.

2.11 Generation of E1A-expressing Cell Lines

The Ad5 E1A coding region was amplified by PCR, and then inserted into lentiviral expression vector pLenti6/v5-mCherrySp100 (kindly gifted by Dr. Thomas Stamminger, University of Erlangen-Nuremberg, Schlossgarten 4, Erlangen 91054, Germany) via *BamH* I and *Xho* I. A lentivirus stock was generated by cotransfection of 3

μg of pLenti-E1A plasmid with ViraPower^{TM} packaging mix (Life Technology), 3 μg of pLP1, pLP2 and pLP-VSVG each, into 293FT cells. At the second day after transfection, transfected cells were resupplied with fresh medium. At fourth-day post transfection (two days after changing medium), virus-containing supernatant was collected, and spined at 500 X g for 5 min to pellet cell debris. Then the supernatant was filtered through Millex-HV 0.45-μm (Millipore). Low passage HDF-TERT cells were transduced with the E1A-expressing lentivirus stock in the presence of 7.5 μg/ml polybrene (Sigma-Aldrich, Germany) at 37 °C overnight. Pools of E1A-expressing HDF-TERT cells were obtained after selection with 1μg/ml blasticidin.

2.12 Generation of Histone H3.1- and H3.3-expressing Cell Lines

Histone H3.1 and H3.3 expression plasmids, pOZ-H3.1FH-IRES-IL2α and pOZ-H3.3FH-IRES-IL2α, did not contain an antibiotic selection marker. The IL2 receptor α coding sequence was replaced by the puromycine coding sequence. The puromycin coding sequence was amplified using primers Puro-F-NcoI (5'-AGACCATGGCCGAGTACAAGCCCAC-3') and Puro-R-BamHI (5'-AGAGGATCCTCAGGCACCGGGC-3') together with pLKO-shneg as the template. Puromycin coding sequence was inserted via NcoI and BamHI. Lentivirus stock was generated by cotransfection of 4 μg of pOZ-H3FH-IRES-Puro plasmid with 4 μg of pCMV-dR8.91 and pVSV-G each, into 293FT cells. HDF-TERT cells were transduced with lentivirus as described above. Pools of H3.1 and H3.3-expressing cells were obtained after selection with 2 μg/ml puromycin.

2.13 Generation of Knockdown Cell Lines

For individual depletion of PML, Daxx or Sp100, retroviral vectors expressing shRNAs directed against PML, Daxx and Sp100 (pSIREN-RetroQ-shPML/-shDaxx/-shSp100), as well as negative control pSIREN-RetroQ-shleer, were provided by Dr. Thomas

Stamminger (University of Erlangen-Nuremberg, Erlangen, Germany) (103, 104). Replication-deficient retroviruses were generated by cotransfection of 293FT cells (Life Technologies) with helper virus and pVSV-G in combination with the respective pSIREN-RetroQ plasmids. Retrovirus-containing medium was repeatedly collected at 2 days, 3 days and 4 days post-transfection. For double and triple depletion of PML-NB components, lentiviral vectors, pLKO-shDP/shPS/shDPS, as well as a scrambled negative control, pLKO-shneg (105), were provided by Dr. Roger Everett (University of Glasgow, Glasgow, Scotland). Lentivirus stocks were prepared as previously described (105). To deplete endogenous IFI16 protein, scrambled shRNA in pLKO-shneg was replaced with shRNA against IFI16. shRNA target sequences against IFI16 were obtained from the RNAi Consortium (TRC) shRNA library, siIFI16-1, GATCATTGCCATAGCAAATT; siIFI16-3, GGAAACTCTGAAGATTGATT. Low passage HDF-TERT cells were transduced with the retrovirus or lentivirus supernatants in the presence of 7.5 μg/ml polybrene (Sigma-Aldrich, Germany) overnight. To increase the transduction efficiency, HDF-TERT cells were reinfected with retroviruses or lentiviruses at day 2 and day 3. Stably-transduced pools of cell populations were selected using 2 μg/ml puromycin. At least two independent pools of cells with efficient knockdown of individual target genes were generated and analyzed.

2.14 Western Blot Analysis

Whole cell extracts were prepared by suspending cell pellets in SDS lysis buffer (50 mM Tris-HCl [pH 6.5], 2% SDS and 10% glycerol) and boiled for 10 min. Lysates were centrifuged at 16,1000 X g for 3 min, supernatants were collected, and the protein concentration was determined using Pierce BCA Protein Assay Kit. Equal amounts of whole cell extracts were resolved on SDS-PAGE and transferred to a nitrocellulose membrane. Membranes were blocked with Tris-HCl-buffered saline (TBS) buffer

containing 3% BSA for 1 hr at room temperature, followed by incubation with primary antibodies (as indicated in the text and figure legends) at 4°C overnight. Membranes were washed with TBS buffer containing 0.1% Tween-20 (TBS-T) and then incubated with IRDye® 800CW-conjugated goat anti-rabbit antibody (926-32211, Li-COR) and IRDye® 680RD-conjugated goat anti-mouse antibody (925-068071, Li-COR) for 1 hr at room temperature. After three wash with TBS-T, images was captured using the ODYSSEY® CLx infrared imaging system (Li-COR). Alternatively, HRP-conjugated secondary antibodies were used in conjunction with ECL western blotting (Millipore Immobilon). Nuclear and cytoplasmic fractions for Western blot analysis were prepared using NE-PER™ nuclear and cytoplasmic extraction kit (Pierce).

2.15 Micrococcal Nuclease (MNase) Accessibility Assays.

IFN-treated or -untreated HDF cells were infected with ΔTP-GFP virus at 5,000 particles/cell or mock infected. Nuclei were prepared at 18 hr post-infection. Approximately 10^7 cells were washed with ice-cold PBS and pelleted by centrifugation at 750 X g for 5 min. Then cells were resuspended in 10ml of PBS containing 0.1% NP-40 (10^6 cells per ml buffer), and homogenized by pipetting up and down five times. Homogenized cells were carefully loaded on 1 ml of sucrose cushion (10 mM Tris pH7.4, 15 mM NaCl, 60 mM KCl, 0.15 mM spermine, 0.5 mM spermidine and 10 % sucrose), and centrifuged at 1,400 X g for 20 min at 4 °C. Nuclei pellets were resuspended in 5 ml wash buffer (10 mM Tris pH7.4, 15 mM NaCl, 60 mM KCl, 0.15 mM spermine, 0.5 mM spermidine) and centrifuge at 1,400 X g for 10 min. Finally, nuclei were suspended in 1 ml wash buffer. Nuclei were aliquot into 10^6 cells/reaction and incubated with MNase at room temperature. At the indicated time points, digestion was terminated by adding an equal volume of stopping buffer (10 mM Tris pH7.6, 10 mM EDTA, 0.5% SDS, 0.5 mg/ml protease K), and incubated at 37 °C overnight. DNA fragments were recovered by

phenol/chloroform extraction and ethanol precipitation, then separated on a 1.5% agarose gel. The DNA gel was stained with ethidium bromide and then transferred to Hybond N+ nylon membrane (Amersham). The DNA was crosslinked using a Stratalinker (Stratagene) and subjected to Southern blot using a ^{32}P-labeld probe generated by random priming with Ad5 genome DNA. The DNA was visualized by autoradiography.

2.16 Lymphocyte Infection

Cell densities of BJAB, Jurkat, and PM1 cells were adjusted to 5 X 10^5 cells/ml, and IFNα, IFNγ or PBS was added to the culture. Twenty-four hr later, cells were washed with TD buffer once, and then their densities were adjusted to 10^7 cells/ml in serum-free RPMI medium. Virus was added to the cell suspension at various multiplicities, as indicated in the figure legend, and incubated at 37°C for 3 hr. The infected cells were washed three times with RPMI complete medium and then resuspended in RPMI complete medium at 5 X 10^5 cells/ml. To determine viral replication, infected cells were harvested at 3 hr and 48 hr post-infection. Cells were washed with PBS once and spun at 1,000 X g 7.5 min to pellet cells. Total DNA was isolated using a DNeasy Blood & Tissue Kit, and then equal amounts of DNA were used in the qPCR reaction to determine viral and cellular copy number as described above.

2.17 Detection of Hexon by FACS (fluorescence activated cell sorting)

BJAB, Jurkat and PM1 cells were pretreated with IFNα, IFNγ or left untreated for 24 hr. Then BJAB and PM1 cells were infected with Ad5-WT or Ad5-mut1 at 2,000 virus particles/cell, and Jurkat cells were infected with the same viruses at 200 virus particles/cell at 37°C for 3 hr. After being washed with RPMI complete medium three times, the cell densities were adjusted to 2.5 X 10^5 cells/ml. Viral late gene expression was monitored for 16 days post-infection by intracellular staining for the hexon protein by

FACS. Cell numbers were determined every 2 days using a Countess Automated Cell Counter (Invitrogen). Cells were subcultured every 4 days. Cells were pelleted by centrifugation at 1,000 X g for 5 min and resuspended in RPMI complete medium containing IFNs or PBS.

For FACS, ~ 1X 10^6 cells were transferred to a FACS tube and centrifuged at 1,000 X g for 5 min. Cell pellets were resuspended in 1 ml ice-cold PBS and spun again. Cells were fixed by adding 1 ml of PBS containing 1% formaldehyde followed by incubation at room temperature for 30 min, flicking tubes occasionally to suspend cells. Cells were permeabilized by adding 1 ml of PBS with 0.2% Tween-20 and then incubated at 37°C for 15 min. Cells were washed with ice-cold FACS buffer (PBS with 2% bovine calf serum), 15 min/time point at room temperature. Then cells were resuspended in 100 µl FACS/Perm buffer (PBS with 2% bovine calf serum, 0.2% Tween-20) containing 1 µg anti-Hexon (clone 3G0, Santa Cruz Biotechnology) antibody and then transferred into a round-bottom 96-well microplate. After incubation for 30 min at room temperature, cells were washed with ice-cold FACS buffer twice. Alexa-488-conjugated goat anti-mouse IgG (2 µg/ml) was added to the cells and incubated at room temperature for 30 min, followed by two washes with FACS buffer and the cells were then subjected to FACS scan analysis.

2.18 Statistical Analysis

All numerical values represent the mean ± sd. Each experiment was done in three replicates, and a representative replicate is shown for each blot. Statistical significance of the differences was calculated using a Student's t-test.

Table 1. Oligonucleotides used for qPCR

Name	Sequence	Targets/Comments
GAPDH 5	CCCCACACACATGCACTTACC	GAPDH genome DNA
GAPDH 6	CCTAGTCCCAGGGCTTTGATT	
GAPDH-1	ACCCAGAAGACTGTGGATGG	GAPDH cDNA
GAPDH-2	TTCTAGACGGCAGGTCAGGT	
PACK-4	GCGAAAATGGCCAAATGTTA	Span ITR and E1A enhancer
PACK-5	TAATGAGGGGGTGGAGTTTG	
loxP7	GTCCGGTTTCTATGCCAAAC	E1A 13S cDNA and E1A coding region
loxP8	CCGTATTCCTCCGGTGATAA	
AdE1A-pan-qPCR-F	ACTCTTGAGTGCCAGCGAG	
Ad5E1A-qPCR-R	TCGTGAAGGGTAGGTGGTTC	Serotype specific reverse oligoes Use as paired with AdE1A-pan-qPCR-F
Ad3E1A-qPCR-R	TACAGATCGTGCAGCGTAGG	
Ad4E1A-qPCR-R	AGCGAAGGTGTCTCAAATGG	
Ad9E1A-qPCR-R	GGGCATCTACCTCCAGATCA	
Ad12E1A-qPCR-R	CGGCAGACTCCACATCAAG	
Ad16E1A-qPCR-R	TACAGATCGTGCAGCGTAGG	
E1A-ENH-F	CGCGGGAAAACTGAATAAGA	Ad5 E1A enhancer specific Not recognize Δ2-CMV virus
E1A-ENH-R	CTTGAGGAACTCACCGGGTA	
E1B-F	TGTGCCTTTTACTGCTGCTG	E1B cDNA
E1B-R	CACAGCCACGCTTTTCACTA	
DBP-F	CCGTAGTGGCATCAAAAGGT	DBP cDNA
DBP-R	GTCTAGCAAGGCCAAGATCG	
E2B-F	CGCGCGTCGAAGTAGTCTAT	E2B cDNA
E2B-R	CGGTGGAAGATGCTACCCTA	
E4ORF6-F	TACCGGGAGGTGGTGAATTA	E4ORF6 cDNA
E4ORF6-R	TTCAAAATCCCACAGTGCAA	
Ad5-mut1-F	ATATCTCCCACTGAATAAGA	Ad5-mut1 specific, paried with PACK-5
GAPDH-Promoter-F	TACTAGCGGTTTACGGGCG	Positive control for H3 K4me3
GAPDH-Promoter-R	TCGAACAGGAGGACAGAGAGCGA	
GAPDH-CHIP-F	GCCATGTAGACCCCTTGAAGAG	Positive control for H3 and H3.3 ChIP
GAPDH-CHIP-R	ACTGGTTGAGCACAGGGTACTTTAT	
Rb-1	GAGCCTCGCGGACGTGACGCCGC	
Rb-2	TGGAGGAGCGCCGGGGAGGACG	
hYAP-1	CCGTTTACCCCTCTCAAGTG	Positive control for H3 K4me3 ChIP
hYAP-2	CTTAAAGCCGCGAGGATAG	
p21-F	CCCACAGCAGAGGAGAAAGAA	Positive control for H3 K9ac ChIP
p21-R	CTGGAAATCTCTGCCCAGACA	
α-Satellite-F	CTGCACTACCTGAAGAGGAC	Positive control for H3 K27me3 ChIP
α-Satellite-R	GATGGTTCAACACTCTTACA	
ZNF554-F	CGGGGAAAAGCCCTATAAAT	Positive control for H3 K9me3
ZNF554-R	TCCACATTCACTGCATTCGT	
CDC2-F	CGCCCTTTCCTCTTTCTTTC	Positive control for DP-1 and E2F-4 ChIP
CDC2-R	ATCGGGTAGCCCGTAGACTT	
DHFR-F	TCGCCTGCACAAATAGGGAC	Positive control for Sp1 ChIP
DHFR-R	AGAACGCGCGGTCAAGTTT	

Table 2. Oligonucleotides used for EMSA

E1A-ENH -1	AATTGGTTCCATTTTCGCGGGAAAACTGCCGC
E1A-ENH -2	AATTGCGGCAGTTTTCCCGCGAAAATGGAACC
Ad5 nt 271-317-1	AATTAGTCCCATTTTCGCGGGAAAACTGAATAAGAGGAAGTGAAATCTGAATAATCCGC
Ad5 nt 271-317-2	AATTGCGGATTATTAGATTTCACTTCCTCTTATTCAGTTTTCCCGCGAAAATGGGAC
GABP-EMSA-1	AATTAGTCATAAGAGGAAGTGAAATCCTGCCGC
GABP-EMSA-2	AATTGCGGCAGGATTTCACTTCCTCTTATGACT
STAT5/6-EMSA-1	AATTGTATTTCCCAGAAAAGGAAC
STAT5/6-EMSA-2	AATTGTTCCTTTTCTGGGAAATAC
STAT5/6-EMSA-1	AATTGTATTTCCCAGAAAAGGAAC
STAT5/6-EMSA-2	AATTGTTCCTTTTCTGGGAAATAC
STAT6-EMSA-1	AATTGTATTTCCCCAGAAAAGGAAC
STAT6-EMSA-2	AATTGTTCCTTTTCTGGGGAAATAC
GAS/IRES-EMSA-1	AATTAAGTACTTTCAGTTTCATATTACTCTA
GAS/IRES-EMSA-2	AATTTAGAGTAATATGAAACTGAAAGTACTT

Chapter 3. Regulation of Ad Replication during an IFN Response in Normal Human Cells

3.1 Introduction

3.1.1 Antagonizing IFN Signaling Pathways by Adenovirus

IFNs fail to inhibit wild-type (WT) Ad replication in established cancer cell lines (46, 106, 107). The resistance of WT Ad to the effects of IFNs is due to multiple counteracting effects of viral gene products. The Ad E1A proteins block IFN signaling by binding STAT proteins and preventing the formation of the transcription complex ISG3 by type I IFNs and GAF complex by type II IFN (106, 108-112). The E1A proteins also bind and disrupt the hBre1 transcription complex and prevent IFN-induced histone H2B monoubiquitination and associated ISG expression (113). Both actions of E1A lead to the global suppression of ISG expression in response to IFNs. A recent study also showed that the E1A proteins interact with STING via its Leu-X-Cys-X-Glu (LXCXE) motif and block cGAS/STING activation in response to cytosolic DNA (114). Ad E1B-55K protein inhibits the expression of cellular ISGs through its transcriptional repression domain (115, 116). Numerous studies have shown that promyelocytic leukemia nuclear bodies (PML-NBs) play an important role in cellular intrinsic and IFN-induced antiviral immunity (117). The Ad E4-ORF3 protein antagonizes the functions of PML-NB by disrupting these structures and sequestering antiviral components including PML and Daxx (46, 47). The Ad E1B-55K:E4-ORF6 ubiquitin ligase complex also targets Daxx for proteasome degradation. Finally, Ad VA RNA-I inactivates PKR to prevent IFN-induced phosphorylation of the eIF2α translation factor that inhibits global protein translation during the late phase of viral infection (107).

Current models of the interplay between Ad infection and IFN signaling have mostly been conducted in cancer cell lines. Such cells are coupled with abnormal signal transduction, unlimited proliferation, and evasion of apoptosis, and likely are compromised in many normal signaling pathways. Indeed, it has been shown that the Ad E1B-55K protein was able to inhibit a set of ISG expression in response to type I IFN signaling in primary human cells, which has not been reported in established cell lines (115). Moreover, a recent study showed WT Ad exhibits an enhanced virus load in the organs of the STAT2-knockout Syrian hamsters compared to wild-type animals, revealing an important role of type I IFNs in controlling Ad replication *in vivo* (118).

3.1.2 Antiviral Activity of Promyelocytic Leukemia Nuclear Bodies (PML-NBs)

PML-NBs are punctate structures found in the nucleus. It is a dynamic structure that can undergo fission and fusion processes in a cell cycle-dependent manner. PML-NBs also move inside the nucleus, contacting the surrounding chromatin and harboring numerous proteins depending on different stimuli. Thus, it is not surprising that PML-NBs are involved in various cellular biology events, including an antiviral response, apoptosis, gene regulation, tumor suppression, protein degradation and DNA repair, among others (119). Here, I only focus on its antiviral activities here.

Though numerous proteins localize to PML-NBs partially or temporarily, there are only three resident proteins at PML-NBs, PML, Daxx (Death domain-associated protein) and Sp100 (Nuclear antigen Sp100). PML and Sp100 proteins are IFN-inducible genes, and the size and number of PML-NBs increase in response to IFN. However, PML-NBs can inhibit viral infection in both an IFN-dependent and IFN-independent manner (120). The molecular basis of PML-NBs antiviral activity against both DNA and RNA virus infection has been extensively studied in the past two decades. Taking alpha-herpesvirus HSV-1 and beta-herpesvirus HCMV as examples, PML-NBs have an

inhibitory effect on viral immediate early (IE) gene expression. Efficient viral gene expression and viral replication requires the disruption or relocalization of PML-NBs. HCMV tegument protein pp71 and immediate early protein 1 (IE1) target Daxx and Sp100, respectively, for protein degradation, to reverse the repression of viral transcription (121-124). In addition, HCMV IE1 and HSV-1 IE protein, ICP0, can induce the desumolyation of PML and Sp100, leading to the disruption of PML-NBs and efficient viral replication(125).

Our lab found that IFNα and IFNγ can inhibit the replication of an E4-ORF3 deletion mutant (*in*ORF3), but not WT Ad5 (*dl*309) in multiple established cancer cell lines, suggesting that E4-ORF3 counteracts antiviral activity of IFNs. E4-ORF3 is an Ad early protein; it forms a unique nuclear track structure and relocalizes a wide range of cellular proteins, including PML-NB proteins and the Mre11/Nbs1/Rad50 (MRN) DNA repair complex, to ensure spatial separation of these cellular proteins from viral replication centers and viral transcription sites. Depletion of PML or Daxx, but not Sp100, restored the replication of *in*ORF3 in IFNα and γ-treated cells (47). This evidence indicated that E4-ORF3 directly antagonizes a PML-NB-mediated, IFN-induced antiviral response. However, the molecular basis of how PML-NBs inhibit Ad replication is still unknown. A recent study showed that Sp100 could regulate viral gene expression in an isoform-specific manner(126). During Ad infection, Sp100 isoforms B, C, and HMG colocalized with viral replication centers. While Sp100 isoform A is retained in the E4-ORF3-PML tracks, it also partially colocalized with active viral transcription sites. The depletion of total Sp100 proteins increased Ad virus yield by less than two-fold (126). This suggests that Sp100 isoform A might repress Ad early gene expression, but this inhibition is independent of an IFN response.

3.1.3 E1A Immediate Early Protein

The E1A protein is the first viral product following Ad infection, and it is indispensable for virus growth (127). At the early stage of infection, the E1A transcript is alternatively spliced to yield two E1A mRNAs, and proteins encoded by these two mRNA are often referred as 13S and 12S E1A after the sedimentation of the mRNA, or 289R and 243R E1A after the length of polypeptides. At late stages of infection, three other E1A mRNAs accumulate but no distinct function is described for these products. Ad E1A protein contains four evolutionary conserved regions, CR1, CR2, CR3, and CR4 (Figure 3-1A). 13S and 12S E1A share many functional redundancies since they are identical in amino acid sequence, except a 46 amino acid sequence unique to 13S E1A. 13S E1A is considered as the transcription factor primarily responsible for activation of other viral genes. The E1A 13S protein interacts with the TATA box binding protein (TBP) though the N-terminus of CR3, and this interaction stimulates the formation of the transcription initiation complex at viral promoters (127).

In contrast, 12S E1A is primarily known for its ability to regulate cell cycle progression (128, 129). When expressed alone, 12S E1A drives growth-arrested cells to enter S phase. In cooperation with another viral oncogene, E1B55K, E1A transforms primary rodent cells. E1A-induced transformation requires simultaneous interaction of E1A with cellular p300/CBP (CREB-binding protein) and Rb family proteins. p300 and CBP are two closely related lysine acetylases, and they function as transcription co-factors. They regulate transcription by inducing the acetylation of histone proteins or transcription factors that they associate with. The E1A protein can directly interact with p300/CBP via its N-terminus and CR1 motif (Figure 3-1A), causing inhibition of histone acetyltransferase (HAT) activities of p300/CBP and their association with transcription factors (127). The Retinoblastoma (Rb) protein is a tumor suppressor that governs the G1/S transition of the cell cycle (130-132). E2F transcription factors regulate the

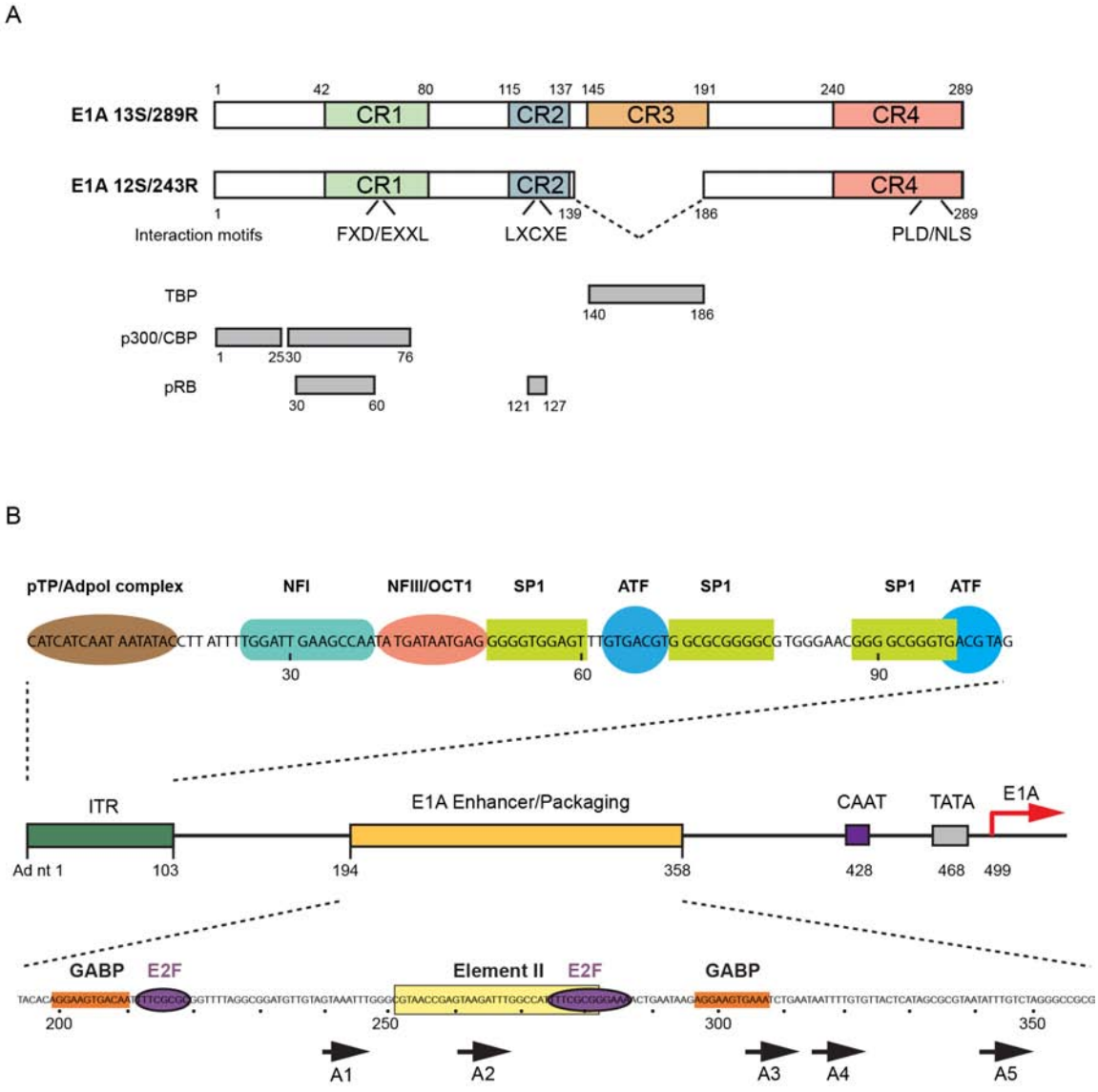

Figure 3-1. Adenovirus E1A protein and organization of adenovirus left end
(A) Schematic view of Ad5 E1A protein structure. The 13S and 12S E1A proteins are shown with the conserved regions CR1, CR2, CR3 and CR4. The domains required for the E1A functions are indicated beneath the E1A protein schematic. The regions necessary for interaction with TBP, p300/CBP and Rb family proteins are indicated as grey boxes.
(B) Schematic view of the left end of the Ad5 genome is shown in the middle including the inverted terminal repeat (ITR), E1A enhancer region, CAAT box, TATA box, and transcription start site (TSS). Shown top are the Sp1 and ATF binding sites in the ITR and the binding sites of protein involved in Ad replication, including pTP/Adpol, NFI and NFIII/Oct1.Shown below are the GABP and E2F binding sites in the E1A enhancer and the boundaries of enhancer element II. Arrow heads indicate packaging sequence repeats.

expression of genes required for S-phase entry. In G1 phase, hypophosphorylated Rb interacts with E2Fs to suppress their transcription activities, as well as recruits repressive chromatin remodeling complexes, such as histone deacetylases (HDACs). When Rb is hyperphosphorylated by CDK4/6 and CDK2, it undergoes a conformational change and releases E2Fs from the E2F/Rb complex. This derepression of E2Fs leads to activation of E2F target genes and S-phase entry. E1A proteins can directly bind to Rb, and two other related pocket proteins p107 and p130, leading to the relief of E2Fs from repression. Different from the E1A-p300 interaction, E1A interacts with pocket proteins primarily through CR2 and 10 amino acids in CR1 (Figure 3-1A).

3.1.4 Regulation of E1A Transcription

E1A transcription is regulated via a constitutively active enhancer located at Ad nt 194-358 and composed of multiple regulatory elements (133). Genetic analyses revealed that there are two distinct *cis*-elements involved in regulation of E1A transcription. Cellular transcriptional factor GA-binding protein (GABP) binds to repeated element I, at -200 (nt 300 from the left end of Ad genome) and -300 (nt 200) relative to the E1A transcription start site, and cooperatively transactivates E1A transcription in Ad-infected cells (134-136). Deletion of individual GABP binding sites only reduces E1A mRNA level by 3 to 4-fold. However deletion of both sites decreases E1A mRNA levels by 40-fold, without altering the transcription from other viral early promoters if E1A is provided *in trans* (136). In contrast, the enhancer element II, located between the two GABP binding sites, transactivates the entire Ad genome in *cis*. Deletion of element II led to decreased mRNAs from all viral early regions (133). Furthermore, there are two E2F binding sites adjacent to both GABP binding sites. EMSA assays suggested that E2Fs and Rb family proteins were indeed associated with the E1A enhancer region *in vitro* (137, 138), but they are dispensable for viral replication since the removal of both

E2F sites did not affect early gene expression (Dr. P. Hearing, unpublished data). Lastly, transcription factor Sp1 binds to multiple sites at the Ad inverted terminal repeat (ITR). Sp1 is not required for activation of the E1A gene in the context of an intact E1A enhancer, but it does support E1A expression when the sequences between ITR and the E1A TATA box are deleted, bringing the ITR immediately upstream of the TATA box.

GABP is the primary transactivator of E1A expression (133, 135, 136). GABP (also known as adenovirus E4 transcription factor 1 [E4TF-1] and nuclear respiratory factor 2 [NRF-2]) belongs to the *Ets* transcription factor family, which contains an evolutionarily conserved DNA binding domain (139). The *Ets* proteins preferentially bind to a purine-rich motif that contains a GGAA/T core. GABP is the only multimeric member among the *Ets* proteins. As a tetrameric transcriptional complex, GABP is composed of two distinct, unrelated subunits, GABPα and GABPβ. The GABPα subunit contains the DNA binding domain (DBD) while the GABPβ subunit contains the transactivation domain (TAD) (140). GABPβ can form a homodimer in the absence of GABPα, but recruitment of GABPβ to the target gene requires proper interaction with GABPα, and GABPβ stabilizes GABPα-DNA interaction. GABP is only functional when α and β subunits form a tetramer, α2β2. The activity of GABP is regulated by post-translational modifications. The oxidation of cysteine residues in the DBD and heterodimerization domains of the GABPα (141) blocks DNA binding and GABPβ interaction, respectively. Also, a recent study showed that GABPβ is phosphorylated by Lats kinase in response to Hippo signaling, blocking GABPβ homodimerization and nuclear localization (142). Both subunits of GABP interact with a variety of transcription factors to regulate target gene transcription, including Sp1, E2F, ATF, PU.1, YEAF, among others (139). Interestingly, GABPα interacts with ATF, and they synergistically transactivate the Ad E4 promoter (143, 144). GABP also interacts with E2F1, but this interaction could either enhance or dampen expression of E2F1 target genes (145-147).

3.2 Specific Aims and Significance

To date, the interplay between Ad and IFN responses were all defined in cancer cell lines. It is known that type I and type II IFNs fail to inhibit WT Ad replication, due to the counteracting effects of viral proteins. But IFNs were able to inhibit the replication of an E4-ORF3 mutant virus mediated by the PML and Daxx proteins. However, the details of the mechanism by which PML and Daxx suppress Ad replication is still unclear. Here I aimed to explore the effect of type I (IFNα) and type II IFNs (IFNγ) on Ad replication in normal human cells. I also wanted to probe the mechanism by which E4-ORF3 antagonizes IFN responses, as well as what role PML-NBs play in the interaction.

Our data demonstrate that both type I and type II IFNs block WT Ad5 (*dl*309) and E4ORF3 deletion mutant (*in*ORF3) replication in primary human bronchial epithelial cells (NHBEC) and normal human diploid fibroblasts (HDF-TERT). The result is opposed to the observation in human adenocarcinomic epithelial cells and other established cancer cell lines (46, 47) where Ad infection is resistant to IFN treatment. Further analysis suggested that this inhibition is the consequence of repression of transcription of the E1A gene. Viral replication and early gene expression were rescued in an HDF-TERT-derived E1A expressing cell line, as well as in HDF-TERT cells that transiently express the E1A protein. Both IFNα and IFNγ impede the association of GABP with the E1A enhancer region *in vivo* before early transcription occurred. I also confirmed that IFNα and IFNγ do not interfere with the assembly of the Ad genome into a chromatin-like structure or specifically alter the post-translational modification of histone H3 at the E1A enhancer region during the early stage of infection.

This is the first study showing that IFNα and IFNγ repress E1A transcription leading to inhibition of WT Ad5 replication. The E4-ORF3 protein only has a minor influence on IFN-signaling in normal human cells.

3.3 Results

3.3.1 Profile of the Adenovirus Life Cycle in HDF-TERT Cells

To evaluate Ad replication in normal human cells during an IFN response, I utilized a normal, non-transformed human diploid fibroblast cell line immortalized by human telomerase (HDF-TERT) that is permissive for Ad infection. *dl*309, a phenotypically wild type Ad5, had an infectious particle/PFU ratio of ~1000:1 in HDF-TERT cells compared to ~20:1 in A549 cells due to reduced infectivity of HDF-TERT cells (data not shown). The particle/PFU ratio of *in*ORF3 was determined to be ~4,800:1 in HDF-TERT cells. Next, I established the timeline of the Ad5 life cycle in HDF-TERT cells. The majority of incoming viral genomes (detected by immunofluorescence using an antibody against the major viral core protein VII) were still in the cytoplasm at 2 hr post-infection; complete entry of viral genomes into the nucleus required ~6 hr (Figure 3-2A). By 16 hr post-infection, the number of core protein VII foci had significantly declined indicating viral early gene transcription had occurred (32). RT-qPCR analysis of Ad immediate early (E1A) and early mRNA levels (E1B, E2A, E2B and E4) showed an exponential increase in early gene expression from 6 to 24 hr post-infection (Figure 3-2B). To assess the kinetics of viral DNA replication, a sensitive qPCR assay was employed. Viral DNA replication began during the 18-24 hr time period and increased substantially thereafter with a 4-log total increase in genome copy number (Figure 3-2D) by 48 hr post-infection and an 1-log additional increase in genome copy number from 48 to 144 hr post-infection (Figure 3-2E). Viral early gene (E4-ORF3) and intermediate gene (IVa2) expression was evident as DNA replication occurred and late gene products continued to accumulate through 144 hr post-infection (Figures 3-2C and 3-5E). There was no cytopathic effect observed up to 6 days post-infection even at a multiplicity of infection (MOI) of 1000 virus particles/cell where all cells were infected (Figure 3-2A and

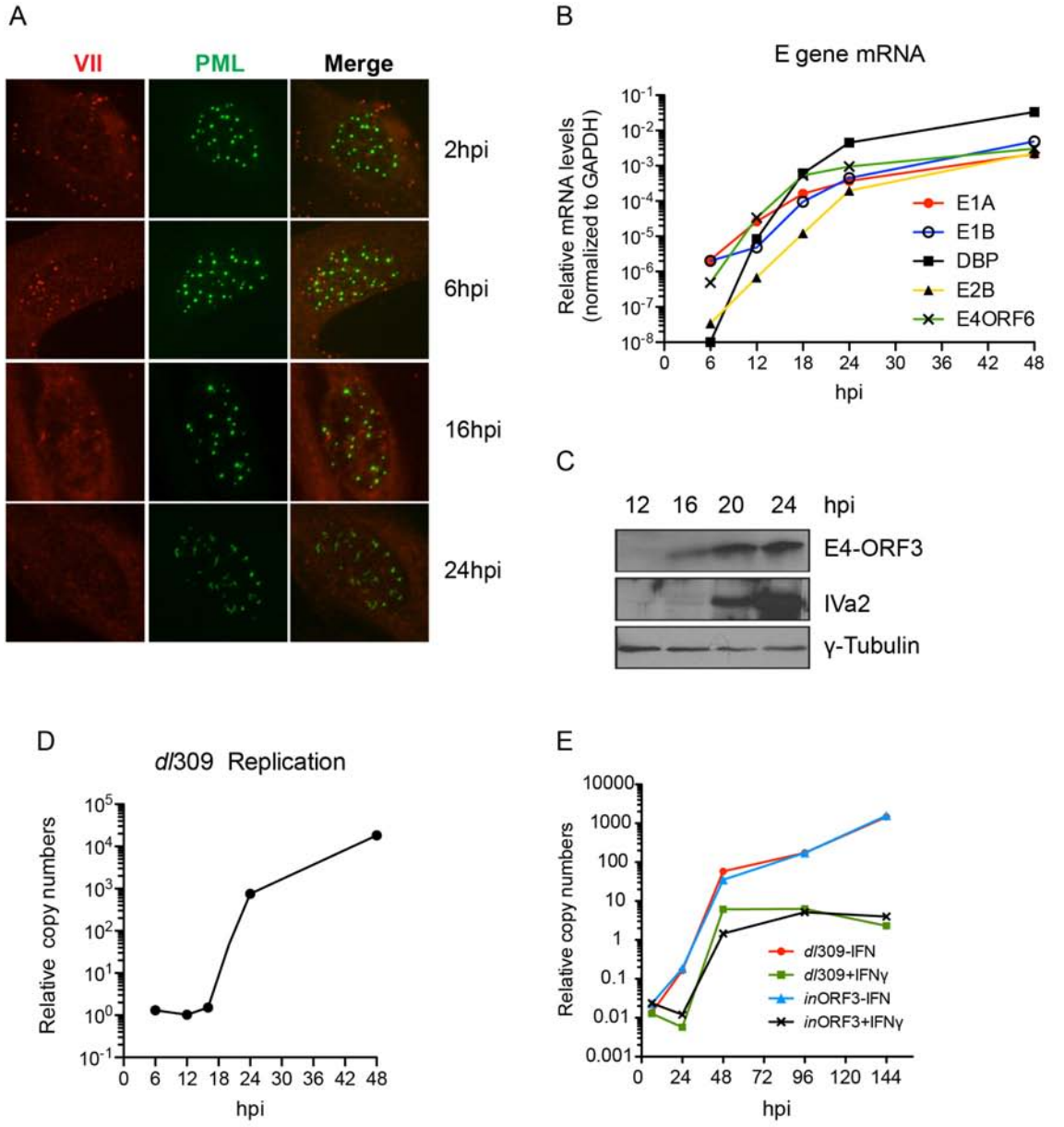

Figure 3-2. Profiling the adenovirus life cycle in HDF-TERT cells
(A) HDF-TERT cells were infected with *dl*309 at 1,000 virus particles/cell, and fixed at various time points. Immunofluorescence assay was carried out using antibodies against viral VII (red) and cellular PML protein (green).
(B, C) HDF-TERT cells were infected with *dl*309 at 25 particles/cell. Total RNA was purified at various time points. Viral mRNA levels were measured by RT-qPCR, and normalized to GAPDH mRNA.
(C) HDF-TERT cells were infected with *dl*309 at 200 particles/cell, and western blot was performed to exam the expression of viral proteins.
(D) HDF-TERT cells were infected with *dl*309 at 200 virus particles/cell. Nuclei DNA were purified at various time points. Viral copy numbers were determined by qPCR and normalized to GAPDH copy numbers.
(E) HDF cells were preteated with 1,000 U/ml IFNγ or left untreated for 24 hr, then infected with *dl*309 and *in*ORF3 at 25 particles/cell. Nuclei DNA were purified at various time points. Viral copy numbers were determined by qPCR and normalized to GAPDH copy numbers.

data not shown). Collectively, Ad exhibits an extended life cycle in HDF-TERT cells compared to that in other permissive cells, such as A549, HeLa and 293. In HDF-TERT cells, it takes 6 hr for incoming genomes to enter the nucleus, in contrast to approximately 45 min in A549 cells. Viral DNA replication starts after 18 hr post-infection, and Ad actively replicates until 48 hr post-infection when the infection goes into the late stage.

3.3.2 IFNα and IFNγ Inhibit Ad5 Replication in Normal Human Cells, but not Cancer Cells.

To evaluate Ad5 replication in HDF-TERT cells in the presence or absence of IFNs, cells were incubated with 500 U/ml IFNα, 1000 U/ml IFNγ or left untreated for 24 hr, followed by infection of WT Ad5 (*dl*309) or an E4-ORF3 mutant (*in*ORF3) at low MOI (25 particles/cell). Viral DNA replication was quantified by qPCR at 48 hr post-infection (Figures 3-3A and 3-3B). It was surprising that IFNα and IFNγ reduced replication of both viruses by more than 20-fold, in contrast to the observation in established cancer cell lines (46, 47) that IFNs did not inhibit WT Ad5 replication. *dl*309 and *in*ORF3 had similar sensitivities to IFNs; this could be due to insufficient accumulation of E4ORF3 to antagonize an IFN response at low MOI. To examine this possibility, I infected HDF-TERT cells with both viruses at higher MOI. The effect of IFNs on virus replication was moderately diminished at high MOIs but replication of both viruses was still inhibited in IFN-treated cells by ~2 fold. The effect of IFNs on infectious virus production was determined by plaque assay. At low MOI, IFNα and IFNγ reduced virus yield of *dl*309 two and three logs, respectively, and virus yield of *in*ORF3 two and four logs, respectively (Figures 3-3C and 3-3D). The reduction in infectious virus yield observed following IFN treatment correlated with reduced viral DNA replication and decreased late gene expression (Figure 3-3E). I also examined Ad5 early mRNA levels by RT-qPCR

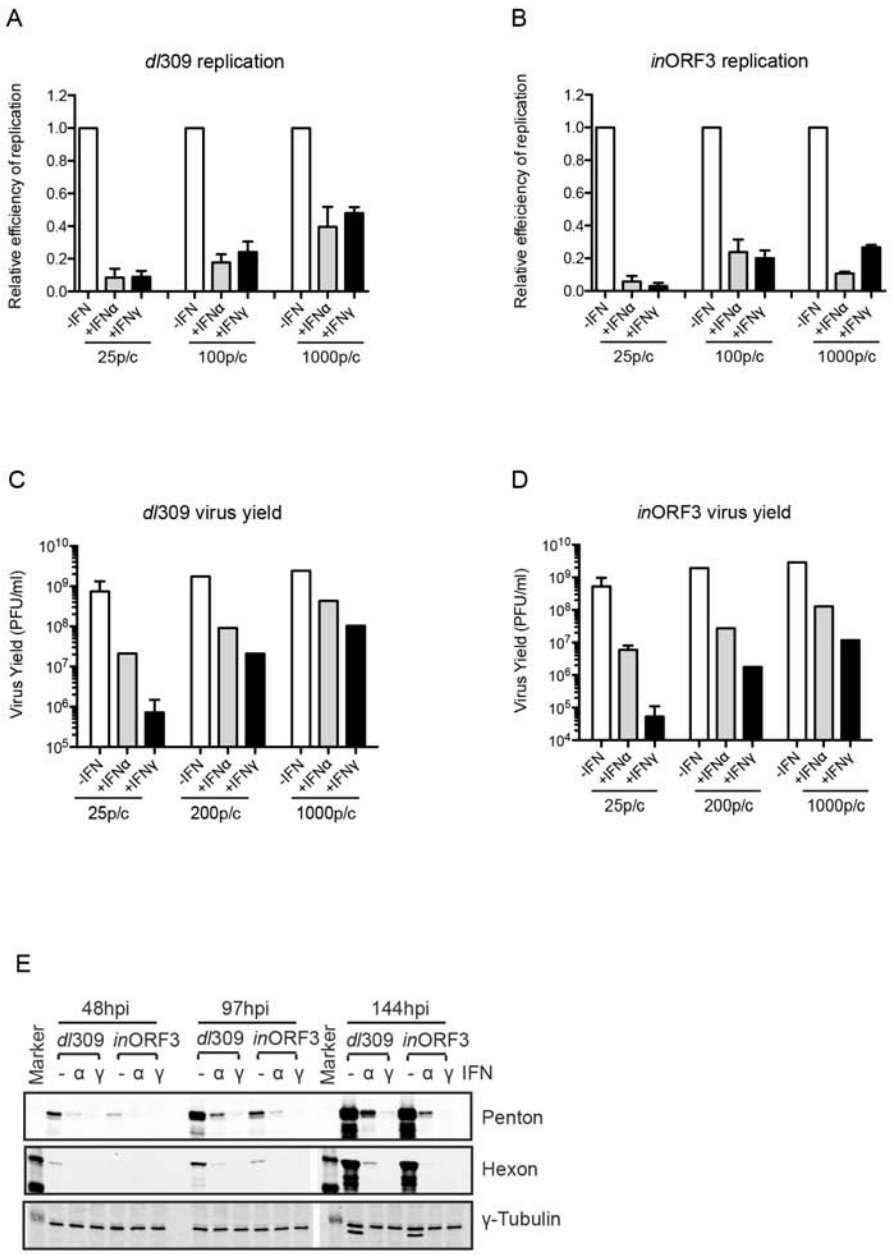

Figure 3-3. IFNα and IFNγ inhibit WT adenovirus replication and early gene expression in normal human cells.
(A, B) IFN-treated and untreated HDF-TERT cells were infected with *dl*309 (C) or *in*ORF3 (D) at 25, 100 and 1,000 particles/cell. Virus replication was determined at 48 hpi by qPCR. Data was plotted as mean ± sd, n=3.
(C, D) HDF-TERT cells cells were infected as described in (C), virus yields were measured at the 144 hpi by plaque assay on A549 cells. For 25 particles/cell infection, data was ploted as mean ± sd, n=3.
(E) Infection was carried out as described in (A) at 25 virus particles/cell. Cells were harvested at 48, 97 and 144 hr post-infection and viral late protein levels (Penton and hexon) were analyzed by western blot. γ-tubulin was used as a loading control for the samples.

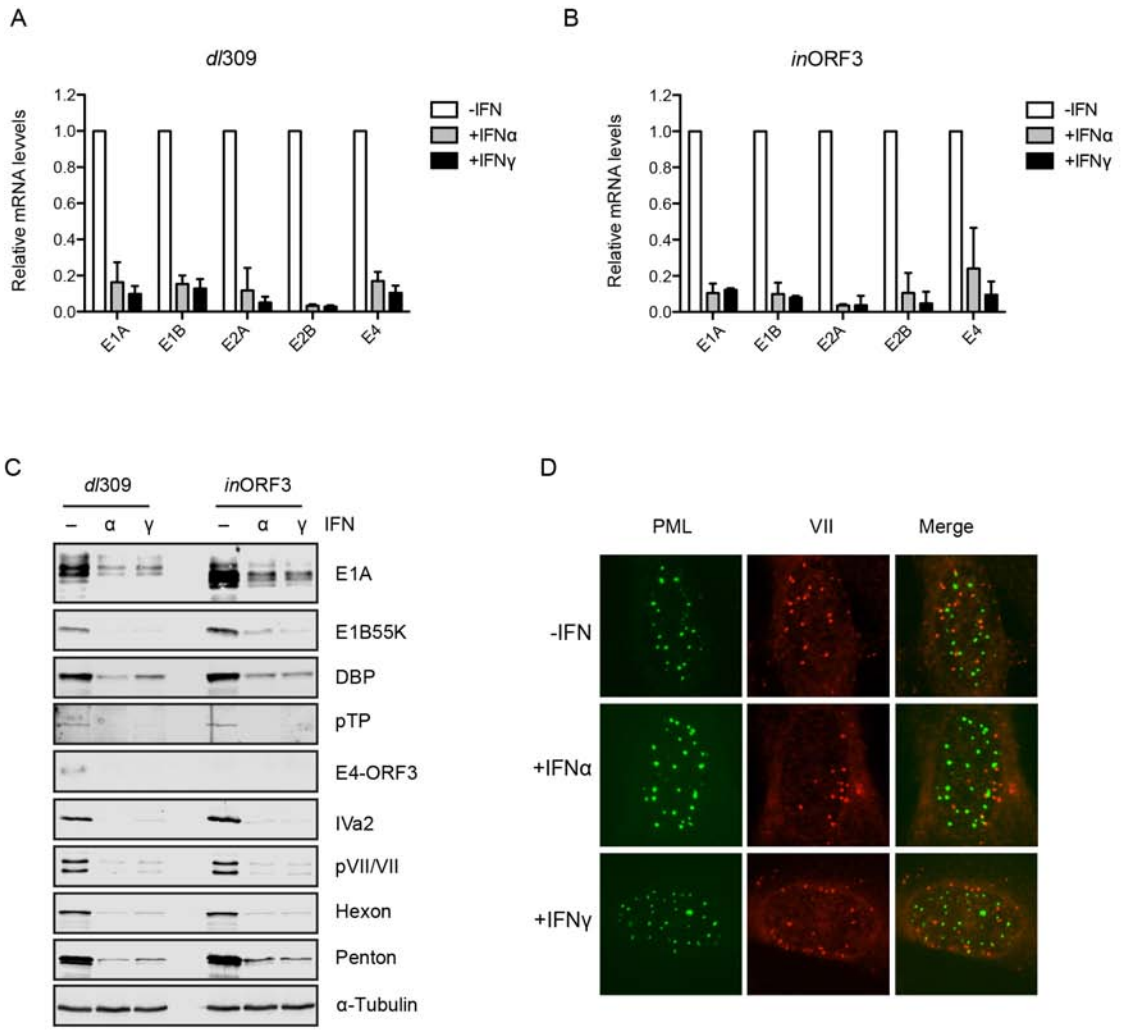

Figure 3-4. Inhibition of Ad5 viral early gene expression by IFNs.
(A, B) HDF-TERT cells were pretreated with IFNs or left untreated for 24 hr and then infected with *dl*309 (A) or *in*ORF3 (B) at 25 virus particles/cell. Ad early mRNA levels were quantified by RT-qPCR with RNA samples isolated at 48 hr post-infection. The results were normalized to GAPDH mRNA levels and the fold-change in Ad early gene expression compared to untreated cells is plotted as mean ± sd, n=3.
(C) HDF-TERT cells were pretreated with IFNs or left untreated for 24 hr and then infected with *dl*309 at 25 virus particles/cell. Ad proteins were analyzed by Western blot using specific antiera directed against early (E1A, E1B55K, DBP, pTP, E4-ORF3), intermediate (IVa2) and late gene products (pVII/VII, Hexon, Penton). α-tubulin is shown in the bottom panel as a loading control for the samples.
(D) HDF cells seeded on glass coverslips were infected with *dl*309 at 1,000 particles/cell. The cells were immonustained for VII (red) and PML (green) at 6 hr post-infection. Merged images are shown in the right column.

with or without IFN treatment. Ad immediate early (E1A) and early gene expression (E1B, E2A, E2B and E4) was significantly suppressed in IFN-treated cells compared to untreated cells (Figures 3-4A and 4B). The reduction in viral mRNA levels correlated with decreased early, intermediate and late gene expression (Figure 3-4C). IFNs did not block the entry of viral genomes into the nucleus, and viral genomes did not colocalize with PML-NB with or without IFN treatment (Figure 3-4D).

I also evaluated Ad replication in primary normal human bronchial epithelial cells (NHBEC), the natural host cell of Ad infection, in comparison to the established epithelial adenocarcinoma cell line A549. Neither IFNα and IFNγ was able to block Ad5 replication in A549 cells (Figures 3-5A). Consistent with the result observed in HDF-TERT cells, WT Ad5 replication in NHBEC was inhibited by IFNα and IFNγ ~40-fold and 70-fold, respectively (Figure 3-5B). Again, the reduced Ad replication in NHBEC was correlated with decreased early transcription (Figure 3-5C).

3.3.3 IFNs Inhibit Ad Replication by Repressing Immediate Early Gene Expression

There are two possible means by which IFNs could reduce Ad early gene expression. IFNs may repress early gene expression directly, or IFNs may inhibit viral DNA replication resulting in a corresponding decrease in early gene expression. To examine these possibilities, HDF-TERT cells were infected with a replication-defective mutant virus ΔTP-GFP. ΔTP-GFP contains a disruption in the coding sequences for Ad5 terminal protein, a protein that is absolutely essential for viral DNA replication (148). The relative copy number of ΔTP-GFP viral genomes in the presence and absence of IFNs did not increase, but E1A mRNA levels were reduced by both IFNα and IFNγ throughout the time course of the experiment (Figures 3-6A and 3-6B). These results demonstrate that IFNs inhibit Ad early gene expression in a replication-independent manner.

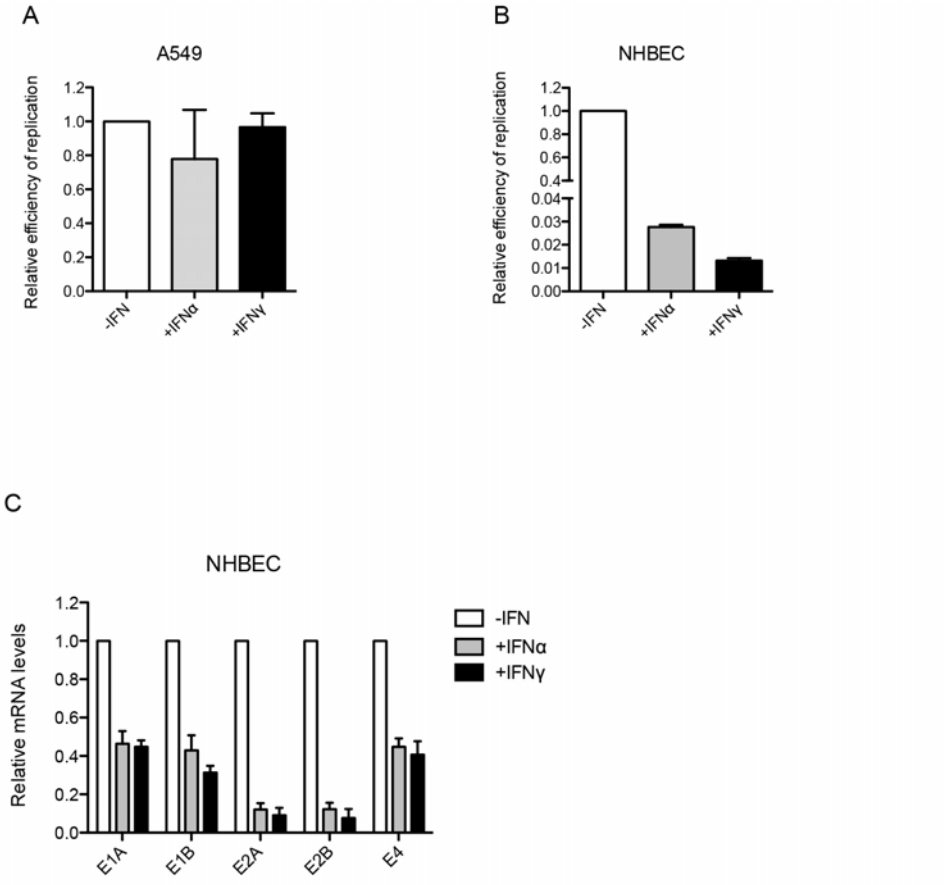

Figure 3-5. IFNα and IFNγ inhibit WT Ad5 replicaion and early gene expression in NHBEC cells.
(A and B) A549 (A) and NHBEC (B) cells were pretreated with IFNα, IFNγ or left untreated for 24h, and infected with *dl*309 (A) or WT Ad5 (B) at 100 particles/cell. Cells were harvested for DNA isolation at 2 hpi and 24hpi, qPCR was performed to determin relative replication efficiencys as described in Materials and Methods.
(C) NHBEC cells were pretreated with IFNs or left untreated for 24 hr and then infected with WT Ad5 at 100 virus particles/cell. Ad early gene mRNA levels were quantified by RT-qPCR at 24 hr post-infection. The results were normalized to GAPDH mRNA levels and the fold-change in Ad early mRNAs compared to untreated cells is polotted. The data represents mean ± sd from two independent experiments.

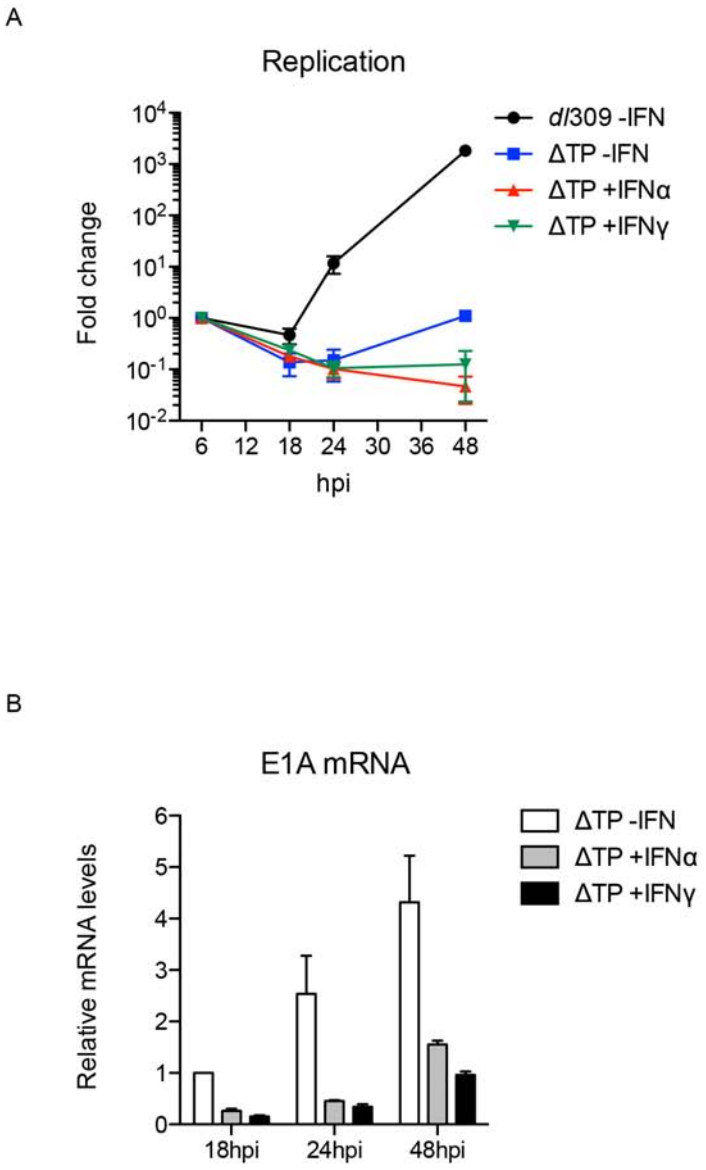

Figure 3-6. Inhibition of Ad E1A expression is replication independent.
(A) HDF-TERT cells pretreated with IFNα, IFNγ or left untreated for 24 hr and then infected with *dl*309 or the replication-defective mutant virus ΔTP-GFP at 25 virus particles/cell. Nuclear DNA was isolated at the indicated time points. Viral DNA copy numbers were normalized to cellular GAPDH, and data is presented as fold change relative to that of the input at 6 hr post-infection.
(B) HDF-TERT cells treated with IFNα, IFNγ or left untreated for 24 hr and then infected with ΔTP-GFP at 25 virus particles/cell. E1A mRNA levels were quantified by RT-qPCR. The results were normalized to cellular GAPDH mRNA levels. The data are plotted as mean ± sd, n=3.

E1A is the first viral protein expressed after infection and it is essential for efficient activation of all Ad gene expression (127). It is possible that IFNs suppress E1A transcription directly, resulting in the observed phenotype, rather than having a global effect on Ad early gene expression. To test this hypothesis, I generated an E1A-expressing HDF-TERT cell line (HDF-TERT-E1A). Western blot showed that the major E1A isoforms were expressed in HDF-TERT-E1A cells (Figure 3-7B, top panel). Since E1A can inhibit IFN signaling (106, 108-112), I examined IFN signaling in HDF-TERT-E1A cells (Figure 3-7B). E1A expression did not impede IFN signaling in these cells; increases in STAT1 protein levels and STAT1 phosphorylation, as well as the induction of IGS54 and ISG15 expression, were observed in HDF-TERT-E1A cells following IFNα and IFNγ treatments. Ad DNA replication and early gene expression of both *dl*309 and *in*ORF3 were almost completely restored in HDF-TERT-E1A cells infected even at low MOI and treated with IFNs (Figures 3-7C and 3-7D). The levels of all Ad early mRNAs and protein levels were also almost completely restored in HDF-TERT-E1A cells infected at high MOI and treated with IFNα or IFNγ (Figures 3-7E and 3-7F).

As a viral oncogene, E1A is able to transform cells (127). HDF-TERT-E1A cells exhibit a different cell morphology as compared to parent HDF-TERT (Figure 3-7A). Stable expression of E1A might lead to transformation of HDF-TERT cells losing the biological property of normal human cells, such as different signaling activities. Thus, I evaluated Ad replication following IFN treatment when E1A was only transiently expressed. Dr. P. Hearing generated an Ad expression vector, *in*340-Δ2-CMV, which contains the CMV promoter/enhancer in place of the E1A enhancer region and E1A/E1B coding sequences. The E1A open reading frame was inserted downstream of the CMV promoter. HDF-TERT cells were infected with *in*340-Δ2-CMV-E1A virus or the control virus *in*340-Δ2-CMV for 1 hr, followed by the addition of IFNα and IFNγ. Twenty-four hr later, cells extracts were prepared and E1A expression was analyzed by Western blot, or

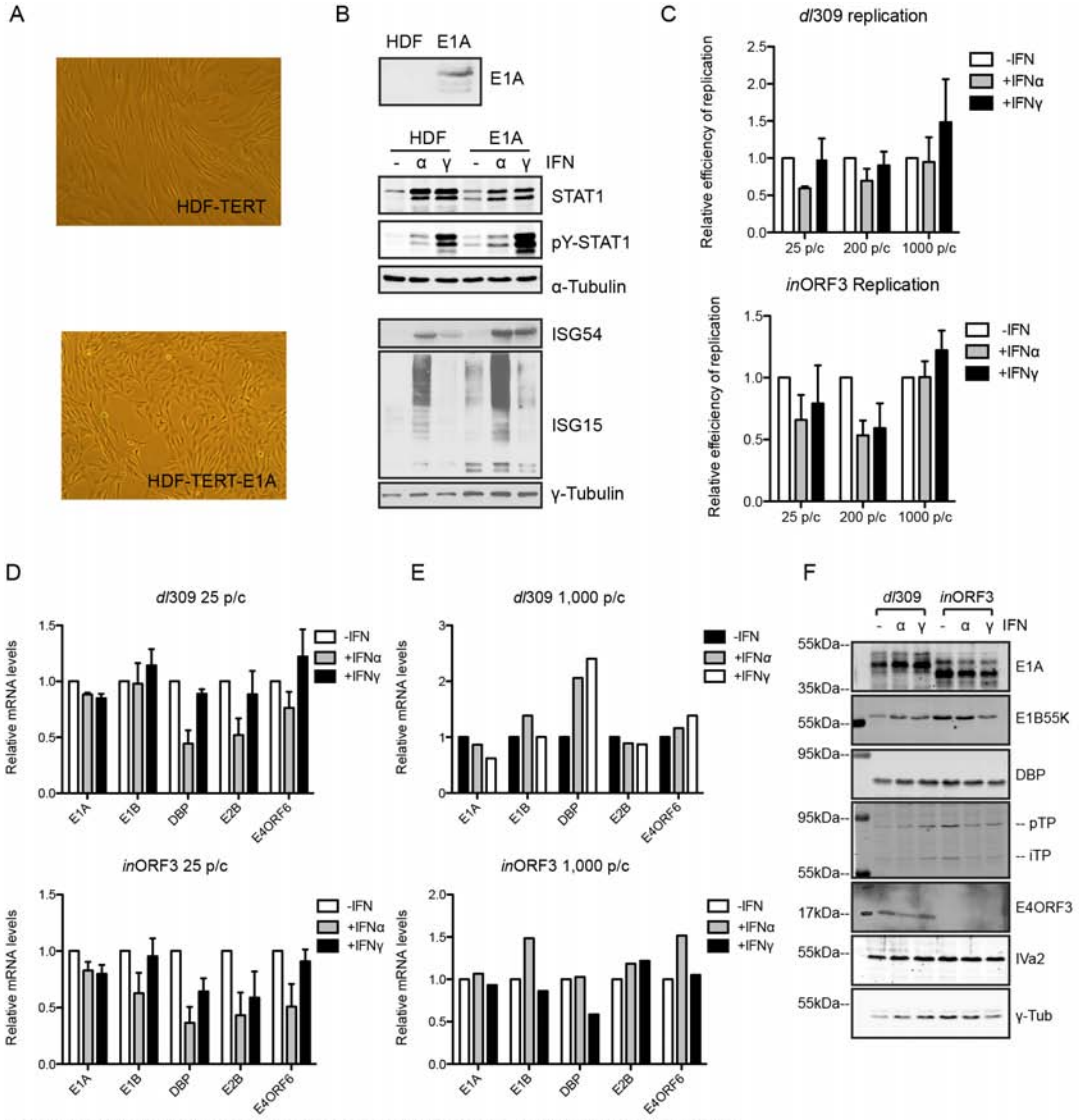

Figure 3-7. Inhibition of Ad replication by IFNs is blocked by E1A expression.
(A) Phase contrast microscopy images of HDF-TERT and HDF-TERT-E1A cells
(B) HDF-TERT-E1A cells were treated with IFNα, IFNγ or left untreated for 24 hr and Western blot analyses were performed at 24 hr post-infection to detect the expression STAT1, phosphorylated STAT1, ISG54, and ISG15. E1A 13S and 12S products are shown in the top panel. α-Tubulin and γ-Tubulin were used as a loading control for the samples.
(C) HDF-TERT-E1A cells were treated with IFNα, IFNγ or left untreated for 24 hr and then infected with *dl*309 (top) or *in*ORF3 (bottom) at 25, 200 or 1000 virus particles/cell. Nuclear DNA was isolated at 48 hr post-infection and viral DNA levels were quantified by qPCR. The values were normalized to 1.0 in untreated cells and are plotted as mean ± sd, n=3.
(E) HDF-TERT-E1A cells were treated with IFNα, IFNγ or left untreated for 24 hr and then infected with *dl*309 (top) or *in*ORF3 (bottom) at 25 virus particles/cell. E mRNA levels were quantified at 24 hr post-infection by RT-qPCR. The values were normalized to 1.0 in untreated cells and are plotted as mean ± sd, n=3.
(E, F) HDF-TERT-E1A cells were infected with *dl*309 or *in*ORF3 at 1,000 particles/cell as described in (E). At 48 hr post-infection, E mRNA levels were quantified by RT-qPCR (E), and E protein levels were quantified be Western blot (F).

the cells were superinfected with *dl*309 and *dl*309 replication was assayed at 48 hr post-infection by qPCR. Neither IFNα and IFNγ reduced E1A expression in cells infected with *in*340-Δ2-CMV-E1A (Figure 3-8B, left). *dl*309 replication was significantly reduced in IFN-treated cells coinfected with *in*340-Δ2-CMV. Consistent with the results obtained using HDF-TERT-E1A cells, ectopic expression of E1A by *in*340-Δ2-CMV-E1A largely restored this defect in IFN-treated cells (Figure 3-8B, right). As observed with HDF-TERT-E1A cells, transient expression of E1A did not impair IFN signaling in these assays (Figure 3-8A). Collectively, these results demonstrate that both IFNα and IFNγ inhibit Ad replication by repressing E1A gene expression and this is the ~~sole~~ defect in the Ad life cycle observed in IFN-treated cells.

3.3.4 IFNs Block Recruitment of GABP to the E1A Enhancer Region

The cellular transcription factor GABP is the major regulator of E1A transcription and binds to two sites in the E1A enhancer region (133, 135, 136). These two sites have synergistic effects on E1A transcription; when both sites are deleted, E1A expression is dramatically diminished. Therefore, I examined the interaction of GABP with the E1A enhancer region *in vivo* plus and minus IFN signaling. I carried out chromatin immunoprecipitation (ChIP) experiments using an antibody against the GABPα subunit. The immunoprecipitated DNA was quantified by qPCR using oligonucleotides spanning the ITR and E1A enhancer. At 18 hr post-infection, prior to the onset of viral DNA replication, IFNα or IFNγ decreased the association of GABP with the E1A enhancer *in vivo* by 3- and 2.5-fold, respectively (Figure 3-9A, left). The specificity of GABPα was ensured by using oligonucleotides spanning the E1A coding region where GABPα did not bind (Figure 3-9A, right).

The transcriptional activity of the GABP can be regulated at the post-translational modification level, including the oxidation of cysteine residues in the DNA binding and

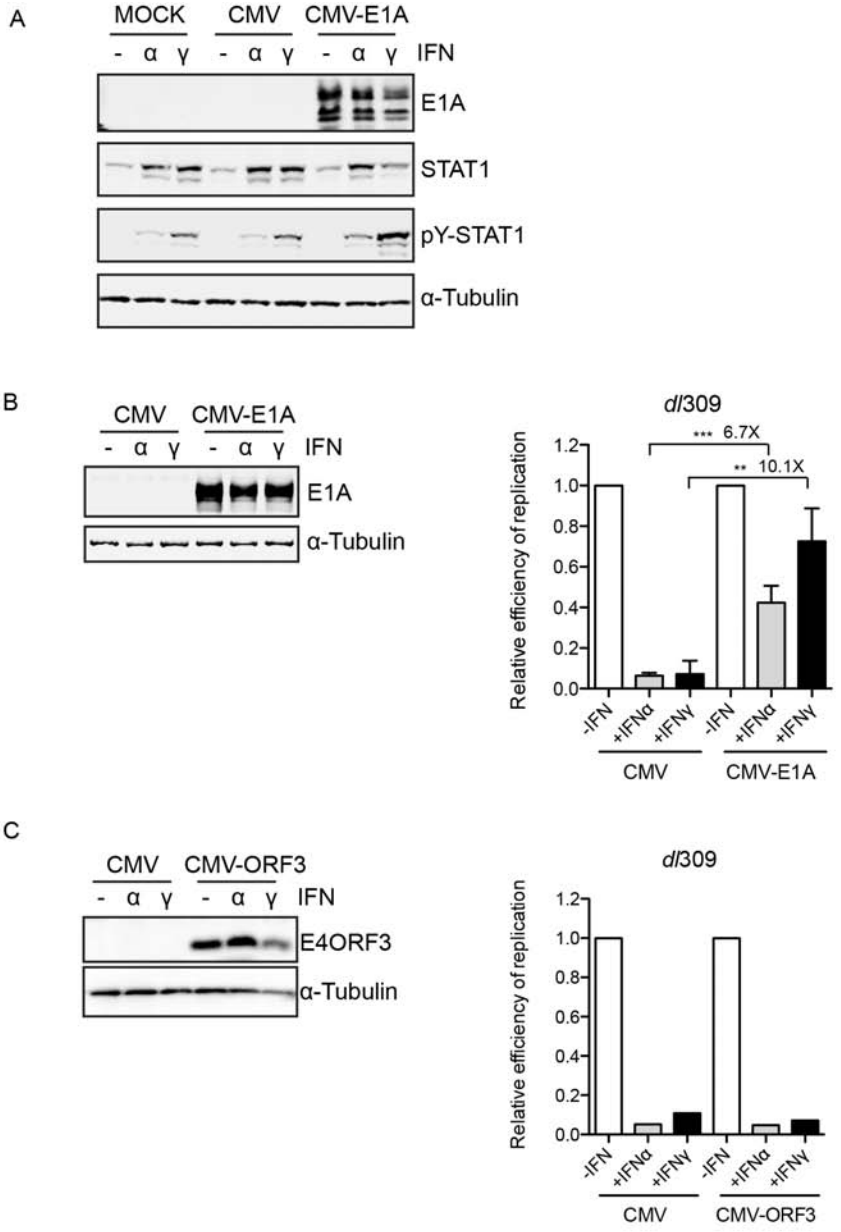

Figure 3-8. Transient expression of E1A gene rescued Ad replication in the presence of IFNs.
(A) HDF-TERT cells were infected with *in*340-Δ2-CMV or *in*340-Δ2-CMV-E1A viruses at 5,000 particles/cell for 1 hr and subsequently treated with IFNα, IFNγ or left untreated. Cellular extracts were prepared at 24 hr post-treatment and analyzed by Western blot using antibodies against E1A, STAT1 and STAT1 (pY701). α-tubulin is shown in the bottom panel as a loading control for the samples.
(B) HDF-TERT cells were infected and treated as in (A) and super-infected with *dl*309 at 200 particles/cell 24 hr after the addition of IFNs. *dl*309 DNA replication was quantified 48 hr post-infection by qPCR using a *dl*309-specific primer pair. The values were normalized to 1.0 in untreated cells and are plotted as mean ± sd, n=3 (** $P \leq 0.01$, *** $P \leq 0.001$).
(C) Experiment was performed as described in (B), except HDF-TERT cells were infected with *in*340-Δ2-CMV-E4-ORF3 virus.

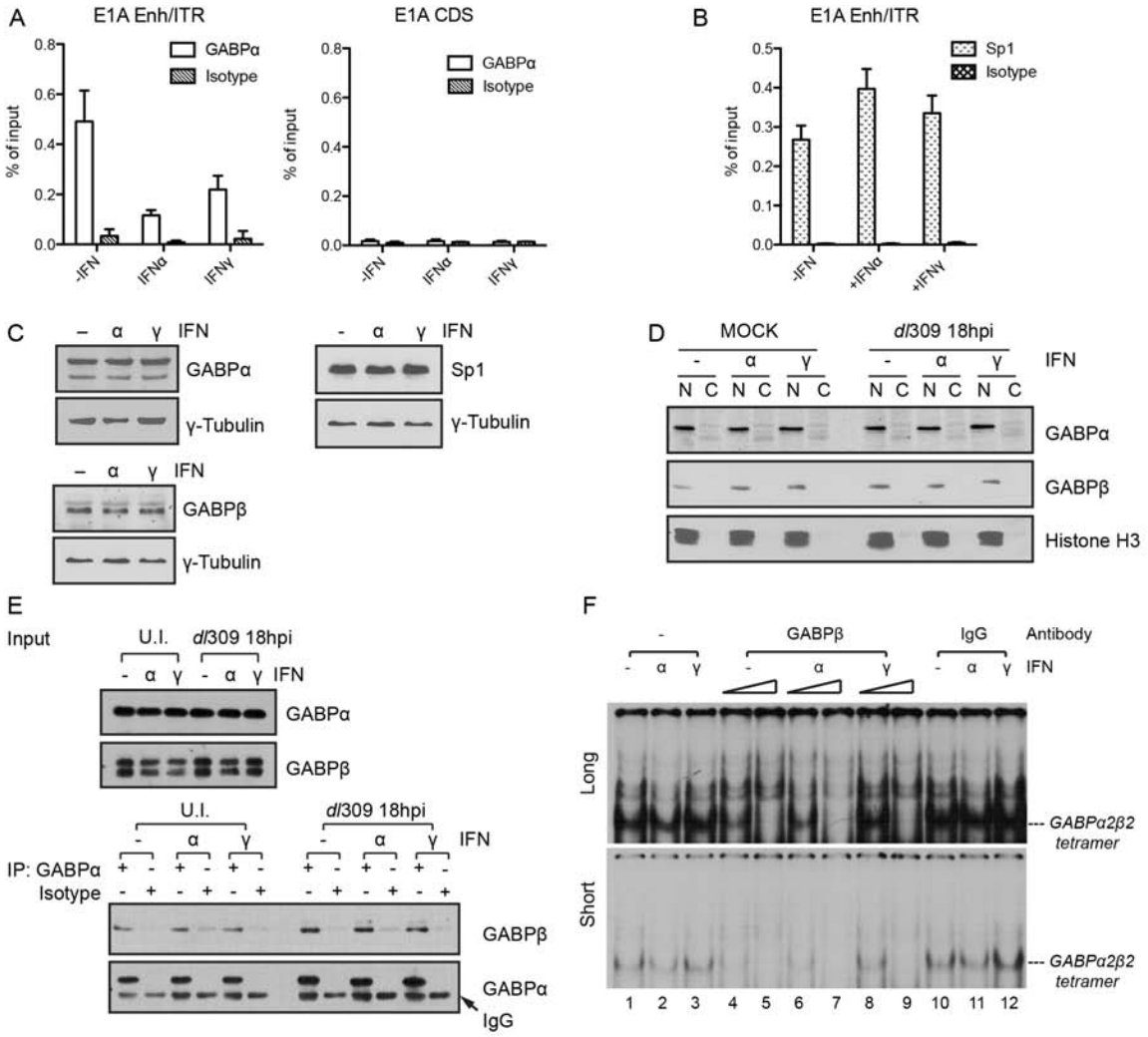

Figure 3-9. IFNs inhibit the association of transcription factor GABP with the E1A enhancer region.
(A and B) HDF-TERT cells were treated with IFNα, IFNγ or left untreated for 24 hr and then infected with *dl*309 at 200 particles/cell. ChIP assays were performed with samples preparedd at 18 hr post-infection using an antibody directed against GABPα or an isotype-matched control (A), or using an antibody directed against Sp1 or an isotype-matched control (B). Immunoprecipited DNA was quantified by qPCR and the enrichment is represented as percentage of input. The values are plotted as mean ± sd, n=3.
(C) HDF-TERT cells were treated with IFNα or IFNγ or left untreated. Cellular extracts were prepared at 24 hr post-treatment and analyzed by Western blot using antibodies directed against GABPα and GABPβ. γ-tubulin was used as a loading control for the samples.
(D) HDF-TERT cells were treated with IFNα, IFNγ or left untreated for 24 hr and then infected with *dl*309 200 particles/cell or mock-infected. Nuclear (N) and cytoplasmic (C) fractions were prepared at 18 hr post-infection. Western blot analyses were performed using antibodies against GABPα and GABPβ. Histone H3 was used a nuclear marker to verify the subcellular fractionation.
(E) IFN treatment and infection of HDF-TERT cells was carried out as described in (D). Total cell extracts were isolated at 18 hr post-infection and used for immunoprecipitation (IP) with an antibody against GABPα or an isotype-matched control. Immunocomplexes were analyzed for GABPβ coIP by Western blot. The top panel shows GABPα and GABPβ protein levels in cell lysates (Input). The bottom panel shows the results of the IPs.
(F) EMSA binding reactions were peformed using a ^{32}P-labeled GABP probe, 4 ug of nuclear extract prepared from IFN-treated or -untreated HDF-TERT cells and 0.2 ug (lane 4, 6 and 8) or 1 ug (lane 5, 7 and 9) GABPβ antibody, 0.2 ug of rabbit IgG (lane 10 to 12) or no Ab (lane 1-3).

dimerization domains of the GABPα (141). Western blot analysis demonstrated that expression of both GABPα and GABP β in IFN-treated cells was the same as that found in the untreated cells (Figure 3-9C). The Hippo pathway promotes the phosphorylation of GABPβ, causing the inhibition of GABPβ homodimerization and nuclear localization (142). In HDF-TERT cells, GABPα and β were primarily nuclear localized, and their localization were not altered by either IFNα or IFNγ (Figure 3-9D). Finally, I performed coimmunoprecipitation assays to determine if IFNs impaired endogenous GABPα:GABPβ interaction. These results did not reveal any differences in IFN-treated cells (Figure 3-9E). I also carried out EMSA to access the binding of GABP to the E1A enhancer region *in vitro*. A ^{32}P labeled the probe of GABP binding site was incubated with nuclear extract from IFN-treated and -untreated HDF-TERT cells. The GABP tetramer complex was detected by supershift using an antibody against GABPβ. A similar amount of GABP:DNA complex was observed in IFN-treated and -untreated cells (Figure 3-9F). This suggested that IFNs only prevent the recruitment of GABP to the E1A enhancer *in vivo*, but not *in vitro*.

The cellular transcription factor Sp1 also binds to several sites in the Ad5 inverted terminal repeat (ITR) (149) that are adjacent to the E1A enhancer region. I analyzed if Sp1 binding to the ITR was altered by IFN signaling *in vivo*. Sp1 bound to the Ad5 ITR at similar levels in the presence and absence of IFNs (Figure 3-9B). This result suggests that reduced binding of GABP to the E1A enhancer following IFN treatment is target-specific and not due to reduced global accessibility of the left end of the Ad5 genome.

3.3.5 PML-NBs are not Required for IFN-mediated E1A Repression

PML-NBs play important roles in intrinsic and IFN-mediated immunity against various viruses (117). Three major components of PML-NB are PML, Daxx and Sp100.

Our laboratory previously reported that PML and Daxx, but not Sp100, mediated IFN-induced antiviral response in the context of Ad infection (47). Thus, we analyzed if PML-NBs participate in repression of Ad replication and E1A expression following IFN treatment. I generated a series of PML, Daxx, and Sp100 knockdown HDF-TERT cell lines using shRNA expression. The knockdown efficiency of individual target genes was accessed by Western blot. PML and Sp100 protein levels were completed depleted in the corresponding knockdown cells, and Daxx expression was completely depleted in two out of four shDaxx-cells and significantly reduced in the other two lines; normal levels of all three proteins were found in cells expressing control shRNA (Figure 3-10A). The integrity of PML-NBs was analyzed using an immunofluorescence assay. As shown in Figure 3-10A, depletion of PML protein completely disrupted PML-NBs structure. With the loss of Sp100 and Daxx proteins, PML-NBs were still intact. Replication of *dl*309 and *in*ORF3 was inhibited by both IFNα and IFNγ in single knockdown cells, as well as the control cells, despite high MOI infection (Figure 3-10C). RT-qPCR confirmed that E1A mRNA levels were correspondingly reduced (data not shown).

A recent study revealed that PML, Daxx and Sp100 have synergistic effects on the suppression of HSV-1 replication with greater effects of multiple knockdown compared to single knockdown (105). Thus, knockdown of individual PML-NB proteins might not be sufficient to prevent IFN-induced repression. Next, I generated HDF-TERT cells in which two or three PML-NB proteins were simultaneously depleted (Daxx plus PML, shDP, PML plus Sp100, shPS, and all three protein, shDPS). Western blot analysis showed that each targeted protein was thoroughly depleted in the corresponding knockdown cells (Figure 3-11A). When both PML and Sp100 proteins were depleted (shPS and shDPS), PML-NBs were completely disrupted and absent in immunofluorescent staining. In shDP cells, Sp100 protein formed a punctate structure that is similar to PML-NBs, but they did not distribute uniformly (Figure 3-11B). A

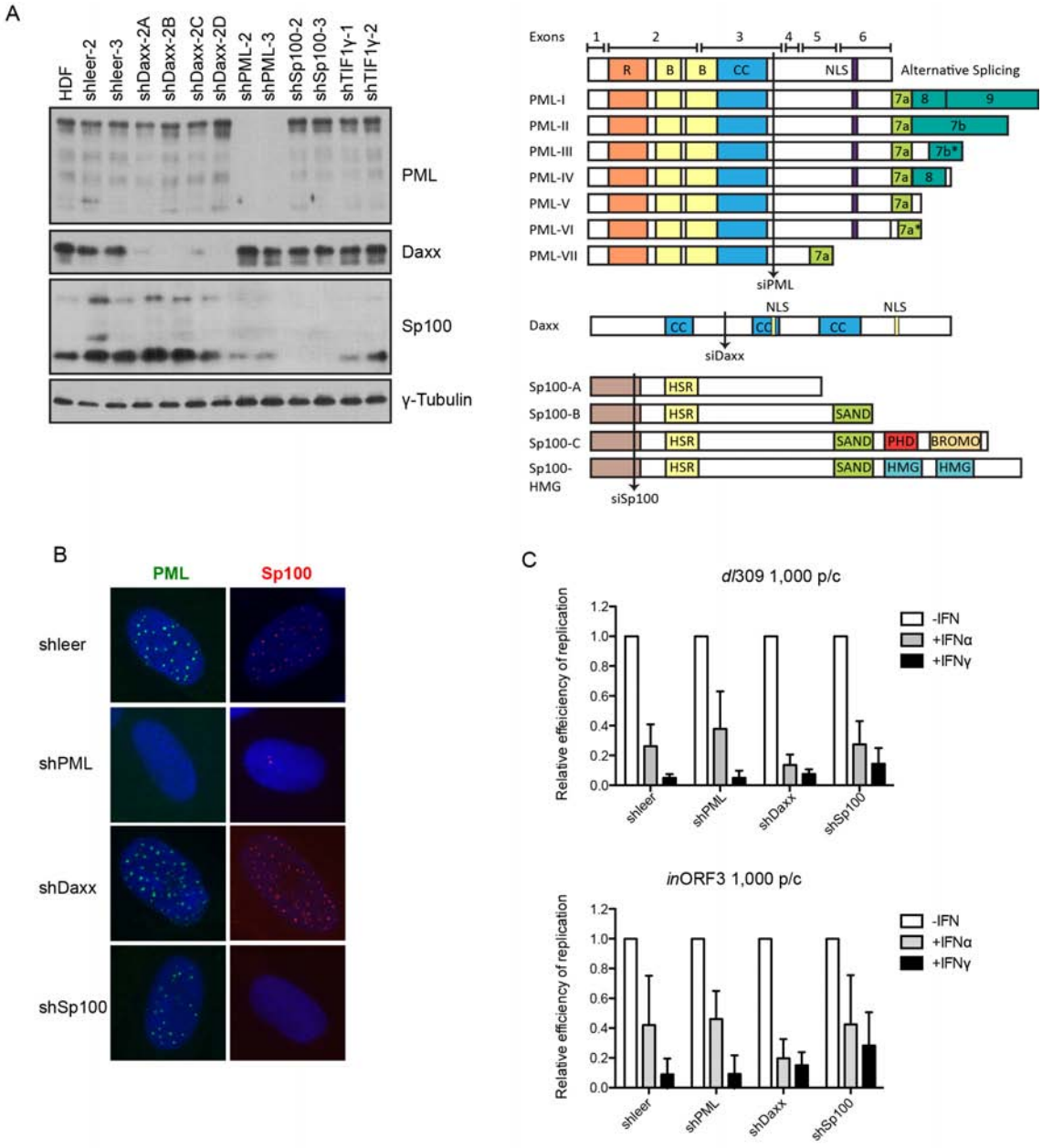

Figure 3-10. Single depletion of PML-NB components does not rescue Ad5 replication in the presence of IFNs.
(A) Expression of PML, Daxx and Sp100 in single knockdown cell lines was examined by Western blot (left panel). Parental HDF-TERT cells (HDF) were used along with different individual knockdown subclones corresponding to control shRNA (shleer) and shRNAs targeting Daxx, PML and Sp100. Domain structures of PML, Daxx and Sp100 are shown at the right panel. Arrows indicate the target sequence of shRNA.
(B) Single-knockdown cells were seeded on cover slips, and immunofluorescence assay was performed using antibodies against PML (green) and Sp100 (red). DAPI (blue) was used to stain nuclear DNA.
(C) Single-knockdown cell lines were infected with *dl*309 or *in*ORF3 at 1,000 particles/cell and viral DNA replication was quantified by qPCR at 48 hr post-infection. Viral DNA replication was plotted as mean ± sd. n=4.

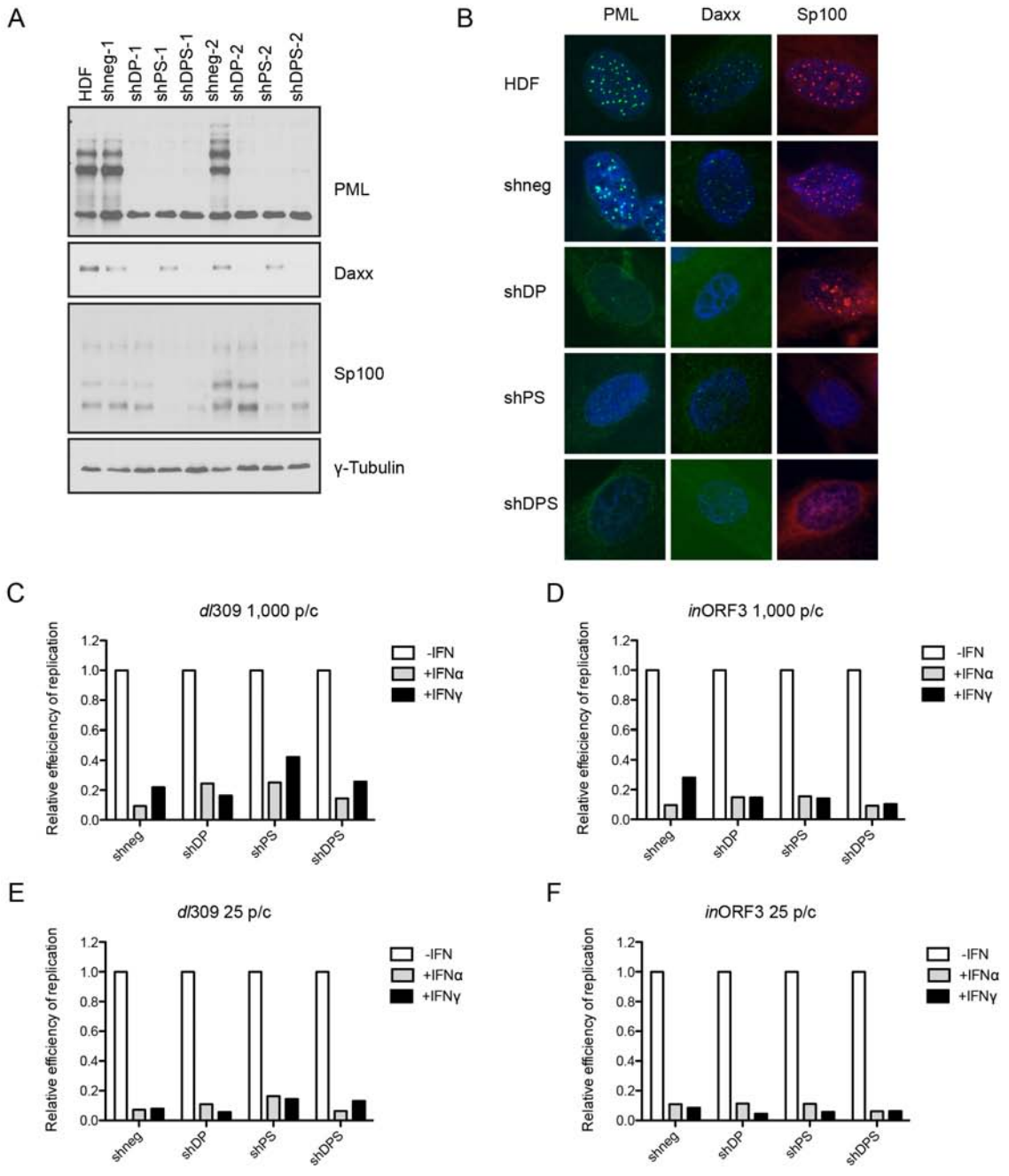

Figure 3-11. Double and triple depletion of PML-NB components does not rescue Ad5 replication by IFNs.
(A) Expression of PML, Daxx and Sp100 in knockdown cell lines was examined by Western blot. Parental HDF-TERT cells (HDF) were used along with pools of cells expressing control shRNA (shneg) and shRNAs targeting Daxx and PML (shDP), PML and Sp100 (shPS), and all thre proteins (shDPS).
(B) Double- and triple-knockdown cells were seeded on cover slips, and immunofluorescence assay was performed using antibodies against PML, Daxx and Sp100. DAPI (blue) was used to staining nuclear DNA.
(C to F) Knockdown cell lines were infected with *dl*309 (C and E) or *in*ORF3 (D and F) and viral DNA replication was quantified by qPCR at 48 hr post-infection.

possible explanation is that trace amount of PML protein serves as the nucleator to recruit SUMOylated Sp100 protein forming a PML-NB-like structure. However, IFNs still repressed *dl*309 and *in*ORF3 replication in these double- and triple-knockdown cells to the same extent as with parental or control knockdown cells (Figure 3-11C).

In all of the experiments carried out in HDF-TERT cells, *dl*309 and *in*ORF3 behaved identically in response to IFNα and IFNγ, and depletion of all three component of PML-NBs was still not able to rescue *in*ORF3 replication. Moreover, transient expression of E4-ORF3 protein in HDF-TERT cells did not affect *dl*309 replication in the presence of IFNs (Figure 3-8C). Thus, I conclude that PML-NBs are not involved in, or only play a minor role in, the IFN-induced anti-Ad response in normal human cells.

3.3.6 IFNs do not Compromise the Chromatinization Process at the Early Stage of Infection

Incoming Ad genomes undergo a chromatinization process, by which VII protein dissociates from Ad DNA, and cellular histones are loaded to Ad DNA (150). Formation of this chromatin-like structure is required for activation of viral early genes. To evaluate the overall structure of input viral genomes at the early phase of infection, HDF-TERT cells were infected with replication deficient virus ΔTP-GFP in the presence or absence of IFNs, and chromatin accessibility was determined at 18 hr post-infection by micrococcal nuclease (MNase) digestion. DNA fragments were detected by the Southern blot using a ^{32}P-labeled Ad genome DNA probe. The periodic oligomeric array pattern (150) was observed in both IFN-treated and -untreated cells (Figure 3-12A). The nucleosome-like structure of input viral genomes had a longer spacer compared with the bulk cellular nucleosome detected using ethidium bromide staining (Figure 3-12A). At 18 hr post-infection, there were similar levels of cellular histone H3 associated with the E1A enhancer region in IFN-treated and -untreated HDF-TERT cells as analyzed by ChIP

(Figure 3-12B). Two-fold more VII protein accumulated at the E1A enhancer region in IFN-treated cells compared to untreated cells (Figure 3-12B). The function of protein VII in regulating early gene transcription is controversial. Previous study suggested that VII condenses viral genome and repress gene transcription, but it also has been shown that VII is required for activation of early genes (30, 34, 151). Moreover, those experiments were conducted at the early phase when all of early promoters has been activated, but not at the immediate early stage that is before E1A transcription occurs. Thus, I could not conclude that increased level of VII protein in the E1A enhancer region causes inhibition of E1A transcription in IFN-treated cells.

In addition to triggering the formation of STAT transcription complexes, IFNs can also regulate target gene expression by altering the epigenetic signature at ISG promoters (152). This prompted me to examine the enrichment of different epigenetic markers at the E1A promoter region plus and minus IFN treatment. Acetylation of histone H3 at lysine 9 (H3K9Ac) and tri-methylation of histone H3 at lysine 4 (H3K4me3) are markers of active transcription, while tri-methylation of histone H3 at lysine 9 (H3K9me3) and lysine 27 (H3K27me3) are markers for repressed transcription (153). I tested the enrichment of these four histone marks at the E1A enhancer, transcription start site (TSS), as well as the coding region (CDS) (Figure 3-13A). I did observe a slight increase in repressive histone marks at the E1A enhancer in IFN-treated cells. However, there was also a slight enhancement of the activtion mark H3K4me3 at the same region. IFNs did not significantly change the H3K4me3 and H3K9me3 protein levels (Figure 3-13B).

Histone H3 has three very similar variants H3.1, H3.2 and H3.3 (154). Histone H3.1 and H3.2 are primarily expressed at the S-phase and incorporated into nucleosomes during DNA synthesis (155, 156). H3.3 is a non-canonical histone H3 variant that is expressed throughout the cell cycle. Histone H3.3 is deposited at

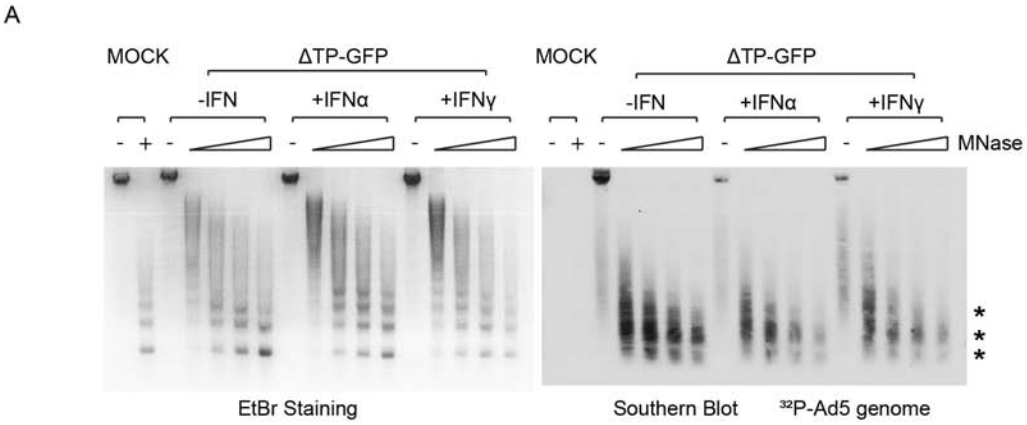

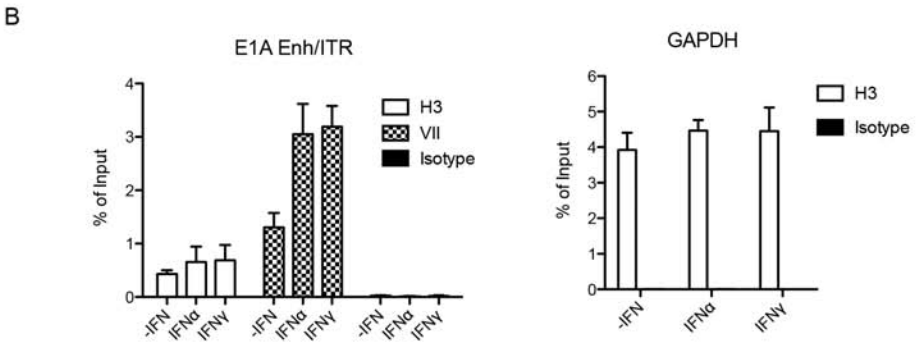

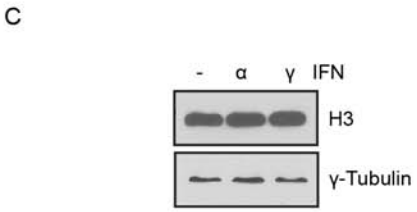

Figure 3-12. Chromatin structure of input Ad genome during the early infection.
(A) IFNα/γ-treated, and -untreated HDF-TERT cells were infected with ΔTP-GFP virus at 5,000 particles/cell, or mock-infected. Nuclei were prepared at 18 hr post-infection followed by incubation with micrococcal nuclease for 10, 20, 30 or 45 min at room temperature. Purified DNA fragments were separated on 1.5% agarose gel, stained with ethidium bromide (EtBr, left) first, and then transferred to a nylon membrane. Southern blot detection was performed using a ^{32}P-labeled Ad5 genome DNA probe.
(B) Enrichment of hisonte H3 and VII protein at the E1A enhancer region. IFNα/γ-treated and -untreated HDF cells were infected with *dl*309 at 200 virus particles/cell. At 18 hr post-infection, ChIP assay was performed using antibodies against tHistone H3 or VII protein. Precipitated DNA was quantified by qPCR using oligonucleotides that detect E1A enhancer or cellular GAPDH gene.
(C) HDF-TERT cells were incubated with IFNα or IFNγ for 24 hr, Histone H3 protein level is analyzed by Western blot.

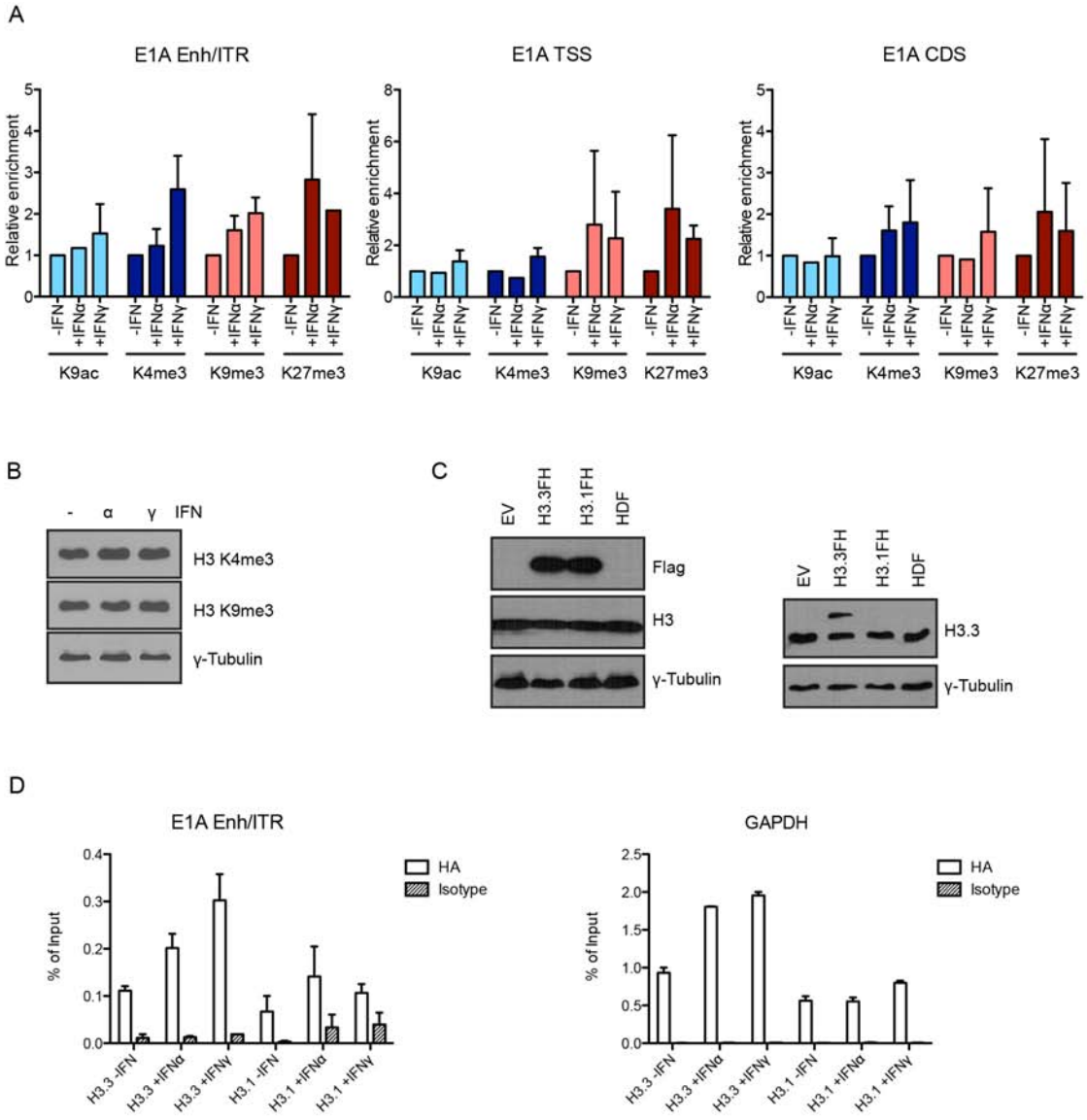

Figure 3-13. Accumulation of histone H3 at the E1A enhancer region.
(A) HDF-TERT cells were treated with IFNs or left untreated for 24 hr and then infected with *dl*309 at 200 particles/cell. ChIP assays were performed with samples prepared at 18 hr post-infection using antibodies against H3K9ac, H3K9me4, H3K27me3 and an isotype-mathched control. Results are presented as relative enrichment compard to IFN-untreated sample.
(B) HDF-TERT cells were incubated with IFNα and IFNγ for 24 hr. Expression of H3 K4me3 and H3 K9me3 were analyzed by Western blot. γ-Tubulin was used as a loading control for the samples.
(C) HDF-TERT cells transduced with Flag/HA-tagged H3.1 (H3.1FH), H3.3 (H3.3FH) or empty vector (EV), along with partent cells (HDF), were treated with IFNα, IFNγ, or left untreated for 24 hr. Expression of each histone H3 variant was analyzed by Western blot.
(D) ChIP assay was perferemed as described in A, and anti-HA antibody was used for immunoprecipitation.

chromatin in replication-dependent and replication-independent manner (156)and marks active chromatin(157). A recent study revealed that H3.3 was associated with the Ad genome at the early stage of infection (29). Thus, I want to know whether IFNα and IFNγ prevented the deposition of H3.3. I generated two HDF-TERT-derived cell lines that stably express HA/Flag-tagged H3.1 or H3.3 at their C-terminus. Western blot showed that tagged H3.1 and H3.3 were expressed at similar levels as determined using anti-Flag antibody (Figure 3-13C), and the expression level of tagged-H3.3 was comparable to endogenous H3.3 (Figure 3-13C, left). ChIP experiments showed that there was relatively more H3.3 associated with the E1A enhancer region compared to H3.1 at 18 hr post-infection following IFN treatment (Figure 3-13D). IFN treatment also slightly increased the enrichment of H3.3 at the cellular GAPDH gene, suggesting this increase is probably due to sample variability. More importantly, this observation opposes the hypothesis stated above that IFNs inhibit E1A expression by altering chromatin structure.

3.4 Discussion

For decades, the regulation of Ad replication by innate and adaptive immunity was poorly understood. This is largely due to the lack of a good animal model and utilizing cancer cell lines to study viral replication in tissue culture. It is known that Ads evolved several means to antagonize IFN signaling. As a result, Ad infection is resistant to IFN treatment in multiple established cancer cell lines. Here, I demonstrate that type I and type II IFN signaling leads to the repression of both WT Ad5 and E4-ORF3 mutant immediate early gene expression in normal human cells, NHBEC and HDF-TERT cells. This reduction in E1A expression leads to suppression of all subsequent aspects of the viral life cycle. Complementation by expression of the E1A transactivation protein reversed the inhibitory effects of IFN signaling on Ad replication demonstrating that this is the sole viral defect in IFN-treated cells. In previous experiments, IFNα caused a

modest reduction in Ad5 E1A and DBP expression and an approximate 5 to 8- fold reduction in viral replication and virus yield in Ad5-infected human foreskin fibroblasts and NHBEC (115). The mechanism of IFNα activity was not determined. We attribute differences in these assays to the profound effects of IFNs in our studies to differences in infection multiplicity and IFNα concentration since other aspects of these analyses were very similar.

I consistently detect a two-fold reduction of *in*ORF3 viral replication and early gene expression in HDF-TERT cells compared to WT *dl*309, which agrees with the observation in cancer cell lines reported previously (Figures 3-3, 3-4 and data not shown)(158). IFNα and IFNγ did exhibit stronger inhibition of *in*ORF3 virus yield compared to *dl*309. This suggests that E4-ORF3 might have a novel function at the later stage of infection. However, generally speaking, *dl*309 and *in*ORF3 exhibited nearly identical phenotypes in HDF-TERT cells. Moreover, transient expression of E4-ORF3 protein did not enhance *dl*309 replication in IFN-treated samples (Figure 3-8C), and knockdown of PML-NB proteins did not rescue *in*ORF3 replication (Figures 3-10 and 3-11). Collectively, I conclude that in normal human cells, E4-ORF3 only has negligible effects on counteracting IFN signaling.

In this chapter, I also showed that repressed E1A expression is correlated with decreased enrichment of GABP at the E1A enhancer region *in vivo* in IFNα- and IFNγ-treated cells. Micrococcal nuclease and ChIP assays indicated that IFNs did not impede the deposition of cellular histone H3 and assembly of the viral genome into a chromatin-like structure at the immediate early stage of infection. It suggests that inhibition of GABP binding to the E1A enhancer by IFNs was irrelevant to the overall accessibility of the Ad genome.

PML-NBs have established intrinsic and IFN-induced activity against many herpesviruses (159, 160) which prompted me to examine if resident PML-NB proteins

Daxx, PML or Sp100 inhibited Ad replication in HDF-TERT cells, plus or minus IFN signaling. These activities were knocked-down individually and combinatorially using shRNAs. Depletion of these proteins singly or in combination did not alter the inhibitory effect of IFNs on Ad replication in a significant manner (Figure 3-10 and 3-11). There was some variation among the cell lines on Ad5 infection minus IFN that we attribute to clonal variation. The lack of effect of these proteins on Ad replication, plus or minus IFN signaling, in comparison to herpesviruses may reflect the nature of the viral genomes within the virus particle. Herpesviruses contain naked viral DNA that may be easily recognized by cellular pattern recognition receptors to trigger IFN signaling and suppress virus infection (161). In contrast, the Ad genome is coated by a histone-like core protein that may protect the genome from such recognition (162). Consistent with this idea, our lab previously showed that Ad core protein VII protects the viral genome from recognition by the DNA damage machinery (28). Thus, Ad may be resistant to the effects of PML-NBs in specific contexts.

Primary human cells, e.g. NHBEC, are difficult to obtain, and costly to maintain in culture. There is also considerable variation in population and preparations. HDF-TERT cells have many advantages in the Ad study. HDF-TERT cells were immortalized by human telomerase and maintained more characteristics of primary cells compared to the cells that were immortalized by viral oncogenes. Despite high particle:PFU ratio of Ad in HDF-TERT cells compared to that in A549, HDF-TERT cells are permissive to Ad infection and yield similar level ($>10^9$ PFU/ml) of infectious particles as A549 cells. In addition to IFN studies, HDF-TERT cells were also suitable for the studying the early events of Ad infection, since Ad has a prolonged life cycle in those cells. For instance, Ad particles take 6 hr to reach the nucleus ($\leq$45 min in epithelial cells), and potentially we can utilize HDF-TERT cells to study individual steps of virus cytoplasmic trafficking in

more precise time frames. I established a novel system to study Ad infection in the context of its natural host cells.

Chapter 4 The Role of IFNs in Establishment of Adenovirus Persistent Infection

4.1 Introduction

4.1.1 E2F/Rb Family Proteins, Cell Cycle Control and Adenovirus

It is well accepted that cancer cells have a characteristic feature of dysregulated proliferation control. The crucial factor in cell cycle control is linked to the retinoblastoma (Rb), a tumor suppressor that governs the G1/S transition to prevent unrestrained S-phase entry. Rb exerts its antiproliferation effects by regulating the expression of genes that are required for DNA replication and mitosis via the E2F family of transcription factors (130, 131, 163). Typically Rb protein remains in an inactive, hypophosphorylated state, which binds the transactivation domain of E2F to repress E2F target gene expression. Upon the activation of cyclin-dependent kinase 4 (CDK4) and CKD6 by cyclin D, CDK4/6 initiates the phosphorylation of Rb, and continued by CDK2, resulting in the hyperphosphorylation of Rb through S-phase and mitosis. Hyperphosphorylated Rb dissociates from E2F-Rb complexes, which results in the relief the repression of E2F target genes. When cell cycle progresses to the M/G0 transition, Rb is dephosphorylated by phosphatases and returns to the hypophosphorylated state that forms the complex with E2F proteins and represses E2F target gene expression. The aberration of the Rb–E2F pathway is frequently found in cancer, including Rb mutations, overexpression of CDK4, and loss of the CDK4 inhibitor $p16^{INK4A}$, which agrees with the essential role of Rb in regulating G1/S transition (131, 164). There are eight different E2F proteins, E2F-1 to E2F-8; E2F-6, E2F-7 and E2F-8 do not a contain transcriptional activation domain and Rb family (pocket protein) binding domains. E2Fs form heterodimers with DP proteins,

which stabilize E2F-DNA interaction and stimulate target gene expression. The transcription activities of E2Fs are suppressed by pocket proteins, including Rb and two Rb-like proteins, p107 and p130. E2F-1, E2F-2 and E2F-3 preferentially interact with Rb, while E2F-4 and E2F-5 interact with p107 and p130.

Virus infection also involves deregulation of Rb function and drives S-phase entry, to make the cellular environment preferable for viral replication. The Ad E1A protein is one of the well-characterized viral oncogenes. E1A directly interacts with Rb at the E2F-interaction domain, and displaces Rb from E2Fs. This also occurs with pocket proteins p107 and p130. As mentioned in Chapter 1, E2F binds to two distinct E2F binding sites in the E1A enhancer region *in vitro*, but the deletion of both E2F sites does not influence E1A expression in Hela cells. It is still unclear whether E2Fs or E2F/pocket proteins are associated with the E1A enhancer *in vivo*. The Ad E2 promoter also contains an inverted E2F binding site. Induction of E2F binding to the E2 promoter *in vitro* is correlated with transcription activation of this promoter *in vivo* (165-170).

4.1.2 Adenovirus Latency

Primary Ad infection occurs in the epithelial cells of the nasopharyngeal mucosa, producing progeny virus, followed by a latent infection in the mucosa-associated lymphoid tissue. Previous studies demonstrated that T lymphocytes at tonsil and adenoid tissue are the primary reservoir for latent adenovirus (171, 172) which is defined as cells harbor Ad genome, but very little infectious virus and hexon are produced. Disseminated Ad infection can cause significant morbidity and mortality in immunocompromised individuals and transplantation recipients, which is suspected to originate from latent Ad infection. Currently, little is known about the mechanism of Ad latency and reactivation. So far, there are only two independent studies attempting to model Ad latency/persistence *in vitro*. The fate of Ad infection of lymphocyte cell lines is

cell type-dependent and serotype-dependent. In the Jurkat cell line, Ad5 entered a lytic life cycle, characterized by high progeny virus titer and cell lysis (173, 174). In contrast, Ad5 established true latency in BJAB cells, a Burkitt lymphoma cell line, which is defined as a high frequency of Ad5 positive cells, but very low amount of progeny virus production and viral gene expression. The persistent infection model was also obtained in Ramos, a Burkitt's lymphoma cell line, and KE37, a T cell lymphoma cell line, which produce a high level of viral genomes and intermediate levels of viral proteins.

4.2 Specific Aims and Significance

In the last chapter, I showed that IFNα and IFNγ block the recruitment of GABP to the E1A enhancer without altering Ad genome chromatin structure. IFNs may also induce the binding of a transcriptional repressor(s) to the E1A enhancer to inhibit E1A transcription. In this chapter, I aimed to identify a *cis* element that negatively regulates E1A expression in response to IFN signaling. I also wanted to explore the role of IFNs in the establishment of Ad persistent infection.

By screening a series of viruses containing mutations at the left end of Ad5 genome, I discovered that the repression of E1A expression by IFNs requires the E2F binding site at Ad nt 280, and this E2F site is conserved among primate Ads. I also established an Ad persistent infection model *in vitro* and demonstrated that IFNγ suppresses productive Ad replication in a manner dependent on the conserved E2F binding site in the E1A enhancer. By comparing the properties of wild-type and E2F site mutant viruses, I show that the IFN–E2F/Rb axis is critical for restriction of Ad replication to promote persistent viral infection. These results reveal a novel mechanism by which adenoviruses utilize IFN signaling to inhibit virus replication to promote persistent infection in the host.

4.3 Results

4.3.1. IFN Signaling Inhibits E1A Expression via a *Cis*-acting Repressor Element

I hypothesized that IFNs might induce the binding of a transcriptional repressor to the E1A promoter/enhancer region. To address this question, I examined the effect of IFNs on E1A expression using a panel of existing (97, 98, 133) and newly created E1A enhancer region mutants (Figures 4-1A and 4-1B). The E1A enhancer overlapped with viral packaging sequences and introducing a deletion in the E1A enhancer causes a defect in encapsidation. *in*340 virus, and its derivatives, contain packaging sequences at the right-end of viral genome to ensure efficient packaging. E1A expression of deletion mutant *in*340-B1, but not of the adjacent deletion mutant *in*340-A5, was completely restored in IFNγ-treated cells, and partially restored in IFNα-treated cells (Figure 4-1A). This finding indicated that an IFN-induced repressor binding site is located in the downstream half of the E1A enhancer region, corresponding to Ad5 nt 270-358. Consistent with this finding, E1A expression of *in*340-dl10 mutant, that carries the deletion of the entire sequence between the ITR and TATA box, was also resistant to IFNα and IFNγ. E1A transcription with *in*340-dl10 can be explained by transactivation by Sp1, which binds to ITR. It was also noted that basal E1A expression with mutant *in*340-B1 was significantly augmented compared to the parent virus *in*340. To identify the minimal sequences required for IFN-mediated repression, I next screened a set of mutants carrying smaller deletions within the *in*340-B1 interval of the E1A enhancer region. Interestingly, *dl*309-21 (Δ271-301) and *dl*309-Δ271/317 exhibited significantly increased basal E1A protein levels and were refractory to IFN-mediated repression. In contrast, E1A expression with the adjacent mutants *dl*309-3 (Δ288-336) and *dl*309-Δ317/358 was still fully repressed by IFN treatment (Figure 4C). I conclude that Ad5

sequences located within nt 271-288 are the target of IFN-mediated repression of E1A expression.

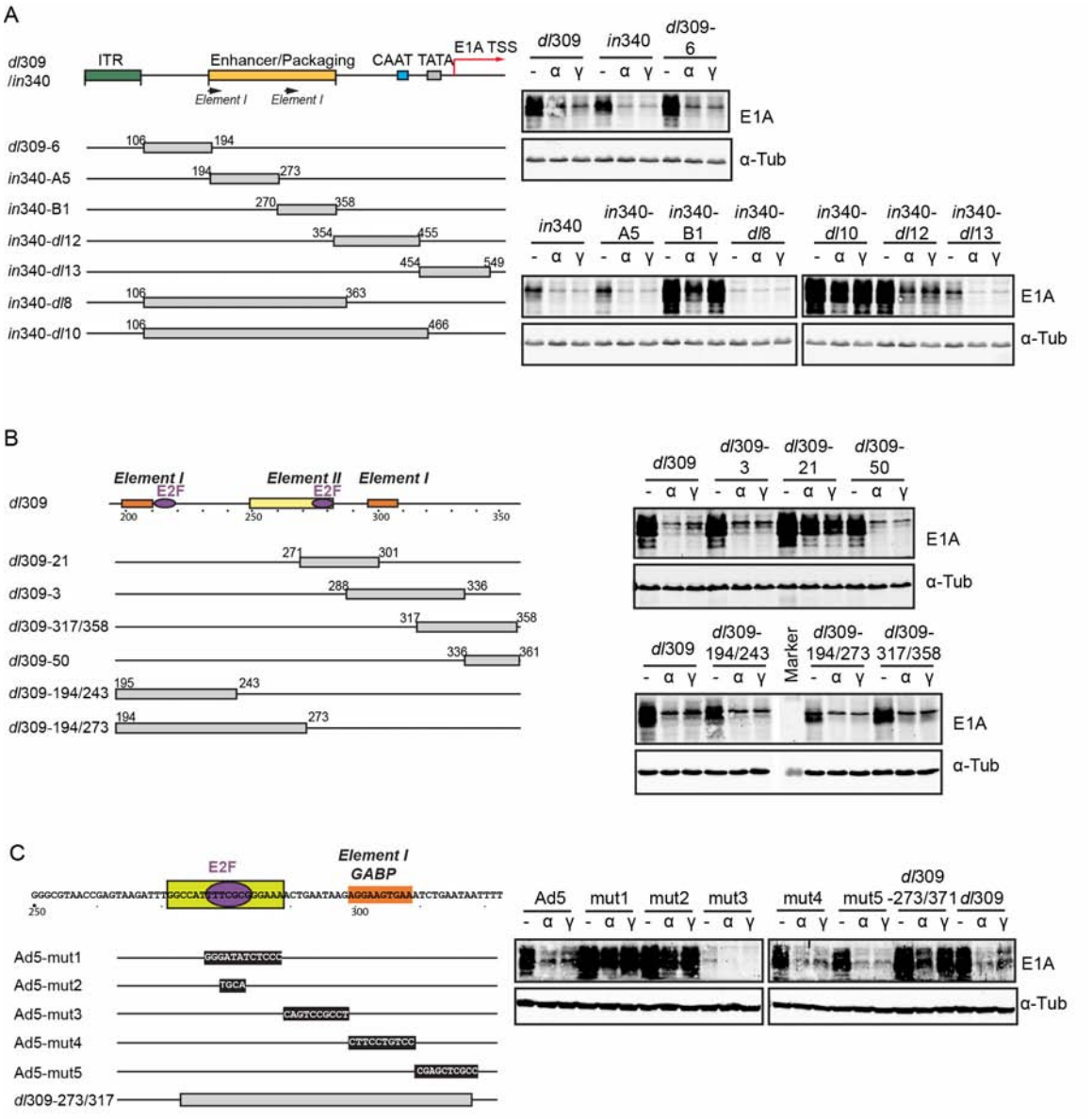

Figure 4-1. The E1A enhancer region contains a repressor element that responds to IFNs.
(A, B) Schematic view of the left end of the Ad5 genome (A) and the downstream half of the E1A enhancer (B) are shown at the left. Deletion mutants are depicted below the schematics.
(C) Schematic view of Ad nt 250-322, including E2F and GABP binding sites. The green box indicates the boundaries of the IFN-induced repressor site delimited by the deletions mutants in (A and B). Linker scanning mutants generated in this region (Ad5-mut1–mut5) are shown below the schematic. The black rectangles with letters indicate nucleotide substitutions.
HDF-TERT cells were treated with IFNα, IFNγ or left untreated for 24 hr and then infected with the mutant viruses illustrated in (A), (B) and (C), as well as the corresponding parent virus (*dl*309, *in*340 and Ad5-WT). E1A protein levels were examined at 48 hr post-infection by Western blot. α-tubulin was used as a loading control for the samples.

4.3.2 STAT6 Does Not Bind to the E1A Repressor Site in Response to IFNs

Further analysis of the 18nt repressor site (Ad5 nt 271-288) revealed that this motif contains a palindrome sequence $TTCN_{2-4}GAA$, the consensus STAT protein binding site. All STAT family proteins recognize the same palindromic core motif, but the number of nucleotides separating two half-palindromes renders the target specificity of STAT proteins. Ad nt 271-288 contains TTCGCGGGAA that be preferentially recognized by STAT6, but not other STATs (175). STAT6 is primarily associated with signaling by two cytokines, IL4 and IL13. It is also activated by the STING/TBP pathway in response to virus infection (176). STAT6 is phosphorylated upon its activation, and translocates into the nucleus to stimulate target gene expression. More importantly, STAT6 can form a complex with STAT2 in IFNα-treated B cells (177). But another study also implied that IFNγ might suppress phosphorylation of STAT6 in Th1 cells (178). HDF-TERT cells were incubated with IFNα, IFNγ, IL4 or in combination, and levels of STAT6 and phosphorylated STAT6 were determined by Western blot. Neither IFNα nor IFNγ induced STAT6 phosphorylation and expression, and IFNγ did not block the activation of STAT6 by IL4 (Figure 4-2A). EMSA experiments indicated that STAT6 indeed bound to a ^{32}P-labeled probe corresponding to Ad5 nt 271-288 using nuclear extract prepared from IL4-treated HDF-TERT cells, but not IFNγ-treated cells (Figure 4-2B). More importantly, activation of STAT6 by IL4 did not result in a reduction of *dl*309 early protein expression (Figure 4-2A, lanes 7,10 and 11). Thus, I conclude that STAT6 does not mediate IFN-induced inhibition of Ad early gene expression.

A

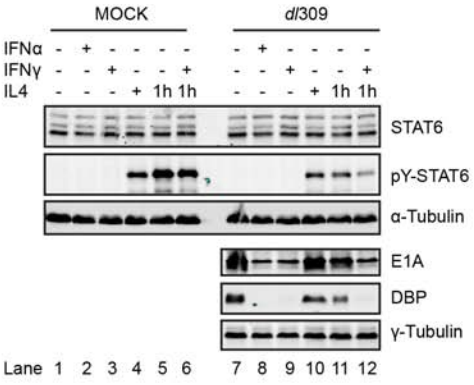

B

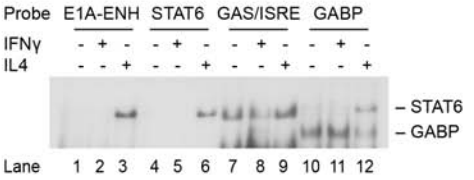

Figure 4-2. Activation of STAT6 does not inhibit early gene expression.
(A) HDF-TERT cells were treated with IFNα (lane 2 and 8), IFNγ (lane 3, 6, 9 and 12), IL4 (lane 4 and 10) or left untreated (lane 1 and 7) for 24 hr; or stimulated with IL4 for 1 hr prior to infection (lane 5, 6, 11, and 12). Cells were infected with *dl*309 at 200 virus particles/cell or mock-infected. At 48 hr post-infection, expression of STAT6, phosphorylated STAT6 and viral proteins E1A and DBP were analyzed by western blot.
(B) Nuclear extracts were prepared from HDF-TERT cells that were treated with IFNγ, IL4 or left untreated for 24 h. EMSA binding reactions were performed using 4 ug nuclear extracts and ^{32}P-labeld probes corresponding to the IFN-regulated E1A enhancer repressor element (E1A-ENH, Ad5 nt 271-288, lane 1-3) or GABP binding site (GABP, Ad5 nt 291-311, lane 10-12). ^{32}P-labeled probes of STAT6 (lane 4-6)and ISRE/GAS (lane 7-9) binding sites were used as positive controls.

4.3.3. IFN Signaling Inhibits E1A Expression via a Conserved E2F Binding Site

To further delineate the repressor target site, linker-scanning mutants were generated within this region. Mutations were introduced in the core of the nt 271-288 interval (Ad5-mut1, Ad5-mut2), in the adjacent GABP binding site (Ad5-mut4), as well as the flanking sequence (Ad5-mut3, Ad5-mut5)(Figure 4-1C). E2F/Rb family proteins bind to sequences positioned at nt 280 (TTTCGCGGGAAA) *in vitro* (135, 138). However, E1A expression in infected Hela cells was not affected by deletion of both E2F sites in the context of the intact E1A enhancer. Ad5-mut1 disrupts this entire sequence, and Ad5-mut2 disrupts the core of the E2F binding site (CGCG). Ad5-mut1 and Ad5-mut2 exhibited efficient E1A expression in the presence of IFNs, compared with Ad5-WT (Figure 4-1C). Basal E1A expression was increased with both mutants minus IFN. Ad5-mut4 and Ad5-mut5 had normal basal expression levels, and E1A expression was fully repressed by IFNs. Ad5-mut3 was defective in E1A expression due to random mutation. The compelling insensitivity of Ad5-mut2 to IFNα and IFNγ strongly suggests that E2F/Rb family protein binding to the IFN-induced repressor site mediates suppression of E1A expression.

DNA sequence alignment of the E1A enhancer regions of divergent human Ad serotypes revealed that the E2F binding site located between nt 270-290 is highly conserved (Figure 4-3A). Thus, I hypothesized that IFNs would repress viral replication of evolutionarily divergent Ads. IFN-treated and untreated HDF-TERT cells were infected with Ad3, Ad4, Ad5, Ad9, and Ad12 (subgroups B, E, C, D and A, respectively) at MOIs that resulted in similar levels of infection. DNA replication of all of these Ad serotypes was inhibited by IFNα and IFNγ treatment to different extents by both IFNα and IFNγ (Figure 4-3B). Next, I expanded the alignment to cover various Ad from different species (Figure 4-4). Overall, the E1A enhancer region is lacking DNA homology among different Ad species. But, strikingly, the DNA sequence alignment revealed that both E2F binding

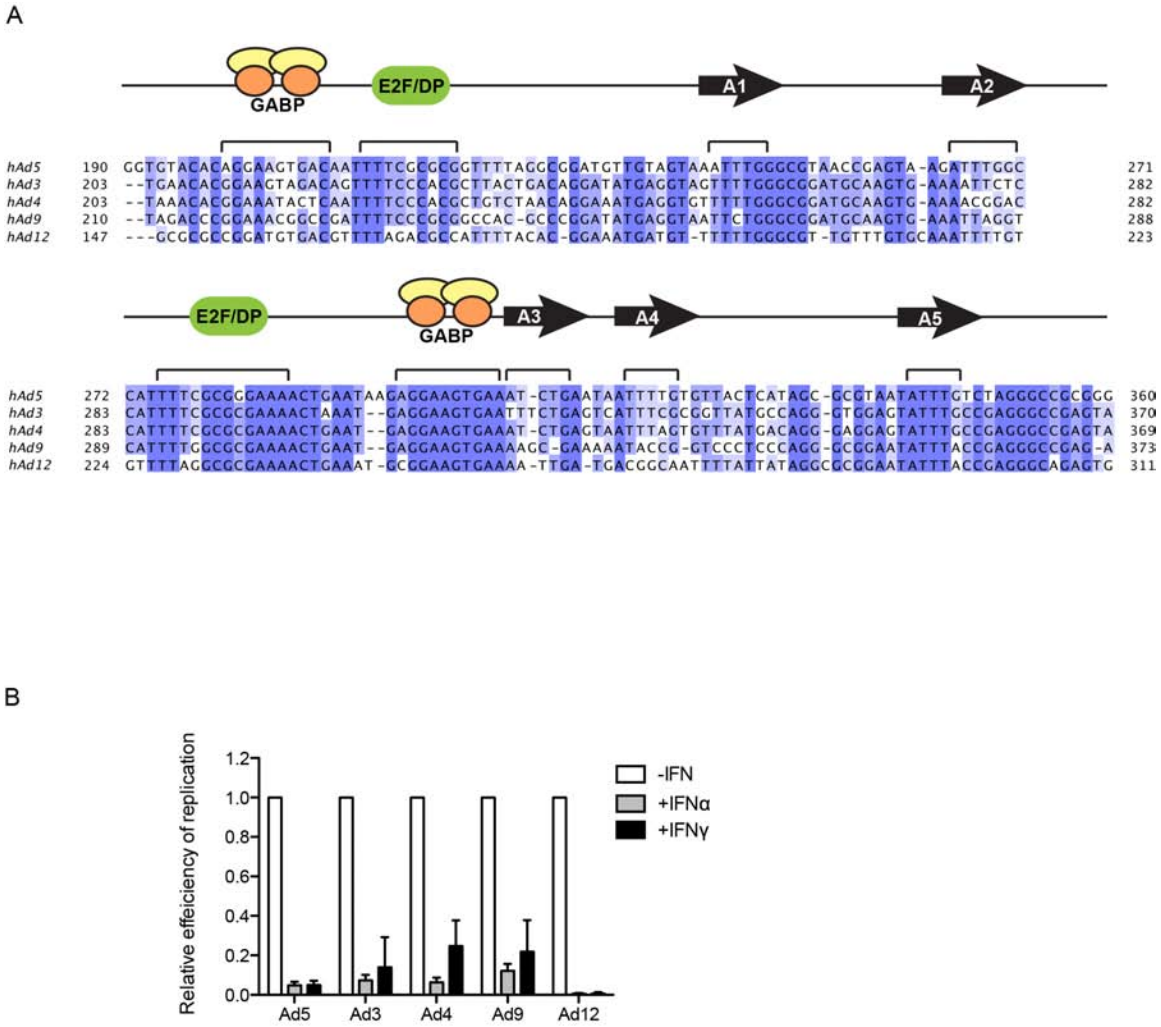

Figure 4-3. IFN Inhibition of replication is conserved among different human Ad serotypes.
(A) Nucleotide sequence alignment of the E1A enhancer regions from different Ad subgroups (serotypes Ad5, Ad3, Ad4, Ad9 and Ad12 corresponding to Ad subgroups C, B, E, D and A, respectively). Homologies (≥75% identity) are shaded in blue. The GABP and E2F binding sites, as well packaging repeats (arrowhead A1-5), are indicated.
(B) HDF-TERT cells were treated with IFNα, IFNγ or left untreated for 24 hr and then infected with 25 virus particles/cell Ad5, Ad3, Ad4, or Ad12 or 5 virus particles/cell Ad9. Nuclear DNA was isolated at 6 hr post-infection to determine virus input and at 72 hr post-infection with Ad3, Ad4, Ad9 and Ad12 or at 48 hr post-infection with Ad5 to measure replication. Viral DNA levels were quantified by qPCR using a primer that recognizes conserved sequence in E1A (AdE1A-Pan) in combination with a serotype-specific primer (Table S1). The values were normalized to 1.0 in untreated cells and are plotted as mean ± sd, n=3.

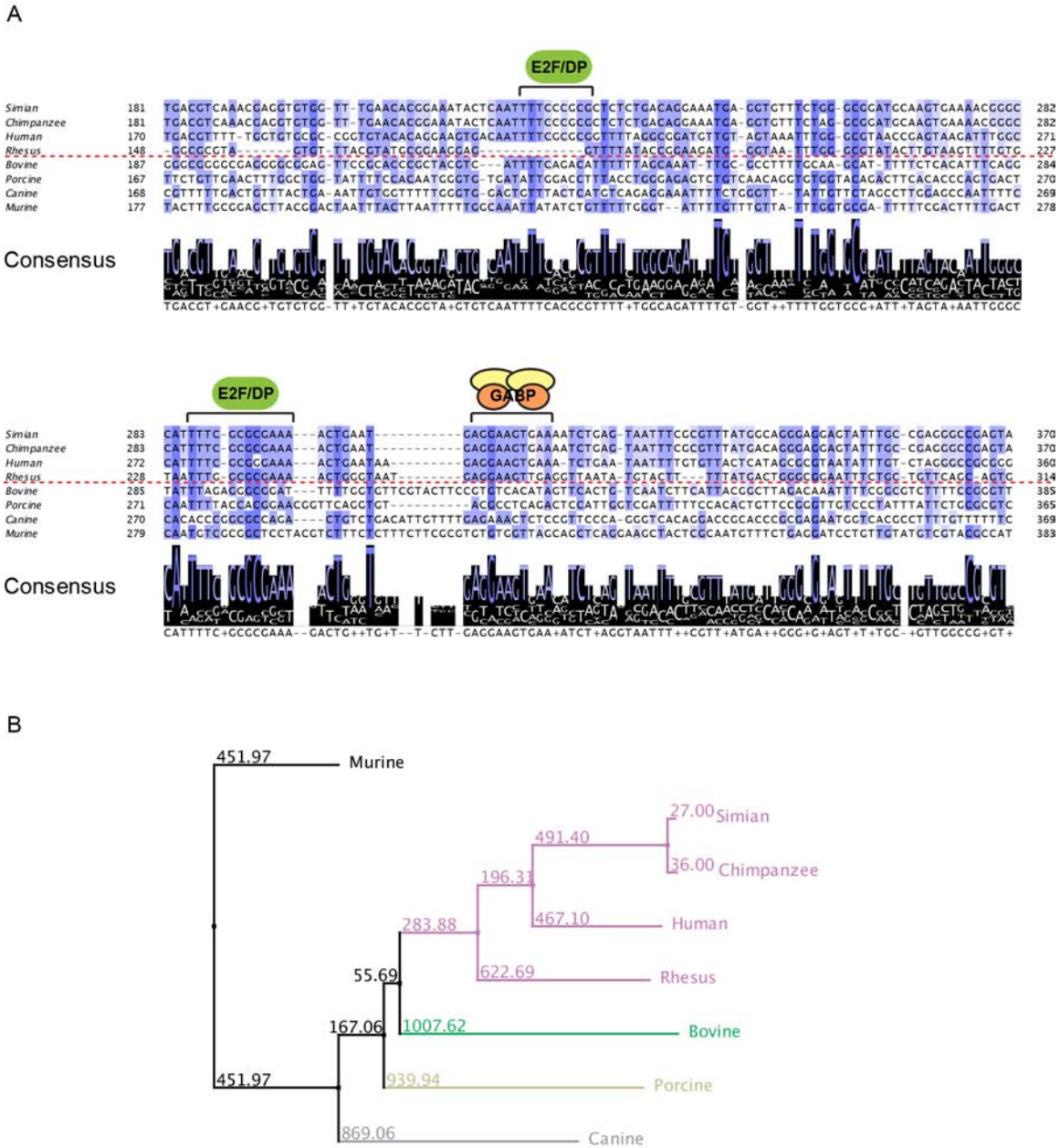

Figure 4-4. Alignment of the adenovirus left end from different species.
(A) Nucleotide sequence alignment of the E1A enhancer regions from different species. Consensus sequences are shown at the bottom and individual base letter height indicates the level of conservation. Red dash line separetes primate Ads from other species. E2F/DP and GABP binding sites are marked according to human Ad sequence.
(B) Neighbor-joining phylogenetic tree derived from the nucleotide sequence of Ad E1A enhancer region.

sites and the second GABP site are conserved among primates, including human, simian, chimpanzee and rhesus, except rhesus does not contain the first E2F site. This raised the interesting question of why do Ads carry a *cis* element that restricts E1A expression?

4.3.4 E2F/Rb Family Proteins Associate with the E1A Repressor Site *in vitro* and *in vivo.*

The E2F/Rb pathway is disrupted in nearly all human cancers (164) and all previous analyzes of the E1A enhancer region were conducted using nuclear extracts prepared from established cancer cell lines (135, 138). Thus, I examined E2F binding to the E1A repressor element using HDF-TERT cells. Nuclear extract was prepared from HDF-TERT cells and analyzed by EMSA using a radiolabeled probe corresponding to the IFN-induced E1A repressor site (Ad5 nt 271 to 288)(Figure 4-5A). Multiple DNA-protein complexes were observed that were identified using specific antibodies to E2F/Rb family proteins. The fastest migrating complex contained E2F-4 and DP-1 while slower migrating complexes contained E2F3/DP1/Rb and E2F1/DP1/Rb (Figure 4-5A lanes 2–4, 8, 12 and 13). The complexes with the slowest migration contained E2F-4/DP1 with p107 or p130 (lanes 5–8). The specificity of each antibody was ensured by competition using the corresponding peptides used to generate the antibodies (data not shown). Identical complexes were observed using nuclear extracts from IFN-treated HDF-TERT cells (Figure 4-5A, lanes 14–16). I performed ChIP experiments to evaluate the enrichment of Rb family proteins at the E1A enhancer early after infection with or without IFN treatment. These results showed an increase in Rb association and p107 with the E1A enhancer region following IFNα and IFNγ treatment, respectively (Figures 4-5B and 4-5C, 2-fold and 5-fold, respectively). The binding of Rb and p107 to the E1A enhancer of Ad5-mut1 was reduced 4-fold compared to wild-type Ad5 without IFN

treatment, and no significant increase in binding of either of these proteins to Ad5-mut1 was observed following IFN treatment (Figures 4-5B and 4-5C). These results demonstrate that IFN treatment induces the binding of repressive E2F/Rb complexes to the E1A enhancer region following IFN treatment. The reduction in Rb and p107 binding to near background levels with Ad5-mut1 suggests that E2F family proteins primarily associate with the downstream E2F site centered at the IFN-induced repressor site rather that at the upstream E2F binding site. This conclusion is consistent with the E1A enhancer mutant screen where a mutant in the upstream E2F binding site showed repression of E1A expression following IFN treatment (Figure 4-1A, *dl*309-A5). Protein p107 does not associate with the E1A enhancer in the untreated cells, but it is recruited by IFNγ signaling pathway.

I also performed EMSA experiment using nuclear extract prepared from HDF-TERT-E1A cells, in which IFNα and IFNγ failed to inhibit Ad E1A expression and viral replication. There were three DNA:protein complex identified, E2F-3/DP-1, E2F-4/DP1 and E2F-1/DP1/Rb (Figure 4-5D). In comparison to DNA:protein complexes formed in HDF-TERT cells, I found E2F-3 was released from repression by Rb, and the association of p107 and p130 to the E1A enhancer was completely diminished in HDF-TERT-E1A cells (Figure 4-5D). This strongly suggests that p107 and p130 might be the primary mediators for IFN-induced repression of E1A gene expression.

4.3.5 Releasing E2Fs from Pocket Proteins Mimics IFN Signaling

PD0332991 (Palbociclib) is a specific CDK4/6 inhibitor and can cause cell cycle arrest through dephosphorylation of Rb family proteins (179). To avoid changes in Rb family protein phosphorylation by contact inhibition, low-density HDF-TERT cells were incubated with PD0332991 and Rb, p107 and p130 phosphorylation was evaluated by Western blot. Rb, p107 and p130 were quickly dephosphorylated within 6 hr of

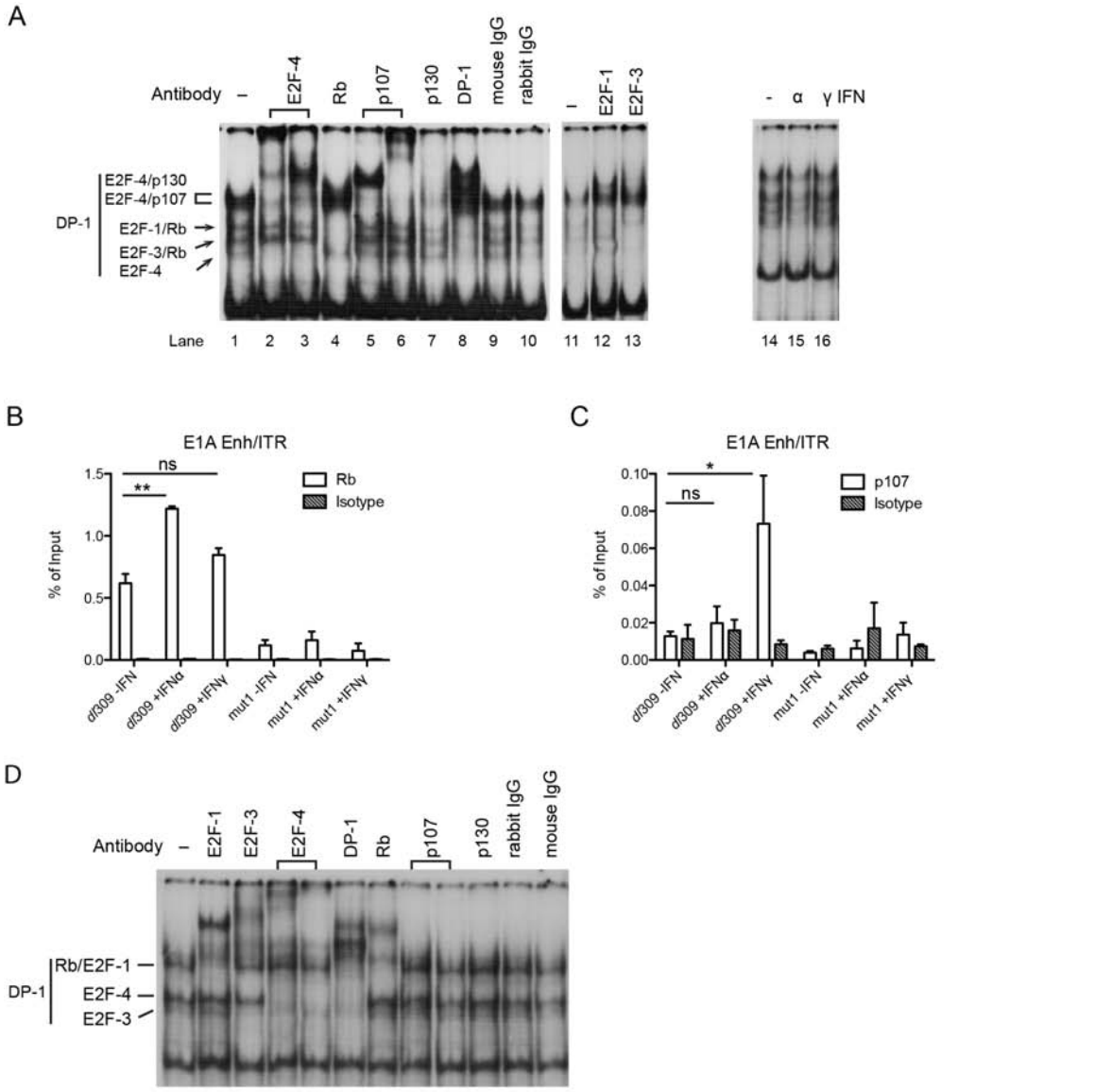

Figure 4-5. E2F/Rb Family Proteins Associate with the E1A enhancer *in vitro* and *in vivo*

(A) EMSA binding reactions were performed using nuclear extract from HDF-TERT cells and a ^{32}P-labeled probe corresponding to the IFN-regulated E1A enhancer repressor element (E1A-ENH, Ad5 nt 271-288, lane 1). Lanes 2–10 show EMSA binding reactions that contained specific antibodies directed E2F, DP, and Rb family members (E2Fs 1, 3 and 4, Rb, p107, p130, and DP1) or control antibodies (normal mouse and rabbit IgG). The compositions of DNA-protein EMSA complexes are indicated on the left. Lanes 11–13 show binding reactions with HDF-TERT nuclear extracts prepared from untreated cells or cells treated with IFNα or IFNγ for 24 hr.

(B and C) ChIP assays were performed to examine the binding of Rb and p107 to the E1A enhancer region *in vivo* with or without IFN treatment. HDF-TERT cells were treated with IFNα, IFNγ or left untreated for 24 hr and then infected with 200 virus particles/cell *dl*309 or Ad5-mut1. ChIP assays were performed at 18 hr post-infection using antibodies against Rb (B), p107 (C), or an isotype-matched control. Immunoprecipited DNAs were quantified by qPCR (primer pairs are listed in Table 1). Enrichment is represented as percentage of input DNA and the values represent the mean ± SD, n=3. (* $P \leq 0.05$, ** $P \leq 0.01$).

(D) EMSA binding reactions were performed using nuclear extract from HDF-E1A cells as described in (A).

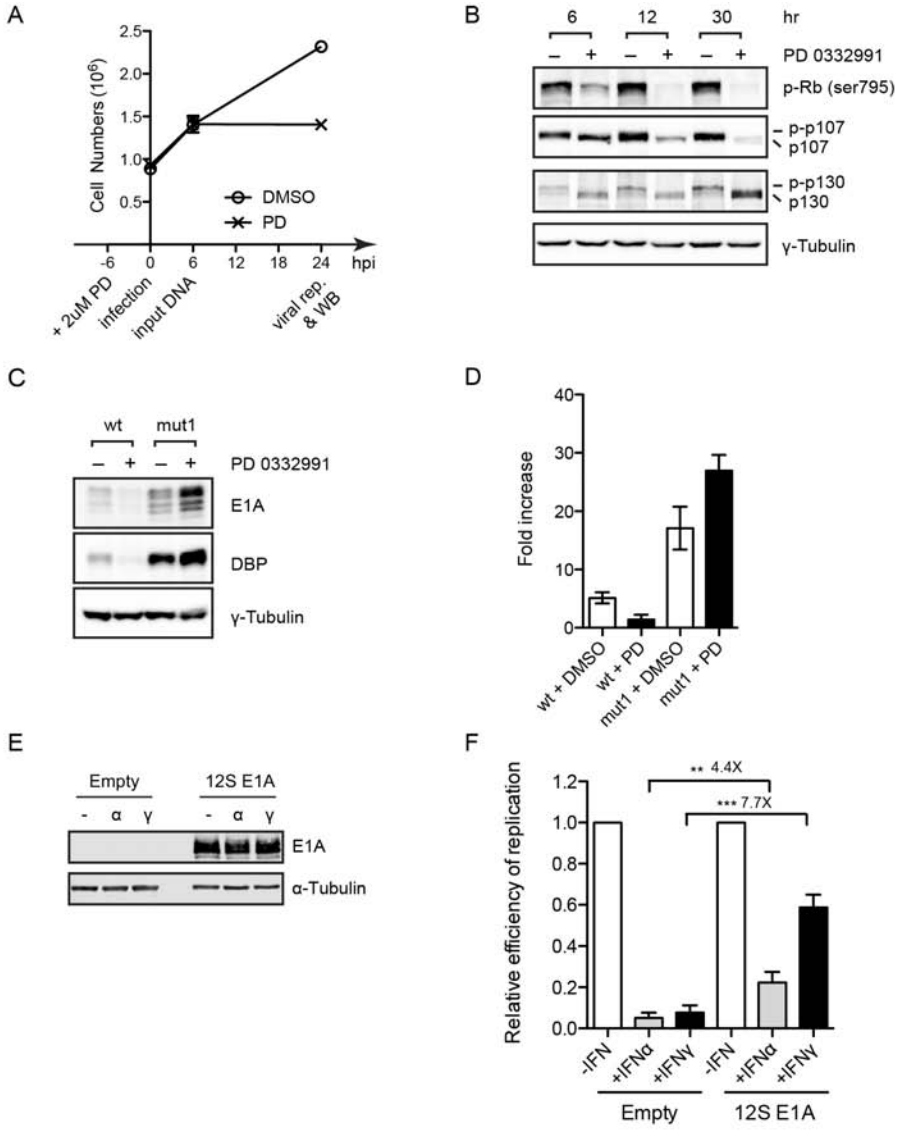

Figure 4-6. Relief of E2F/Rb repression counteracts IFN signaling to restore viral replication.

(A-D) The effect of the cdk4 inhibitor PD0332991 on Ad5 replication via the E2F binding site in the E1A enhancer region was evaluated. HDF-TERT cells were incubated with 2 μM PD0332991 or DMSO for 6 hr prior to virus infection. (A) Cell numbers were determined after 6 hr PD0332991 pretreatment (0), and in virus-infected cells at 6 and 24 hr post-infection. (B) Cell extracts were prepared at 0, 6 and 4 hr following PD0332991 pretreatment and Rb, p107 and p130 phosphorylation was examined by Western blot. (C) PD0332991 pretreated cells were infected with Ad5-WT and Ad5-mut1 at 200 particles/cell and Ad early gene expression (E1A, DBP) was analyzed by Western blot at 24 hr post-infection. γ-tubulin was used as a loading control for the samples. (D) Cells were pretreated with PD0332991 and infected as described in (D) and viral DNA replication was quantified at 24 hr post-infection by qPCR. The values were normalized to the input and are plotted as mean ± sd. n=3.
(E and F) HDF-TERT cells were infected Ad-CMV-12S-E1A or the empty control virus, Ad-CMV, at 5,000 virus particles/cell for 1 hr and the cells were left untreated or treated with IFNα or IFNγ for 24 hr. The cells were super-infected with dl309 at 200 virus particles/cell. (E) Cells were harvested at 24 hr after Ad-CMV-12S-E1A virus infection, and E1A expression was analyzed by Western blot. α-tubulin was used as a loading control for the samples. (F) Cells were harvested at 48 hr after *dl*309 infection and viral DNA replication was quantified by qPCR using a *dl*309-specific primer pair (see Table 1). The values were normalized to 1.0 in untreated cells and are plotted as mean ± sd. n=3. (** $P \leq 0.01$, *** $P \leq 0.001$)

PD0332991 addition (Figure 4-6B, 0 hr post-infection) although growth arrest was not evident until later times (Figure 4-6A). PD0332991 inhibited Ad5-WT replication whereas Ad5-mut1 replication was increased (Figure 4-6D); these results correlated with E1A and E2A DNA binding protein (DBP) expression levels (Figure 4-6C). Thus, PD0332991 treatment mimicked the effects of IFNs. It is well established that the E1A 12S protein can directly interact with Rb family proteins, leading to their dissociation from E2Fs and activation of E2F target gene expression (127). Ectopic expression of the E1A12S protein significantly restored Ad5 replication in the presence of IFNs (Figure 4-6F); IFN treatment did not reduce E1A 12S protein expression with the vector used in these experiments (Figure 4-6E). Collectively, these experiments reveal that IFNs inhibit Ad replication and E1A expression via E2F/Rb family proteins and IFN induction of transcriptional repressor activity.

It is well known that IFNs have anti-proliferative properties and can inhibit the growth of cells from multiple hematological malignancies (180). IFNα and IFNγ can induce the expression of p21 and p27, cyclin kinase inhibitors (CKIs), ultimately leading to decreased phosphorylation of Rb and the formation of repressive E2F-Rb complexes (181-183). There were no changes in the expression of CKIs p27 and p16 when HDF-TERT cells were incubated with IFNα and IFNγ for 24, 48 or 72 hr (Figure 4-7A), as well as IFN-treated HDF-TERT-E1A cells and Ad-infected cells (Figure 4-7B). Expression of the CKI p21 was not detectable in HDF-TERT cells (Figures 4-7A and 4-7B). Due to contact inhibition, Rb, p107 and p130 were dephosphorylated at 72 hr. There was slightly more loss of phosphorylated Rb, p107 and p130 in IFN-treated cells than untreated cells. However, it is hard to correlate the dramatic inhibition of Ad replication with the negligible effects on pocket protein phosphorylation. Consistent with the EMSA result that p107 and p130 do not associate with the E1A enhancer when E1A is

expressed, there were no detectable levels of phosphorylated p107 and p130 (Figure 4-7C) suggesting HDF-TERT-E1A lost the normal cell cycle control. This evidence emphasizes the important role of pocket protein in regulating Ad E1A expression in normal human cells.

4.3.6 IFI16 is not Required for IFN-mediated E1A Repression

IFI16, a HIN-200 family protein, senses intracellular viral DNA leading to IRF3 activation and IFNβ expression (161). Ectopic expression of IFI16 in prostate cancer cell lines increases p21 expression and inhibits E2F-stimulated transcription (184-186). Taken together, these results suggested that IFI16 might regulate global E2F transcription activity upon IFN treatment in HDF-TERT cells. I generated three independent pools of IFI16 knockdown cells, shIFI16-1-1, shIFI16-1-2 and shIFI16-3-1; IFI16 expression was significantly depleted in all cell pools, compared to control cells (Figure 4-8A, top). Although treatment of the IFI16 knockdown cells with IFNs slightly increased IFI16 protein levels, it was still less than that in untreated control cells (Figure 4-8A, bottom). When IFI16 protein was depleted, Ad5 replication was still inhibited by IFNα and IFNγ treatment to the extent observed in control cells (Figure 4-8B). Thus, I conclude IFI16 is not required for IFN-mediated repression of Ad5 replication.

4.3.7 The IFN-regulated Repressor Element in the E1A Enhancer Region is Important for the Establishment of Persistent Ad5 infection

Previous studies demonstrated that T lymphocytes in tonsil and adenoid tissues are the primary reservoirs for latent Ad (187, 188). As important cytokines mediating innate and adaptive immunity, type I and type II IFNs could inhibit Ad replication and promote the establishment of persistent infection. The conserved IFN-induced repressor element in the E1A enhancer region may be involved in Ad latency by repressing E1A expression in response to IFNs and allow Ad to evade immune surveillance and

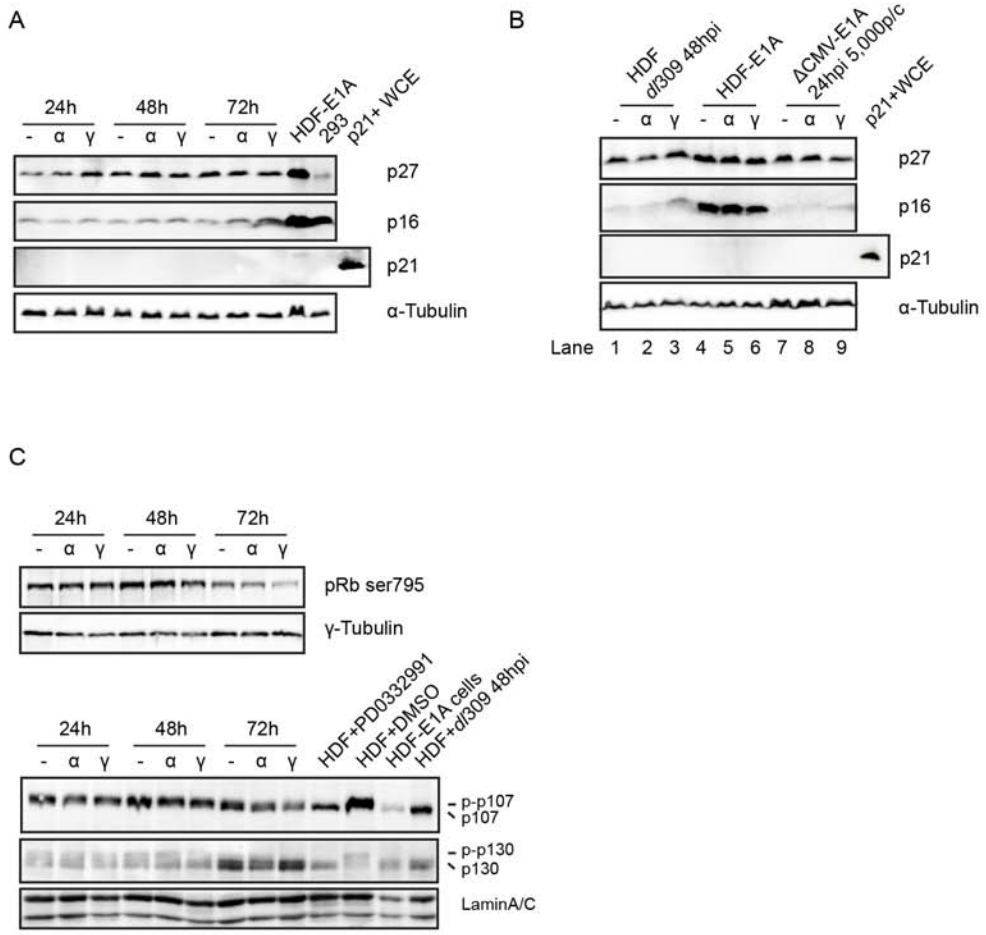

Figure 4-7. Phosphorylation of pocket proteins in HDF-TERT cells
(A) HDF-TERT cells were treated with IFNα, IFNγ or left untreated for 24, 48 and 72 hr. Expression levels of three CDK inhibitors, p27, p16 and p21, were analyzed by Western blot. α-Tubulin was used as a loading control. p21 positive whole cell extracts (p21+WCE) were generously provided by Dr. Ji'an Pan.
(B) HDF-TERT cells were treated with IFNα, IFNγ or left untreated for 24 hr, followed by infection with dl309 at 200 particles/cell (lane 1-3). HDF-TERT-E1A cells were treated with IFNs (lane 4-6) or left untreated for 24 hr. HDF-TERT cells were infected with in340-Δ2-CMV-E1A at 5,000 particles/cell and subsequently treated with IFNα, IFNγ or left untreated for 24 hr. Expression levels of p21, p27 and p16 were analyzed by Western blot.
(C) HDF-TERT cells were treated with IFNα, IFNγ or left untreated for 24, 48 and 72 hr. Western blot analysis was performed using antibodies against phospho-Rb (ser795), p107 and p130. Whole cell extracts from DMSO- or PD0332991-treated HDF-TERT cells were used to identify hyperphosphorylated and hypophosphorylated p107 and p130. Levels of p107 and p130 were also analyzed in HDF-TERT-E1A cells and dl309-infected HDF-TERT cells. γ-Tubulin and Lamin A/C were used as loading controls.

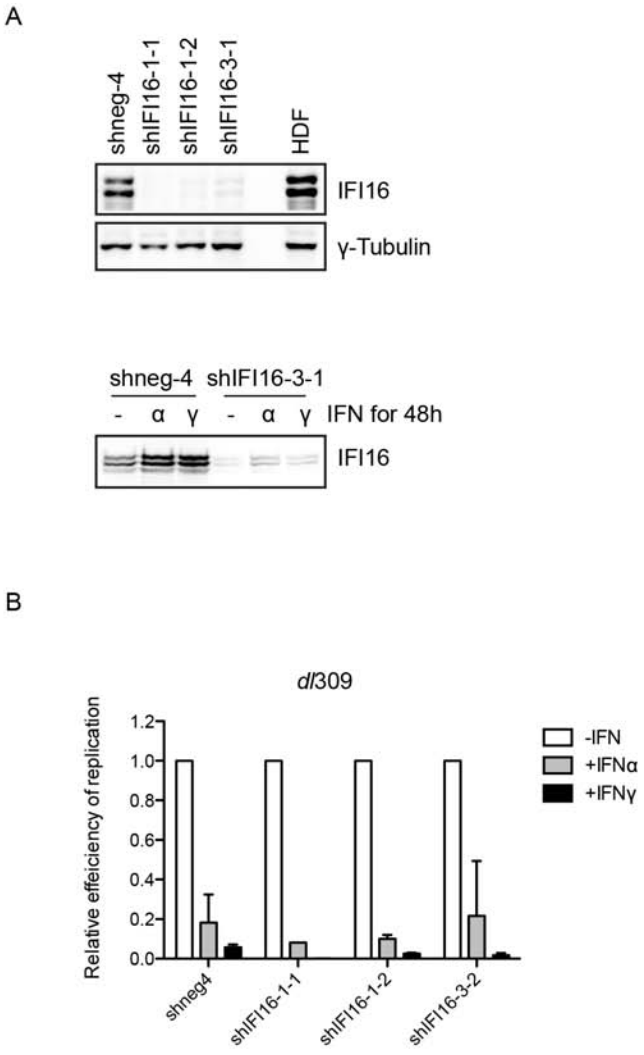

Figure 4-8. Effect of IFI16 on Ad replication and E1A expression
(A) IFI16 protein levels (top panel) were examined by Western blot in parental HDF-TERT cells (HDF), along with different individual knockdown subclones corresponding to control shRNA (shneg) and shRNAs targeting IFI16. γ-Tubulin was used as a loading control. shRNA control and IFI16 knockdown cells were treated with IFNs or left untreated for 48 hr (bottom panel). IFI16 protein levels were examined by Western blot.
(B) shRNA control and IFI16 knockdown cells were pretreated with IFNs or left untreated for 24 hr and then infected with dl309 at 1000 virus particles/cell. Viral DNA replication was quantified by qPCR at 48 hr post-infection and are plotted as mean ± sd.

clearance. To test this hypothesis, HDF-TERT cells were infected with *dl*309 and *in*ORF3 at low MOI in the presence or absence of IFNs. Infected cells were cultured for an extended period of time and the production of infectious virus quantified by plaque assay (Figure 4-9A). During the first 10 days of infection, no cytopathic effect was observed in any infected cells. In the absence of IFNs, peak virus yield was reached at 10 days post-infection (~10^8 PFU/ml). Full cytopathic effect was observed at 15 days post-infection. In contrast, in IFN-treated cells, virus yields gradually increased over 25-30 days, giving a peak of 1-2x10^7 PFU/ml. IFNα postponed the onset of cytopathic effect in *dl*309 and *in*ORF3 infected cells until 45 days post-infection. IFNγ also postponed the onset of CPE until 45 days post-infection. In contrast, in IFNγ-treated *dl*309-infected cells, no cytopathic effect was observed throughout the entire period (up to 100 days post-infection). These results demonstrate that both IFNα and IFNγ can promote the establishment of long-term Ad infection. An intermediate amount of infectious virus was produced throughout the course of infections with IFNγ treatment (10^6–10^7 PFU/ml) indicating the establishment of persistent, not latent, infection. qPCR was also performed to detect the different regions across the entire genome. There were similar copy numbers of left-end (E1A region), middle region (E2B and L2) and right-end (E4), suggesting that *dl*309 genome remained intact in persistently infected HDF-TERT cells (Figure 4-9B).

Next, I examined the role of the E2F binding site in the E1A enhancer region in an IFN response during long-term infection of HDF-TERT cells. HDF-TERT cells were infected with Ad5-WT or Ad5-mut1 in the presence of absence of IFNγ. Both infectious virus yield and viral genome copy number were measured during the course of infection (Figures 4-9C and 4-9D). Ad5-WT displayed identical infection course with or without IFNγ treatment as compared to *dl*309. In the absence of IFNγ, both Ad5-WT and Ad5-mut1 reached peak virus production at 10 days post-infection. Cytopathic effect started

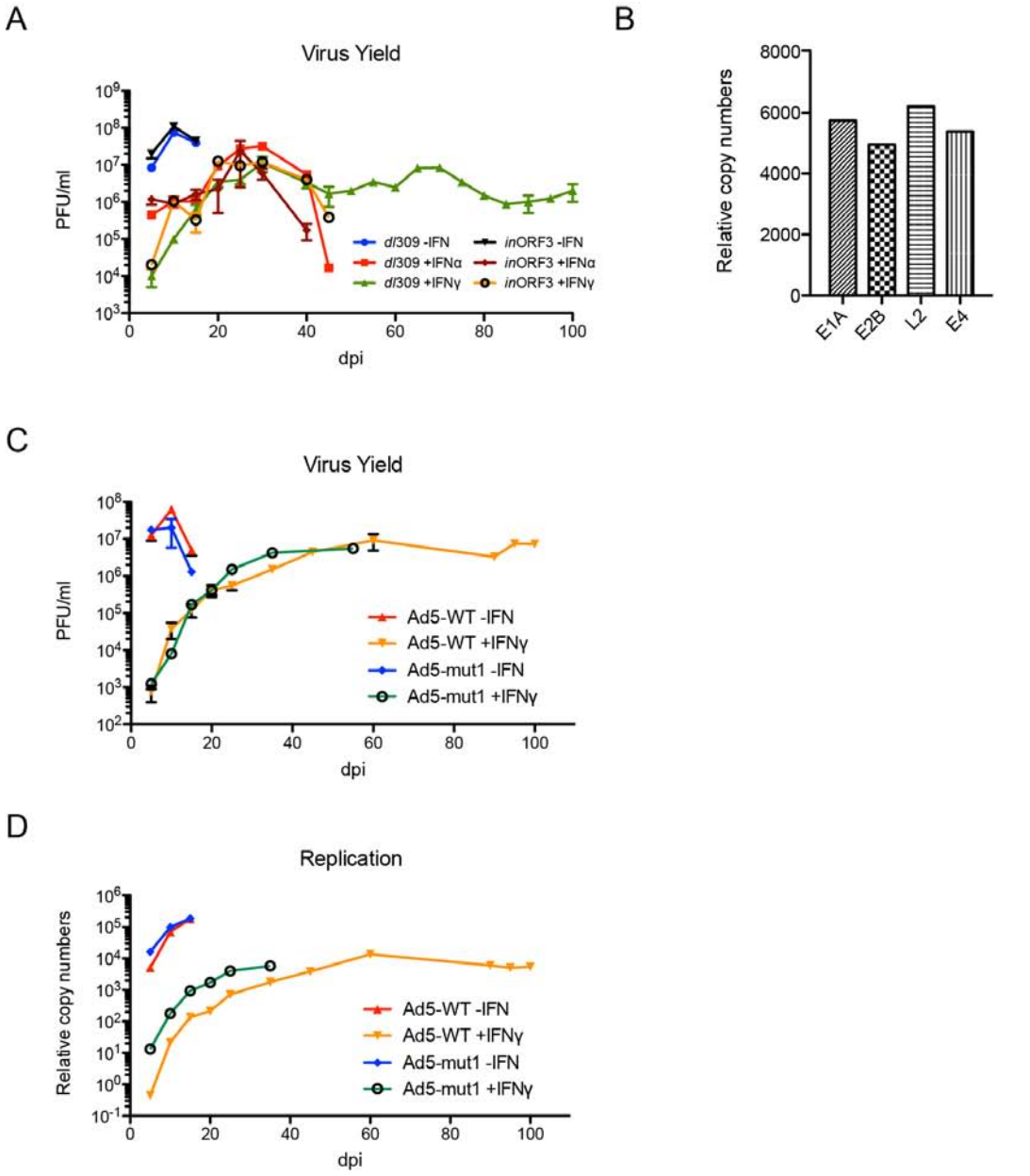

Figure 4-9. IFNs promote the establishment of persistent Ad infection
(A, B) HDF-TERT cells were infected with dl309 or inORF3 at 25 particles/cells and cultured grown in the presence or absence of IFNα or IFNγ. Growth media plus or minus IFNs were replenished every 5 days. Infectious virus yields were determined by plaque assay (A).
(B) Viral DNA was prepared from dl309-infected IFNγ-treated cells at 70 days post-infection. The viral copy number was determined by qPCR using oligonucleotides that recognize different regions of Ad genome.
(C to E) The experiment was performed as described in (A) with infection using WT Ad5 or Ad5-mut1 viruses. At the indicated times post-infection, infectious virus yields were determined by plaque assay (C) and viral DNA replication was quantified by qPCR (D). Phase contrast microscopy images of infected cells at various time points are shown in (E).
(F) Immunofluorescence assays were used to determine the percentage of Ad protein-positive cells. At 113 days post-infection, Ad5-infected HDF-TERT cells treated with IFN were immunostained for Ad early proteins (E1A, DBP, E4-ORF3) and late proteins (pVII, Hexon). Cells were scored as either positive or negative for the expression of viral proteins, and the percentages of 250 cells in 5-6 random views were plotted. E and L stand for early and late protein expression, respectively.

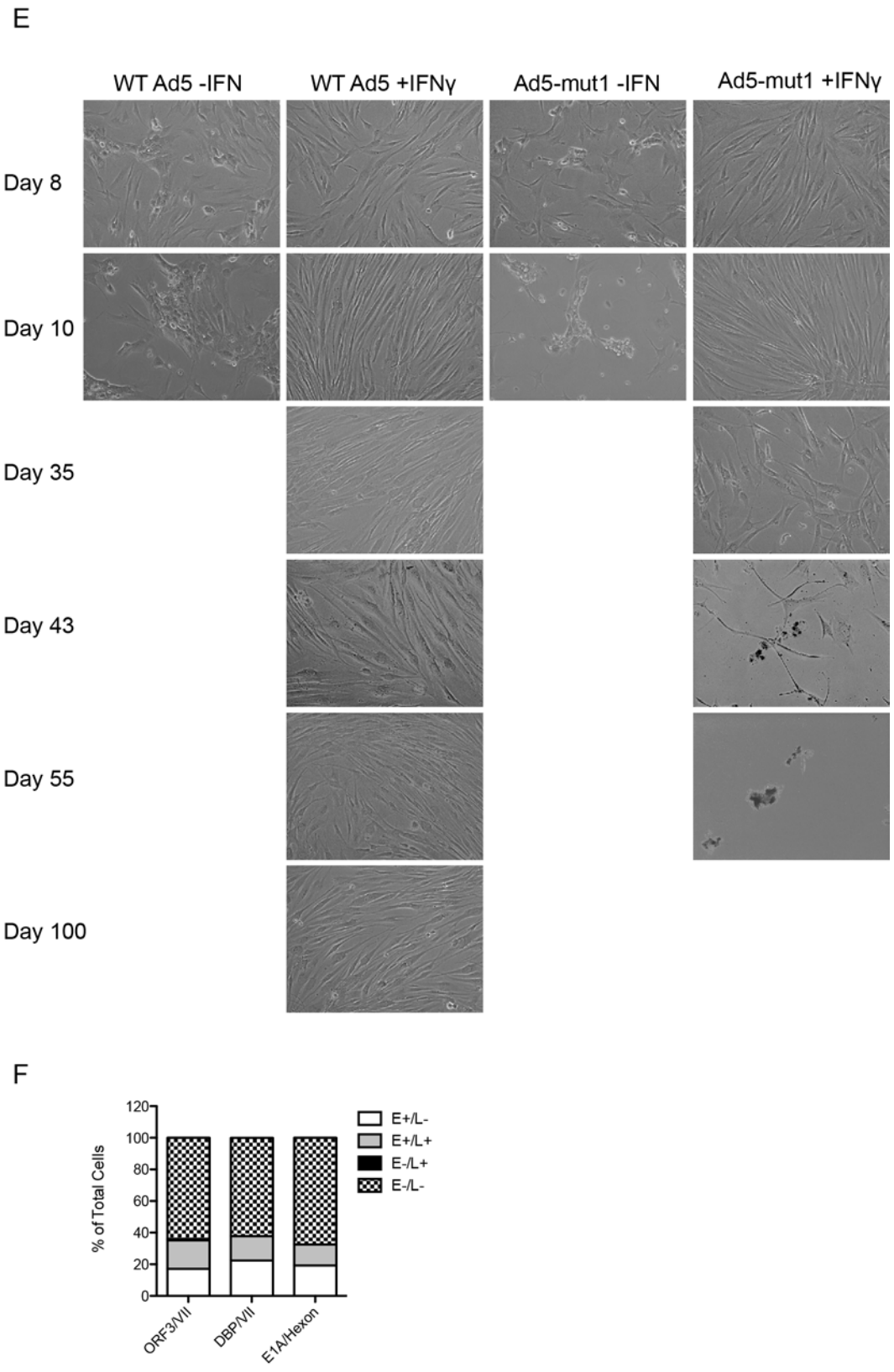

Figure 4-9. IFNs promote the establishment of persistent Ad infection

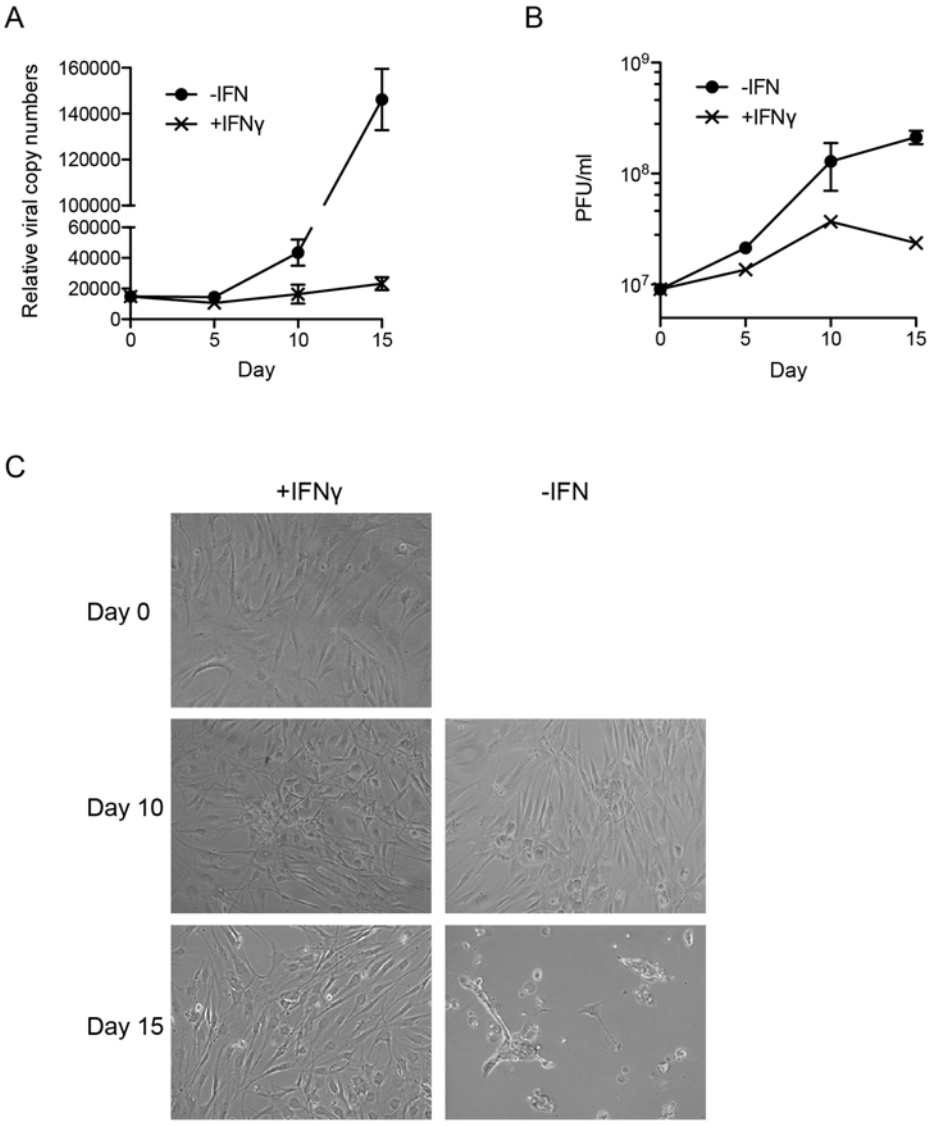

Figure 4-10. Ad enters lytic infection upon withdrawal of IFNγ
At 107 days post-infection, WT Ad5-infected HDF-TERT cells treated with IFN (shown in C) were seeded into new plates in duplicate. When the cells reached ~80% confluence, IFN was removed from one set and maintained in the second set. Cells were subcultured at day 5 and growth medium was replenished at day 10. Ad5 DNA replication was quantified by qPCR (A) and infectious virus yield was determined by plaque assay (B) at day 5, 10 and 15. The plots represent the average of two independent experiments. Phase contrast microscopy images of infected cells were taken at day 0, 10 and 15 (C).

merging around 8 days post-infection, and full cytopathic effect was observed at 15 days post-infection (Figure 4-9E and data not shown). In IFNγ-treated cells, virus production of Ad5-WT and Ad5-mut1 gradually increased from 0 to 30 days post-infection. Ad5-mut1 infection in the presence of IFNγ was terminated at 55 days post-infection due to full cytopathic effect, while Ad5-WT infection continued for 100 days without cell death (Figure 4-9E). Viral genome copy number correlated well with infectious virus yields throughout the course of these infections (Figure 4-9D). IFNγ-treated cells infected with Ad5-WT-infected were analyzed by immunofluorescence at 113 days post-infection to examine viral early and late gene expression in individual cells (Figure 4-9F). These result showed that ~40% of the infected cells were positive for viral gene expression with some cells expressing only early proteins and other cells expressing both early and late proteins.

I also examined the fate of long-term infected cells upon the withdrawal of IFNγ. As shown in Figures 4-10A and 4-10B, there was no significant changes in viral genome copy number and infectious virus yield 5 days after IFNγ removal compared to IFNγ-treated cells. However, significant increases in viral genome copy number and infectious virus yield were observed by 10 and 15 days following IFNγ removal; full cytopathic effect was observed by day 15 (Figure 4-10C). Collectively, I conclude that IFNγ treatment represses the Ad5 lytic cycle in infected HDF-TERT cells and promotes persistent infection, and that this effect requires the E2F binding site in the E1A enhancer region.

4.3.8 Adenovirus Infection in Lymphocyte Cell Lines

The fate of Ad following the infection of T and B lymphocyte cell lines is cell type and serotype dependent (173, 174). I wanted to test whether IFNs plays any role in promoting the establishment of Ad latency in lymphocytes. Previous studies suggested

that Ad5 established latency and persistent infection following infection of BJAB and PM1 cell lines. In contrast, Ad exhibited a lytic life cycle in the Jurkat cell line (173, 174). Our result of persistent Ad infection in HDF-TERT cells prompted us to test whether Ad can establish latent infection in PM1 and Jurkat cells with IFNγ treatment. I found all three cell lines responded to the IFN stimuli. STAT1 was phosphorylated by the incubation with 25 U/ml IFNα and IFNγ for 1 hr (Figure 4-11A), and the expression of STAT1 was also observed after 24 hr (Figure 4-11B) incubation with IFNs. Next, I tested infectivity of Ad5 in those cell lines, since it is known that lymphocyte cell lines are refractory to Ad infection. Three cell lines were infected with Ad5 at various MOI, and input viral copy numbers were measured by qPCR. In Jurkat and PM1 cells, the relative viral copy numbers increased as MOI increased. The infectivity of Ad in Jurkat cells was comparable to that in A549 cells (Figure 4-11C), while PM1 cells were comparable to HDF-TERT cells (Figure 4-11C). However BJAB cells were highly resistant to Ad infection, since input viral genome number reached a peak at 2,000 particles/cell infection and was not increased when the MOI was further increased (Figure 4-11C). To monitor virus growth by flow cytometry for an extended period, BJAB, Jurkat and PM1 were pretreated with 100 U/ml IFNα, 200 U/ml IFNγ, or left untreated for 24 hr. To ensure similar input viral genome numbers, BJAB and PM1 cell lines were infected with Ad5-WT or Ad5-mut1 at 2,000 virus particles/cell, while Jurkat cells were infected at 200 virus particles/cell. Infected cells, along with uninfected cells, were maintained for 12 days, and cell density was adjusted to 2.5×10^5 cells/ml every 4 days. Virus infection was monitored by flow cytometry for expression of hexon protein (Figure 4-12). Infected-Jurkat cells expressed hexon in >80% cells within 8 days following initial infection. At 10 days post-infection, all of hexon-positive Jurkat cells died due to CPE as determined by Ad-mut1 replication. BJAB and PM1 cells reached the peak of hexon expression within 4 days post-infection. At the peak of expression, less than 25% of BJAB cells and 35%

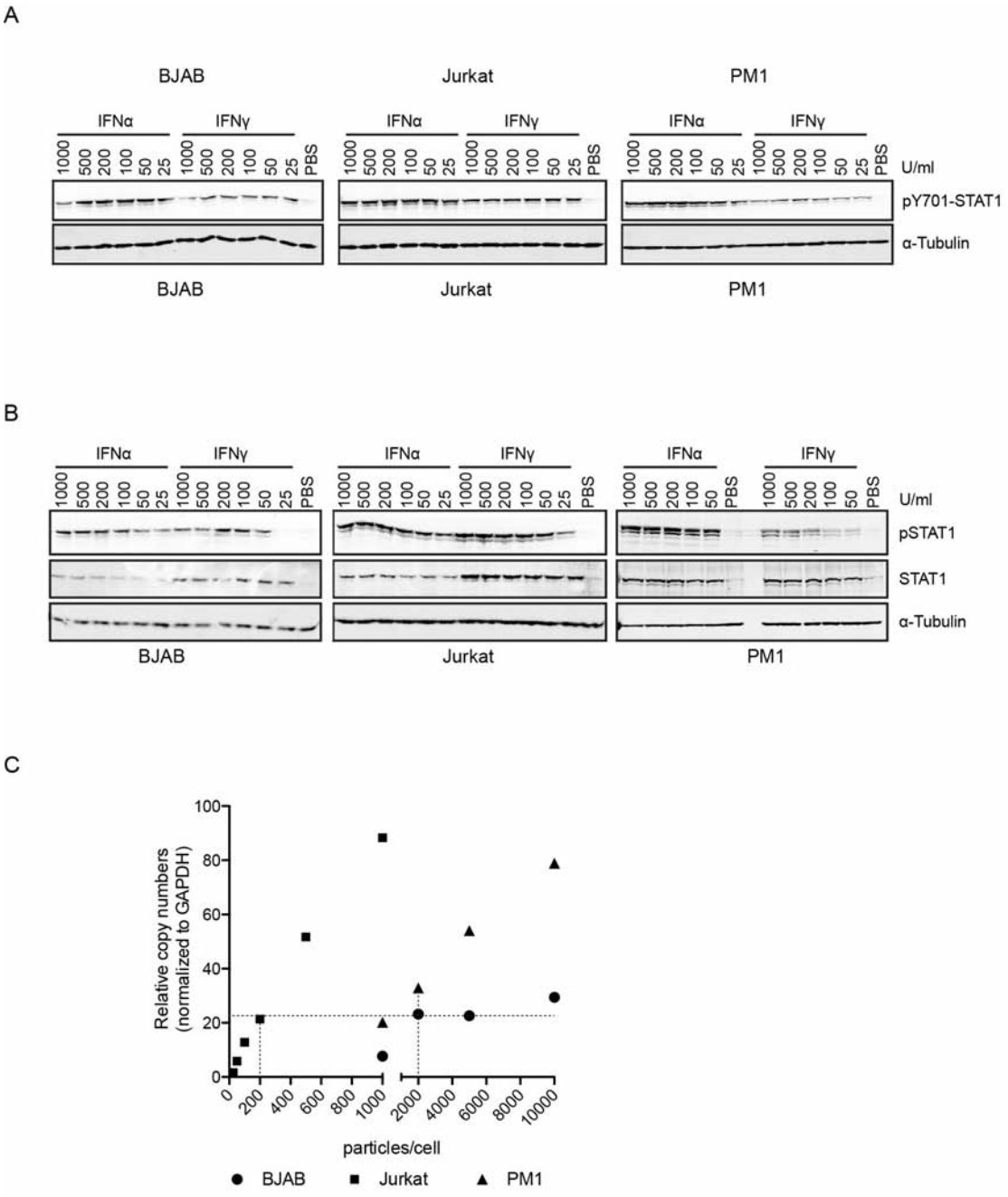

Figure 4-11. Sensitivities to IFNs and Ad infectivity in multiple lymphocyte cell lines
(A, B). Cell densities of BJAB, Jurkat and PM1 cells were adjusted to 5x105 cells/ml and treated with different concentrations of IFNα and IFNγ for 1 hr (A) or 24 hr (B). Expression levels of STAT1 and phosphorylated STAT1 were analyzed by Western blot. α-Tubulin was used as a loading control for the samples.
(C) Cell densities of BJAB, Jurkat and PM1 cell lines were adjusted to 107 cells/ml and were infected with dl309 at different MOIs. Total DNA was isolated at 3 hr post-infection and viral DNA levels were quantified by qPCR.

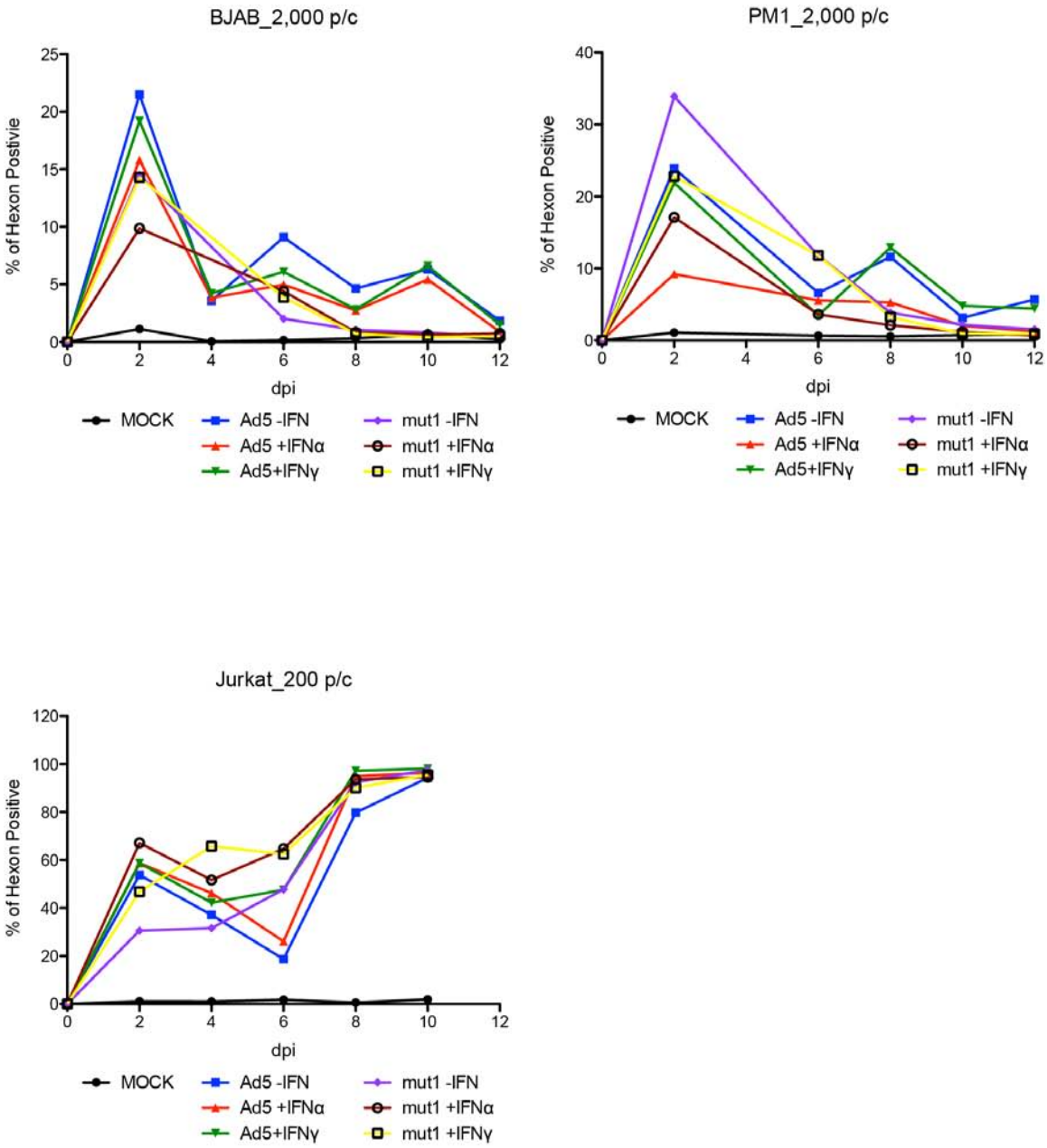

Figure 4-12. Monitoring Ad replication in lymphocyte cell lines
BJAB, PM1 and Jurkat cell lines were treated with 100 U/ml IFNα, 200 U/ml IFNγ or left untreated for 24 hr. BJAB and PM1 cells were infected with WT Ad5 or Ad5-mut1 at 2000 virus particles/cell, and Jurkat cells were infected with the same viruses at 200 particles/cell. Infected cells were cultured in the presence and absence of IFNs. Growth media plus or minus IFNs were replenished every 4 days. Hexon protein expression was determined by flow cytometry at the indicated time points.

PM1 cells were hexon positive. IFNα and IFNγ failed to reduce Ad5-WT and Ad5-mut1 replication in both BJAB and PM1 cells. IFNα only reduced Ad replication by approximately 2-fold in both cell lines, while IFNγ hardly had any effect on Ad replication. More importantly, hexon expresson in Ad5-WT- and Ad5-mut1-infected cells, with or without IFN treatment, wa reduced precipitously and fell below detection by 12 days post-infection. Loss of hexon expression would be an indication of latency establishment. The other possibility is the outgrowth of uninfected cells, since I did not observe hexon protein expressed in the entire cell population. Moreover, when lymphocytes were treated with higher concentration of IFNs (up to 500 U/ml IFNα and 1,000 U/ml IFNγ) and infected with Ad5 at lower MOI (25 particles/cell in BJAB and PM1, 5 particles/cell Jurkat), IFNα only exhibit 2.5- to 5-fold inhibition of Ad replication, and IFNγ hardly inhibited Ad replication in both Jurkat and PM1 cells (Figure 4-13A), which is consistent with results from flow cytometry assays. When viral protein expression was exanimated by Western blot, lFNα only has minimal effect on E1A expression (Figure 4-13B). Thus, B and T lymphocyte cell lines did not give a viable model to study latent or persistent Ad infection.

4.4 Discussion

Adenoviruses establish two different types of infection in the host. Primary infection occurs in epithelial cells, e.g., the nasopharyngeal mucosa with Ad5, resulting in lytic infection and the production of progeny virus. Following acute infection, Ad5 establishes latent infection in the mucosa-associated lymphoid tissue, preferentially T-lymphocytes in tonsil and adenoid tissues (173, 188). Cellular mechanisms that regulate Ad lytic infection are well understood, but the molecular basis for the control of persistent Ad infections was not understood. In this chapter, I showed that repression of E1A expression by IFNs requires a conserved E2F binding site in the E1A enhancer region.

A

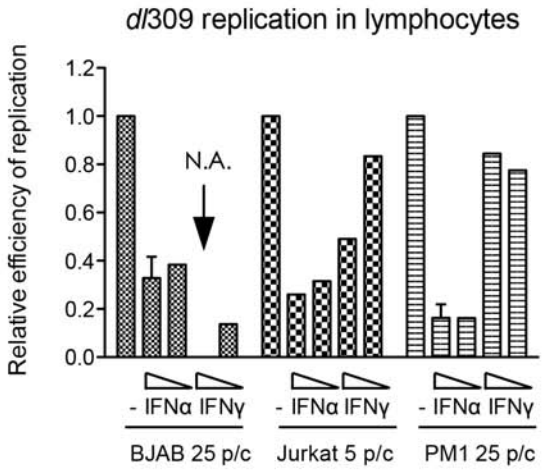

B

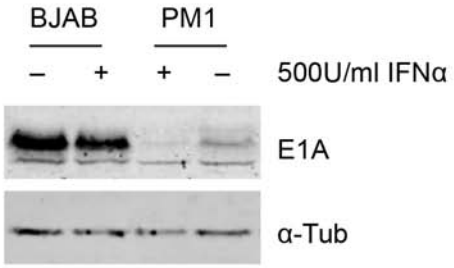

Figure 4-13. Ad infection in lymphocytes treated with high concentration of IFNs
(A) Three lymphocyte cell lines, BJAB, PM1 and Jurkat, were treated with 500 or 100 U/ml IFNα, 1000 or 200 U/ml IFNγ or left untreated for 24 hr and then infected with a low MOI of dl309. Viral DNA replication was quantified by qPCR at 48 hr post-infection.
(B) BJAB and PM1 cells were treated with or without 500 U/ml IFNα and then infected with *dl*309 at200 particles/cell. E1A expression was analyzed at 48 hr post-infection by Western blot.

E2Fs can transcriptionally activate or repress gene expression depending on their interactions with Rb family proteins (132). IFNs augmented the binding of the tumor suppressors Rb and p107, well characterized E2F binding partners and transcriptional repressors (132), to the E1A enhancer region *in vivo*. Mutation of the conserved E2F binding site in the E1A enhancer abrogated the effects of IFNs on E1A expression and Ad replication. Two additional compelling results link E2F/Rb family proteins with the inhibition of Ad infection by IFN signaling. First, ectopic expression of the small E1A oncoprotein that lacks transactivation function but efficiently dissociates E2F-Rb family protein complexes (127) blocks the effects of IFN signaling on Ad replication. Second, treatment of cells with the CDK4/6 inhibitor PD0332991, which promotes Rb family phosphorylation and disrupts E2F-Rb complexes (179), has the same effect. Collectively, these results demonstrate that the IFN–E2F/Rb axis is critical for restriction of adenovirus replication during type I and type II IFN responses.

Rb protein is associated with the E1A enhancer in the absence of IFN (Figure 4-5B). The viruses that contain a mutation at the E2F site exhibited higher E1A expression compared to parent viruses (*in*340 vs. *in*340-B1, -*dl*10 and -*dl*12, *dl*309 vs. *dl*309-21 as well as Ad5-WT vs. Ad5-mut1) (Figure 4-1). Relief E2F repression from pocket protein by PD0332991 treatment enhanced E1A expression (Figure 4-6). Taken together, my results suggest that the E2F binding site in the Ad5 E1A enhancer region has effects on both basal and IFN-regulated immediate early gene expression. It was surprising that this E2F site is conserved across divergent Ad serotypes. Indeed, both IFNα and IFNγ treatment of cells repressed the replication of Ads in five evolutionarily distinct subgroups. These observations suggested that Ads may utilize the conserved E2F site in the E1A enhancer to suppress E1A expression in certain infection contexts, for example during persistent Ad infections. I established a persistent Ad infection model *in vitro* and demonstrated that IFNγ suppresses productive Ad replication in a manner

dependent on this conserved E2F binding site (Figure 4-9). Relief of this repression by removal of IFN resulted in a transition from persistent to lytic Ad infection (Figure 4-10). A viral mutant that lacks the conserved E2F binding in the E1A enhancer region was resistant to the effects of IFNs and was unable to establish persistent infection *in vitro*. IFN signaling reduced the binding of the major E1A enhancer transactivator complex GABPα/β to the E1A enhancer *in vivo*. The E2F binding site is located immediately adjacent to the GABPα/β binding site in the E1A enhancer. It is possible that GABPα/β and E2F/Rb proteins compete for binding to the enhancer given the proximity of their binding sites. Alternatively, IFNs may regulate the binding of GABPα/β and E2F/Rb family proteins to the E1A enhancer through independent mechanisms. If the competition binding is true, the similar level of Ad5-mut1 should be immunoprecipitated by GABP antibody. However, mixed results were observed, both equal and reduced amount of GABP was associated with Ad5-mut1 virus. IFNs may block the binding of GABP to both enhancer element I sites, and deletion of the second E2F binding site at nt 280 might not sufficient to reverse the defect of GABP binding by IFNs.

In addition to the E1A enhancer region, E2Fs bind to sites in the Ad5 E2 promoter *in vitro* (137). In NHBEC and HDF-TERT cells, IFNs exhibited stronger inhibition of transcription from the E2A and E2B regions compared with other early regions (Figures 4-3A and 4-5C) consistent with the idea that E2Fs also directly negatively regulate E2 expression in addition to the E1A. This effect also was observed in HDF-TERT-E1A cells (Figure 3-7D).

These results reveal a novel mechanism by which adenoviruses utilize IFN signaling to inhibit lytic virus replication and promote persistent infection. It is well established that IFNs fail to inhibit wild-type Ad replication in established cell lines (46, 106, 107). The resistance of wild-type Ad to the effects of IFNs is due to multiple counteracting effects of viral gene products. Additionally, this is due to the nature of

established cancer lines that contain alterations in different signaling pathways. The same experimental conditions were utilized in experiments that demonstrated significant effects of IFNs in normal human cells but a distinct lack of effect in an adenocarcinoma cell line (Figure 3-3 and 3-5). Given the association of IFN signaling with E2F/Rb family protein function shown in our studies, The defects observed in IFN signaling in cancer cell lines likely due to perturbations in the regulation of E2F/Rb family members since the E2F pathway is mutated in numerous cancer cells (164).

ONYX-1520, an Ad5 E1B 55K null mutant, has been used as a potential cancer therapy agent. The clinical data suggests that ONYX-1502 is safe, and selectively replicates and lyses cancer cells, but not normal cells (189). However, the further development of ONYX-1520 for therapeutic use in the U.S. was abandoned during Phase III trials in the early 2000s, in part due to the unclear mechanism of action. Development of the third generation of Ad-based oncolytic vectors involves taking advantage of hyperactive E2Fs in cancer cells to improve tumor specificity. Adenovirus was re-engineered by replacing viral early promoters with the cellular E2F-1 promoter, and/or delivering E2F-1 promoter driven transgenes (190-192). Gene expression and cell killing activities of these viruses are tightly regulated in normal cells in an Rb-dependent fashion. Considering the finding that IFN-E2F/Rb axis is important for inhibition of Ad gene expression and replication, innate and adaptive immunity might reinforce the tumor selectivity of E2F-driven oncolytic Ads by selectively diminishing vial replication and transgene expression in normal cells.

Though IFNs have anti-proliferation properties by manipulating the E2F/Rb pathway, I failed to detect any significant changes in p16 and p27 expression in IFN-treated and untreated cells. Minimal changes of phospho-Rb and -p107 levels were detected in IFN-treated cells. The murine protein p202, a HIN200 family member, is an IFN-inducible gene product that represses gene expression via E2F4/DP1 in transient

expression assays (193, 194). These results and the known role of IFI16 in regulating cellular proliferation via CKIs, which impact E2F-Rb activity (184-186), prompted us to examine if the human p202 homolog, IFI16, is involved in IFN-mediated repression of Ad replication. Knockdown of human IFI16 in HDF-TERT cells using shRNAs (Figure 4-8). This result is not surprising since p202 regulates the DNA binding activity of E2F4/DP1 (194) and I found no effect of IFNs on E2F DNA binding properties *in vitro* plus or minus IFNs (Figure 4-5A). In addition to antiviral activities, PML can induce cell senescence in an Rb-dependent manner (195-197). PML relocalized Rb and induced heterochromatin formation and silencing of E2F target genes, leading to cell cycle arrest. However, depletion of PML-NB proteins individually and combinatorially did not alter the inhibitory effect of IFNs on Ad replication in a significant manner, indicating that PML does not regulate the function of the Rb protein.

I found that HDF-TERT cells infected with wild-type Ad5 continued proliferating without lysis over 100 days of maintenance in the presence of IFNγ (Figure 4-9). Viral DNA replication was restricted and maintained at a steady state level (1,000-10,000 viral genomes/cell). This number is comparable to persistent Ad infection in the BJAB and Ramos B cell lines (173). In contrast, HDF-TERT cells infected with wild-type Ad5 and treated with IFNα initially maintained persistent Ad infection but succumbed by day 45 (Figure 4-9). It is not clear why cells treated with IFNα displayed this pattern of infection. Ad5-infected HDF-TERT cells continuously produced low amounts of infectious virus in these experiments suggesting that Ad established a persistent infection, rather than a latent infection, in the presence of IFNs. I attempted to study the effect of IFNs on the properties of Ad infection in lymphocytes (Jurkat and PM1 T cells and BJAB B cells). Even though these cells responded to IFN signaling (STAT1 phosphorylation was detected 1 hr after IFN treatment, STAT1 expression was induced by 24 hr, IFNα and

IFNγ only had a minimal effect on Ad5 replication and E1A expression. Considering these cell lines were derived from leukemias and lymphomas, they likely contain alterations in E2F/Rb signaling.

This is the first study that probes the molecular basis of lytic versus persistent adenovirus infection and reveals a novel mechanism by which adenoviruses utilize IFN signaling to suppress virus replication and promote persistent infection. I established a persistent Ad infection model *in vitro* and demonstrated that IFNγ suppresses productive Ad replication in a manner dependent on the conserved E2F binding site in the E1A enhancer region. These results show that the IFN-E2F/Rb-E1A axis plays a crucial role in the establishment of Ad persistent infection.

Chapter 5 Summary and Future Directions

In this study, I have shown that the E2F binding site located in the E1A enhancer is critical for regulating E1A transcription and subsequential aspects of Ad infection during an IFN response in normal human cells. In contrast, IFNs failed to inhibit WT Ad5 infection in multiple established cancer cell lines. Considering cancers and tumors are featured by uncontrolled cell cycle division, I propose that E2F transcription activity is the key determinant of Ad infection in response to IFN signaling in various cell types. Cancer cells are often associated with aberrant regulation of the E2F/Rb pathway. Disruption of Rb family proteins, activating mutations in cyclinD or CDK4/6, or inactivating mutations in the CDK inhibitors leads to a high level of transcriptionally active E2Fs. Thus, in cancer cells, IFNs are not able to modulate the transcription activities of E2Fs and Ad infection is insensitive to IFN signaling (Figure 5). While in normal cells, the E2F/Rb pathway is intact, E2F transcription activity is controlled by pocket proteins, and E2F/Rb can also be regulated by IFNs. When Ad infects normal cells, E1A transcription is activated by the cellular GABP proteins. Upon IFN stimuli, pocket proteins are enriched in the E1A enhancer to represses E1A transcription. IFNs also prevent the binding of GABP to the E1A enhancer. Consequently, E1A expression is repressed by IFNs in normal cells and Ad infection exits from a lytic life cycle and enters a persistent state (Figure 5).

Although I demonstrated that the IFN-E2F/Rb axis is essential to control E1A transcription, I did not identify the mediator(s) that bridges IFNα/γ to E2F/Rb activity. My data suggested that IFNs are unlikely to modulate E2F/Rb activity canonically. This is because: 1) expression levels of the CDK inhibitors, p16 and p27, are not altered by

IFNs in both infected and uninfected HDF-TERT cells (Figure 4-7A and 4-7B); 2) dephosphorylation of Rb, p107 and p130 are not significantly detected IFN-treated HDF-TERT cells (Figure 4-7C); and, 3) the interaction between E2Fs and pocket proteins is not significantly altered by IFNs as determined using a coIP approach (data not shown). Rb associates with the E1A enhancer in the absence of IFN, while p107 is only recruited to the E1A enhancer following IFNγ treatment. Moreover, p107 and p130 only bind to the E2F site at Ad nt 280 *in vitro* using nuclear extract prepared from HDF-TERT cells, but not HDF-TERT-E1A cells. I speculate that p107 and p130 are the key players regulating E1A expression in response to IFNs, but not Rb. A multisubunit DREAM (DP, Rb-like, E2F and multi-vulval class B [MuvB]) complex is a cell cycle regulator that is only assembled at G_0 phase to repress all cell cycle-dependent gene expression. The DREAM complex contains p107/p130, DP, E2F4/5 and five MuvB proteins (LIN9, LIN37, LIN52, LIN54 and RBBP4) (198). Phosphorylation of LIN52 at Ser28 by dual-specificity Yak1-related kinase 1A (DYRK1A) triggers the association of MuvB with the p107/p130/E2F complex (199). Interestingly, E1A has been shown to interact with DYRK1A via its CR4 region, but the functional significance of this interaction is not fully elucidated (200). Taken together, I postulate that IFNs might induce the formation of the DREAM complex at the E1A enhancer region to repress E1A expression. The following approachs should be useed to test this hypothesis: 1) phosphorylation of LIN52 minus and plus IFNs can be assessed by Western blot--phosphorylated LIN52 can be easily distinguished from unphosphorylated form based on protein mobility on a SDS-PAGE gel; 2) the formation of the DREAM complex can be examined by a coIP assay--Rb-like proteins, p107 and p130, can be immunoprecipitated using specific antibodies, and then LIN52 and other MuvB proteins can be detected by Western blot; 3) the laboratory of Dr. James A. DeCaprio (Dana Farber Cancer Center) established three BJ-hTERT cell lines, a TERT-immortalized human skin fibroblast cell line stably expressing V5-tagged WT

LIN52 or the LIN52 S28A mutant, or LIN52-shRNA. If the DREAM complex mediates the IFN-induced anti-Ad effect, WT Ad5 replication and E1A expression should be resistant to IFN signaling in both LIN52 S28A-expressing and LIN52 shRNA cell lines. LIN52 can also be pulled down using V5-tag from BJ-hTERT-WT LIN52 cells, and then Western performed to detect p107 and p130 in the presence and absence of IFNα/γ; and 4) Harmine, a DYRK inhibitor, blocks the assembly of DREAM complex. If harmine treatment enhanced E1A expression in IFNγ-treated HDF-TERT cells, it suggests that IFNs inhibit E1A transcription in a DREAM complex-dependent manner. In addition to CDK inhibitors and the DREAM complex, we could also examine mRNA levels of a full panel of cell cycle proteins using an RT^2 Profiler^{TM} PCR array (Qiagen Cat. No. PAHS-020Z) to identify the proteins that are regulated by IFNα/γ in HDF-TERT cells.

It is known that IFNs also activate MAPK and PI3K signaling cascades independent of STAT proteins (61). JNK1, also known as MAPK8, reduces DNA binding activities of E2F-1 while p38 can inactivate Rb (201). We could examine the activation of MAPK and PI3K as well as their downstream effectors in IFN-treated HDF-TERT cells. If all of the proposals above failed, a screening of kinase inhibitors should be conducted to identify the inhibitor(s) that counteracts IFN-induced anti-Ad activity.

I only observed the changes of GABP and pocket proteins enrichment in the E1A enhancer region by IFNs *in vivo*, but not *in vitro* (Figure 3-9 and 4-5). An unbiased protemic approach needs to be established to isolate the E2F/Rb co-factor(s), or other repressors associated with the E1A enhancer, only in the presence of IFNs. I propose to perform a reverse ChIP experiment, which requires the efficient capture of a DNA sequence of interest followed by analysis of DNA-bound proteins by mass spectrometry. Particularly, two approaches are reported for the identification of proteins associated with specific genomic loci. Dejardin and Kingston developed a proteomics approach using a

chromatin segments isolation strategy (PICh) to recover telomere-associated proteins (202). This approach does not require genetic engineering of the target sequence. Briefly, cells were fixed and denatured, and chromatin was hybridized with a desthiobiotinlated probe. Then the chromatin-probe complex was pulled down using biotin beads. The chromatin-associated proteins were subjected to MS for identification. PICh requires a large amount of material, and it is very challenging to achieve the requirement if the Ad infection was carried out using the ChIP conditions described in Chapter 2, Materials and Methods. However, HBEC3-KT cells, primary human bronchial epithelial cells immortalized by CDK4 and hTERT, are permissive to Ad5 infection and E1A expression is inhibited by IFNα and IFNγ (data not shown). Thus, we could infect HBEC3-KT cells at 100-200 particles/cell to achieve higher input viral genome copy number as compared to HDF-TERT cells, and then carry out PICh at the early stage of infection. Pourharzad and colleagues established another approach named targeted chromatin purification (TChP) (203). TChP takes advantage of the specific interaction between tetracycline repressor (TetR) and tetracycline operator (TetO) to enrich the genome locus that has been engineered with TetO sites. Ad has low infectivity in HDF-TERT cells compared with that in A549 or NHBEC cells, ~1-4 viral genomes enter the nucleus when cells are infected at 200 virus particles/cell. TChP is more promising since it has been applied for pull-down of the γ-globin locus with only 2 copies per cell. I propose to utilize TChP to identify proteins that recruited to the E1A enhancer region in response to IFN treatment: 1) a replication-deficient Ad5 carrying TetO sites upstream of the E1A enhancer can be constructed. I propose to replace the E1A coding region with GFP sequences, and then insert 7 copies of the TetO sequence (7xTetO) between the ITR and E1A enhancer. This GFP-expressing Ad, named as Ad-ENH-GFP, can be used for the study of E1A transcription solely without viral protein expression and replication. Theoretically, the fluorescent intensity of GFP protein reflects the expression level of E1A

during Ad infection, and can be determined by fluorescence microscopy or flow cytometry rapidly; 2) TetR3T is a triple-tagged TetR protein with a CFP-3xNLS-HA tag-biotinylation triple tag fused to TetR DNA binding domain at the C-terminus (203). The TetR3T protein enables sequential purification using anti-HA and streptavidin beads. Coding sequences of TetR3T and BirA biotin ligase will be inserted into lentiviral expression vectors, and HDF-TERT cells will be transduced with TetR3T and BirA expressing lentivirus; 3) If we could successfully detect GABP by Western blot from Ad-ENH-GFP infected HDF-TERT-TetR3T/BirA cells following TChP, we could infect IFN-treated and -untreated cells with Ad-ENH-GFP virus on a larger scale, and uses MS to identify the proteins specifically enriched at the E1A enhancer in IFN-treated cells. This is a very attractive approach that potentially could be applied in the study of different viral promoters at different stages of Ad infection.

I showed that the enrichment of GABP to the E1A enhancer was negatively correlated with that of E2F/Rb family protein binding *in vivo*. One possibility is that GABP and E2F/Rb proteins compete for binding to the enhancer given the proximity of their binding sites. The other possibility is that IFNs may regulate the binding of GABP and E2F/Rb family proteins to the E1A enhancer through independent mechanisms. I failed to answer this question using an EMSA assay because the formation of GABP-DNA and E2F/Rb-DNA complexes *in vitro* requires different non-specific competitors. When either the 18nt probe or GABP probe was used in EMSA, IFNs did not alter the pattern of protein-DNA complexes (Figures 3-9F and 4-5A), suggesting that it is likely that GABP and E2F/Rb are competing for binding in the E1A enhancer *in vivo*. If IFN regulated GABP and E2F/Rb activities independently, reduced GABP binding and enhanced E2F/Rb binding should also be observed *in vitro*. However, further analysis needs to be carried out. I attempted to quantify the enrichment of cellular proteins in the E1A

enhancer at the input virus level; it is not feasible to perform a ChIP-re-ChIP assay to evaluate co-occupation of GABP and pocket proteins. I can introduce the mut1 mutation into *dl*309-194/243 that does not contain GABP and E2F binding sites at Ad nt 200. If IFNs were still able to block the binding of GABP to this *dl*309-194/243-mut1 virus, it means IFNs regulate GABP and E2F/Rb family proteins independently. In contrast, if GABP and E2F/Rb family proteins compete with each other then a similar level of GABP would be detected in the E1A enhancer region of *dl*309-194/243-mut1 minus and plus IFNs.

So far, it is an open area of research to establish persistence and latency models of Ad infection *in vivo*. Although I successfully established a persistent infection model of Ad5 *in vitro*, it is not clear whether IFNγ promotes Ad persistence or latency *in vivo*. To address this question, we are collaborating with Dr. William S. M. Wold, (Saint Louis University, Missouri) to test our hypothesis in a Syrian hamster infection model using WT Ad5 and Ad5-mut1 viruses. We expect that Ad5-mut1 may have a more pronounced acute phase of infection and/or exhibit reduced persistent or latent infection compared to Ad5 WT. IFNα and IFNγ only have negligible effects on WT Ad5 E1A expression as well as viral replication in human B/T lymphoma cell lines (Figure 4-12 and 4-13). Ad infection is host species restricted, but Ad5 can infect mouse embryonic fibroblasts (MEFs) with low infectivity (data not shown). Ad5 E1A expression and viral replication are repressed by mouse IFNγ (mIFNγ) in MEFs (data not shown). In the next step, we should infect mouse T lymphocytes with WT Ad5 and Ad5-mut1 and test whether mIFNγ is sufficient to driven Ad infection into latency.

IFN signaling induces the expression of hundreds of ISGs. I did not rule out the possibility that certain ISGs might participate in the repression of E1A transcription. Considering that fact that the E4-ORF3 protein only plays a minor role in IFN signaling in normal human cells, Dr. Hearing and I have generated a GFP-tagged Ad5 whose E4-

ORF3 coding sequences were replaced by the GFP gene. This virus replicates similarly to Ad5 WT and is sensitive to IFNα and IFNγ in HDF-TERT cells (data not shown). GFP expression is correlated with viral replication as determined by flow cytometry (data not shown). As an ongoing collaboration, the laboratory of Dr. Charles M. Rice (Rockefeller University) is conducting a high-throughput screen to identify the ISGs that inhibit Ad replication in $STAT1^{-/-}$ MEFs (204)

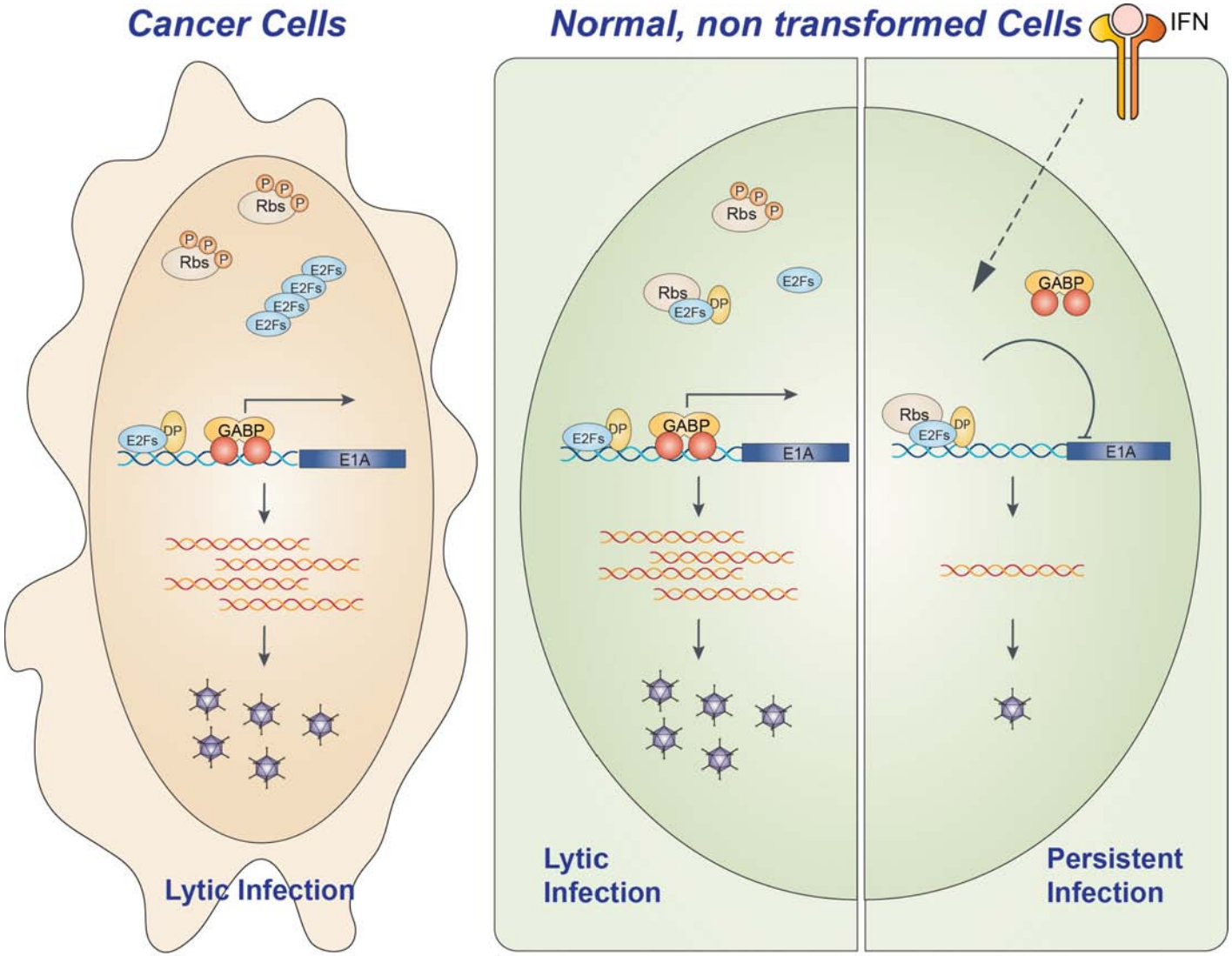

Figure 5-1. A proposed model of the regulation of Ad replication by IFN in normal human cells vs. cancer cells

Reference

1. **HILLEMAN MR**, **WERNER JH**. 1954. Recovery of new agent from patients with acute respiratory illness. Proc. Soc. Exp. Biol. Med. **85**:183–188.

2. **ROWE WP**, **HUEBNER RJ**, **GILMORE LK**, **PARROTT RH**, **WARD TG**. 1953. Isolation of a cytopathogenic agent from human adenoids undergoing spontaneous degeneration in tissue culture. Proc. Soc. Exp. Biol. Med. **84**:570–573.

3. **TRENTIN JJ**, **YABE Y**, **TAYLOR G**. 1962. The quest for human cancer viruses. Science **137**:835–841.

4. **Green M**, **Wold WS**, **Brackmann K**, **Cartas MA**. 1980. Studies on early proteins and transformation proteins of human adenoviruses. Cold Spring Harbor symposia on quantitative biology **44 Pt 1,**:457–469.

5. **Mackey JK**, **Rigden PM**, **Green M**. 1976. Do highly oncogenic group A human adenoviruses cause human cancer? Analysis of human tumors for adenovirus 12 transforming DNA sequences. Proc Natl Acad Sci U S A **73**:4657–4661.

6. **Davison AJ**, **Benkő M**, **Harrach B**. 2003. Genetic content and evolution of adenoviruses. The Journal of general virology **84**:2895–2908.

7. **Liu H**, **Jin L**, **Koh SBS**, **Atanasov I**, **Schein S**, **Wu L**, **Zhou ZH**. 2010. Atomic structure of human adenovirus by cryo-EM reveals interactions among protein networks. Science **329**:1038–1043.

8. **Ginsberg HS**, **Pereira HG**, **Valentine RC**, **Wilcox WC**. 1966. A proposed terminology for the adenovirus antigens and virion morphological subunits. Virology **28**:782–783.

9. **Prage L**, **Pettersson U**. 1971. Structural proteins of adenoviruses. VII. Purification and properties of an arginine-rich core protein from adenovirus type 2 and type 3. Virology **45**:364–373.

10. **Everitt E**, **Lutter L**, **Philipson L**. 1975. Structural proteins of adenoviruses. XII. Location and neighbor relationship among proteins of adenovirion type 2 as revealed by enzymatic iodination, immunoprecipitation and chemical cross-linking. Virology **67**:197–208.

11. **Russell WC**, **Precious B**. 1982. Nucleic acid-binding properties of adenovirus structural polypeptides. The Journal of general virology **63 (Pt 1)**:69–79.

12. **Lonberg-Holm K**, **Philipson L**. 1969. Early events of virus-cell interaction in an adenovirus system. Journal of virology **4**:323–338.

13. **Bergelson JM**, **Cunningham JA**, **Droguett G**, **Kurt-Jones EA**, **Krithivas A**, **Hong JS**, **Horwitz MS**, **Crowell RL**, **Finberg RW**. 1997. Isolation of a common receptor for Coxsackie B viruses and adenoviruses 2 and 5. Science **275**:1320–1323.

14. **Mayr GA**, **Freimuth P**. 1997. A single locus on human chromosome 21 directs the expression of a receptor for adenovirus type 2 in mouse A9 cells. Journal of virology **71**:412–418.

15. **Tomko RP**, **Xu R**, **Philipson L**. 1997. HCAR and MCAR: the human and mouse cellular receptors for subgroup C adenoviruses and group B coxsackieviruses. Proc Natl Acad Sci U S A **94**:3352–3356.

16. **Nemerow GR**, **Stewart PL**. 1999. Role of alpha(v) integrins in adenovirus cell entry and gene delivery. Microbiol. Mol. Biol. Rev. **63**:725–734.

17. **Stewart PL**, **Chiu CY**, **Huang S**, **Muir T**, **Zhao Y**, **Chait B**, **Mathias P**, **Nemerow GR**. 1997. Cryo-EM visualization of an exposed RGD epitope on adenovirus that escapes antibody neutralization. The EMBO journal **16**:1189–1198.

18. **Greber UF**. 2002. Signalling in viral entry. Cell Mol Life Sci **59**:608–626.

19. **Wickham TJ**, **Mathias P**, **Cheresh DA**, **Nemerow GR**. 1993. Integrins alpha v beta 3 and alpha v beta 5 promote adenovirus internalization but not virus attachment. Cell **73**:309–319.

20. **Nakano MY**, **Boucke K**, **Suomalainen M**, **Stidwill RP**, **Greber UF**. 2000. The first step of adenovirus type 2 disassembly occurs at the cell surface, independently of endocytosis and escape to the cytosol. Journal of virology **74**:7085–7095.

21. **Burmeister WP**, **Guilligay D**, **Cusack S**, **Wadell G**, **Arnberg N**. 2004. Crystal structure of species D adenovirus fiber knobs and their sialic acid binding sites. Journal of virology **78**:7727–7736.

22. **Greber UF**, **Webster P**, **Weber J**, **Helenius A**. 1996. The role of the adenovirus protease on virus entry into cells. The EMBO journal **15**:1766–1777.

23. **Dales S**, **Chardonnet Y**. 1973. Early events in the interaction of adenoviruses with HeLa cells. IV. Association with microtubules and the nuclear pore complex during vectorial movement of the inoculum. Virology **56**:465–483.

24. **Greber UF**, **Way M**. 2006. A superhighway to virus infection. Cell **124**:741–754.

25. **Leopold PL**, **Kreitzer G**, **Miyazawa N**, **Rempel S**, **Pfister KK**, **Rodriguez-Boulan E**, **Crystal RG**. 2000. Dynein- and microtubule-mediated translocation of adenovirus serotype 5 occurs after endosomal lysis. Hum Gene Ther **11**:151–165.

26. **Suomalainen M**, **Nakano MY**, **Keller S**, **Boucke K**, **Stidwill RP**, **Greber UF**.

1999. Microtubule-dependent plus- and minus end-directed motilities are competing processes for nuclear targeting of adenovirus. J Cell Biol **144**:657–672.

27. **Trotman LC**, **Mosberger N**, **Fornerod M**, **Stidwill RP**, **Greber UF**. 2001. Import of adenovirus DNA involves the nuclear pore complex receptor CAN/Nup214 and histone H1. Nature cell biology **3**:1092–1100.

28. **Karen KA**, **Hearing P**. 2011. Adenovirus core protein VII protects the viral genome from a DNA damage response at early times after infection. Journal of virology, 2011 ed. **85**:4135–4142.

29. **Komatsu T**, **Nagata K**. 2012. Replication-uncoupled histone deposition during adenovirus DNA replication. Journal of virology, 2012 ed.

30. **Komatsu T**, **Haruki H**, **Nagata K**. 2011. Cellular and viral chromatin proteins are positive factors in the regulation of adenovirus gene expression. Nucleic acids research, 2010 ed. **39**:889–901.

31. **Nakanishi Y**, **Maeda K**, **Ohtsuki M**, **Hosokawa K**, **Natori S**. 1986. In vitro transcription of a chromatin-like complex of major core protein VII and DNA of adenovirus serotype 2. Biochem Biophys Res Commun, 1986 ed. **136**:86–93.

32. **Chen J**, **Morral N**, **Engel DA**. 2007. Transcription releases protein VII from adenovirus chromatin. Virology, 2007 ed. **369**:411–422.

33. **Gyurcsik B**, **Haruki H**, **Takahashi T**, **Mihara H**, **Nagata K**. 2006. Binding modes of the precursor of adenovirus major core protein VII to DNA and template activating factor I: implication for the mechanism of remodeling of the adenovirus chromatin. Biochemistry, 2006 ed. **45**:303–313.

34. **Xue Y**, **Johnson JS**, **Ornelles DA**, **Lieberman J**, **Engel DA**. 2005. Adenovirus protein VII functions throughout early phase and interacts with cellular proteins SET and pp32. Journal of virology, 2005 ed. **79**:2474–2483.

35. **Haruki H**, **Gyurcsik B**, **Okuwaki M**, **Nagata K**. 2003. Ternary complex formation between DNA-adenovirus core protein VII and TAF-Ibeta/SET, an acidic molecular chaperone. FEBS Lett **555**:521–527.

36. **Nevins JR**, **Ginsberg HS**, **Blanchard JM**, **Wilson MC**, **Darnell JEJ**. 1979. Regulation of the primary expression of the early adenovirus transcription units. Journal of virology, 1979 ed. **32**:727–733.

37. **Cuconati A**, **Mukherjee C**, **Perez D**, **White E**. 2003. DNA damage response and MCL-1 destruction initiate apoptosis in adenovirus-infected cells. Genes Dev **17**:2922–2932.

38. **Cuconati A**, **White E**. 2002. Viral homologs of BCL-2: role of apoptosis in the regulation of virus infection. Genes Dev **16**:2465–2478.

39. **Harada JN**, **Shevchenko A**, **Shevchenko A**, **Pallas DC**, **Berk AJ**. 2002.

Analysis of the adenovirus E1B-55K-anchored proteome reveals its link to ubiquitination machinery. Journal of virology **76**:9194–9206.

40. **Querido E**, **Blanchette P**, **Yan Q**, **Kamura T**, **Morrison M**, **Boivin D**, **Kaelin WG**, **Conaway RC**, **Conaway JW**, **Branton PE**. 2001. Degradation of p53 by adenovirus E4orf6 and E1B55K proteins occurs via a novel mechanism involving a Cullin-containing complex. Genes Dev **15**:3104–3117.

41. **Teodoro JG**, **Branton PE**. 1997. Regulation of p53-dependent apoptosis, transcriptional repression, and cell transformation by phosphorylation of the 55-kilodalton E1B protein of human adenovirus type 5. Journal of virology **71**:3620–3627.

42. **Yew PR**, **Berk AJ**. 1992. Inhibition of p53 transactivation required for transformation by adenovirus early 1B protein. Nature **357**:82–85.

43. **Carson CT**, **Schwartz RA**, **Stracker TH**, **Lilley CE**, **Lee DV**, **Weitzman MD**. 2003. The Mre11 complex is required for ATM activation and the G2/M checkpoint. The EMBO journal **22**:6610–6620.

44. **Boyer J**, **Rohleder K**, **Ketner G**. 1999. Adenovirus E4 34k and E4 11k inhibit double strand break repair and are physically associated with the cellular DNA-dependent protein kinase. Virology **263**:307–312.

45. **Stracker TH**, **Carson CT**, **Weitzman MD**. 2002. Adenovirus oncoproteins inactivate the Mre11-Rad50-NBS1 DNA repair complex. Nature, 2002nd ed. **418**:348–352.

46. **Ullman AJ**, **Reich NC**, **Hearing P**. 2007. Adenovirus E4 ORF3 protein inhibits the interferon-mediated antiviral response. Journal of virology, 2007 ed. **81**:4744–4752.

47. **Ullman AJ**, **Hearing P**. 2008. Cellular proteins PML and Daxx mediate an innate antiviral defense antagonized by the adenovirus E4 ORF3 protein. Journal of virology, 2008 ed. **82**:7325–7335.

48. **Temperley SM**, **Hay RT**. 1992. Recognition of the adenovirus type 2 origin of DNA replication by the virally encoded DNA polymerase and preterminal proteins. The EMBO journal **11**:761–768.

49. **Chen M**, **Mermod N**, **Horwitz MS**. 1990. Protein-protein interactions between adenovirus DNA polymerase and nuclear factor I mediate formation of the DNA replication preinitiation complex. The Journal of biological chemistry **265**:18634–18642.

50. **Mul YM**, **van der Vliet, P. C.** 1992. Nuclear factor I enhances adenovirus DNA replication by increasing the stability of a preinitiation complex. The EMBO journal **11**:751–760.

51. **Mul YM**, **Verrijzer CP**, **van der Vliet, P. C.** 1990. Transcription factors NFI and NFIII/oct-1 function independently, employing different mechanisms to enhance

adenovirus DNA replication. Journal of virology **64**:5510–5518.

52. **van Leeuwen HC**, **Rensen M**, **van der Vliet, P. C.** 1997. The Oct-1 POU homeodomain stabilizes the adenovirus preinitiation complex via a direct interaction with the priming protein and is displaced when the replication fork passes. The Journal of biological chemistry **272**:3398–3405.

53. **Smart JE**, **Stillman BW**. 1982. Adenovirus terminal protein precursor. Partial amino acid sequence and the site of covalent linkage to virus DNA. The Journal of biological chemistry **257**:13499–13506.

54. **Nagata K**, **Guggenheimer RA**, **Hurwitz J**. 1983. Adenovirus DNA replication in vitro: synthesis of full-length DNA with purified proteins. Proc Natl Acad Sci U S A **80**:4266–4270.

55. **Ostapchuk P**, **Hearing P**. 2008. Adenovirus IVa2 protein binds ATP. Journal of virology, 2008 ed. **82**:10290–10294.

56. **Ostapchuk P**, **Almond M**, **Hearing P**. 2011. Characterization of Empty adenovirus particles assembled in the absence of a functional adenovirus IVa2 protein. Journal of virology, 2011 ed. **85**:5524–5531.

57. **Chen PH**, **Ornelles DA**, **Shenk T**. 1993. The adenovirus L3 23-kilodalton proteinase cleaves the amino-terminal head domain from cytokeratin 18 and disrupts the cytokeratin network of HeLa cells. Journal of virology **67**:3507–3514.

58. **Tollefson AE**, **Scaria A**, **Hermiston TW**, **Ryerse JS**, **Wold LJ**, **Wold WS**. 1996. The adenovirus death protein (E3-11.6K) is required at very late stages of infection for efficient cell lysis and release of adenovirus from infected cells. Journal of virology **70**:2296–2306.

59. **Walters RW**, **Freimuth P**, **Moninger TO**, **Ganske I**, **Zabner J**, **Welsh MJ**. 2002. Adenovirus fiber disrupts CAR-mediated intercellular adhesion allowing virus escape. Cell **110**:789–799.

60. **McNab F**, **Mayer-Barber K**, **Sher A**, **Wack A**, **O'Garra A**. 2015. Type I interferons in infectious disease. Nat Rev Immunol **15**:87–103.

61. **Platanias LC**. 2005. Mechanisms of type-I- and type-II-interferon-mediated signalling. Nat Rev Immunol, 2005 ed. **5**:375–386.

62. **Chen J**, **Baig E**, **Fish EN**. 2004. Diversity and relatedness among the type I interferons. Journal of interferon & cytokine research : the official journal of the International Society for Interferon and Cytokine Research **24**:687–698.

63. **Darnell JE**. 1997. STATs and gene regulation. Science **277**:1630–1635.

64. **Bach EA**, **Aguet M**, **Schreiber RD**. 1997. The IFN gamma receptor: a paradigm for cytokine receptor signaling. Annu. Rev. Immunol. **15**:563–591.

65. **Zhou Z**, **Hamming OJ**, **Ank N**, **Paludan SR**, **Nielsen AL**, **Hartmann R**. 2007. Type III interferon (IFN) induces a type I IFN-like response in a restricted subset of cells through signaling pathways involving both the Jak-STAT pathway and the mitogen-activated protein kinases. Journal of virology **81**:7749–7758.

66. **Levraud J-P**, **Boudinot P**, **Colin I**, **Benmansour A**, **Peyrieras N**, **Herbomel P**, **Lutfalla G**. 2007. Identification of the zebrafish IFN receptor: implications for the origin of the vertebrate IFN system. J. Immunol. **178**:4385–4394.

67. **Sadler AJ**, **Williams BR**. 2008. Interferon-inducible antiviral effectors. Nat Rev Immunol, 2008 ed. **8**:559–568.

68. **Rebouillat D**, **Hovanessian AG**. 1999. The human 2“,5-”oligoadenylate synthetase family: interferon-induced proteins with unique enzymatic properties. Journal of interferon & cytokine research : the official journal of the International Society for Interferon and Cytokine Research **19**:295–308.

69. **Malathi K**, **Dong B**, **Gale M**, **Silverman RH**. 2007. Small self-RNA generated by RNase L amplifies antiviral innate immunity. Nature **448**:816–819.

70. **Dar AC**, **Dever TE**, **Sicheri F**. 2005. Higher-order substrate recognition of eIF2alpha by the RNA-dependent protein kinase PKR. Cell **122**:887–900.

71. **Dey M**, **Cao C**, **Dar AC**, **Tamura T**, **Ozato K**, **Sicheri F**, **Dever TE**. 2005. Mechanistic link between PKR dimerization, autophosphorylation, and eIF2alpha substrate recognition. Cell **122**:901–913.

72. **Borden EC**, **Sen GC**, **Uze G**, **Silverman RH**, **Ransohoff RM**, **Foster GR**, **Stark GR**. 2007. Interferons at age 50: past, current and future impact on biomedicine. Nat Rev Drug Discov **6**:975–990.

73. **Blasius AL**, **Beutler B**. 2010. Intracellular toll-like receptors. Immunity, 2010 ed. **32**:305–315.

74. **Rathinam VA**, **Fitzgerald KA**. 2011. Innate immune sensing of DNA viruses. Virology, 2011 ed. **411**:153–162.

75. **Takaoka A**, **Wang Z**, **Choi MK**, **Yanai H**, **Negishi H**, **Ban T**, **Lu Y**, **Miyagishi M**, **Kodama T**, **Honda K**, **Ohba Y**, **Taniguchi T**. 2007. DAI (DLM-1/ZBP1) is a cytosolic DNA sensor and an activator of innate immune response. Nature, 2007 ed. **448**:501–505.

76. **Roberts TL**, **Idris A**, **Dunn JA**, **Kelly GM**, **Burnton CM**, **Hodgson S**, **Hardy LL**, **Garceau V**, **Sweet MJ**, **Ross IL**, **Hume DA**, **Stacey KJ**. 2009. HIN-200 proteins regulate caspase activation in response to foreign cytoplasmic DNA. Science, 2009 ed. **323**:1057–1060.

77. **Schattgen SA**, **Fitzgerald KA**. 2011. The PYHIN protein family as mediators of host defenses. Immunol Rev **243**:109–118.

78. **Fernandes-Alnemri T**, **Yu JW**, **Datta P**, **Wu J**, **Alnemri ES**. 2009. AIM2

activates the inflammasome and cell death in response to cytoplasmic DNA. Nature, 2009 ed. **458**:509–513.

79. **Panchanathan R**, **Duan X**, **Shen H**, **Rathinam VA**, **Erickson LD**, **Fitzgerald KA**, **Choubey D**. 2010. Aim2 deficiency stimulates the expression of IFN-inducible Ifi202, a lupus susceptibility murine gene within the Nba2 autoimmune susceptibility locus. J. Immunol., 2010 ed. **185**:7385–7393.

80. **Unterholzner L**, **Keating SE**, **Baran M**, **Horan KA**, **Jensen SB**, **Sharma S**, **Sirois CM**, **Jin T**, **Latz E**, **Xiao TS**, **Fitzgerald KA**, **Paludan SR**, **Bowie AG**. 2010. IFI16 is an innate immune sensor for intracellular DNA. Nat Immunol, 2010 ed. **11**:997–1004.

81. **Kerur N**, **Veettil MV**, **Sharma-Walia N**, **Bottero V**, **Sadagopan S**, **Otageri P**, **Chandran B**. 2011. IFI16 acts as a nuclear pathogen sensor to induce the inflammasome in response to Kaposi Sarcoma-associated herpesvirus infection. Cell Host Microbe, 2011 ed. **9**:363–375.

82. **Johnson KE**, **Bottero V**, **Flaherty S**, **Dutta S**, **Singh VV**, **Chandran B**. 2014. IFI16 Restricts HSV-1 Replication by Accumulating on the HSV-1 Genome, Repressing HSV-1 Gene Expression, and Directly or Indirectly Modulating Histone Modifications. PLoS Pathog **10**:e1004503.

83. **Orzalli MH**, **Conwell SE**, **Berrios C**, **DeCaprio JA**, **Knipe DM**. 2013. Nuclear interferon-inducible protein 16 promotes silencing of herpesviral and transfected DNA. Proc Natl Acad Sci U S A **110**:E4492–501.

84. **Zhang Z**, **Yuan B**, **Bao M**, **Lu N**, **Kim T**, **Liu YJ**. 2011. The helicase DDX41 senses intracellular DNA mediated by the adaptor STING in dendritic cells. Nat Immunol, 2011 ed. **12**:959–965.

85. **Wu J**, **Sun L**, **Chen X**, **Du F**, **Shi H**, **Chen C**, **Chen ZJ**. 2013. Cyclic GMP-AMP is an endogenous second messenger in innate immune signaling by cytosolic DNA. Science **339**:826–830.

86. **Sun L**, **Wu J**, **Du F**, **Chen X**, **Chen ZJ**. 2013. Cyclic GMP-AMP synthase is a cytosolic DNA sensor that activates the type I interferon pathway. Science **339**:786–791.

87. **Cerullo V**, **Seiler MP**, **Mane V**, **Brunetti-Pierri N**, **Clarke C**, **Bertin TK**, **Rodgers JR**, **Lee B**. 2007. Toll-like receptor 9 triggers an innate immune response to helper-dependent adenoviral vectors. Mol Ther, 2007 ed. **15**:378–385.

88. **Zhu J**, **Huang X**, **Yang Y**. 2007. Innate immune response to adenoviral vectors is mediated by both Toll-like receptor-dependent and -independent pathways. Journal of virology, 2007 ed. **81**:3170–3180.

89. **Stein SC**, **Falck-Pedersen E**. 2012. Sensing Adenovirus Infection: Activation of Interferon Regulatory Factor 3 in RAW 264.7 Cells. Journal of virology, 2012 ed. **86**:4527–4537.

90. **Lam E**, **Stein S**, **Falck-Pedersen E**. 2014. Adenovirus detection by the cGAS/STING/TBK1 DNA sensing cascade. Journal of virology **88**:974–981.

91. **Stein SC**, **Lam E**, **Falck-Pedersen E**. 2012. Cell-specific regulation of nucleic Acid sensor cascades: a controlling interest in the antiviral response. Journal of virology **86**:13303–13312.

92. 1995. Activation of interferon-inducible 2“-5” oligoadenylate synthetase by adenoviral VAI RNA, 1995 ed. **270**:3454–3461.

93. **Yu J**, **Boyapati A**, **Rundell K**. 2001. Critical role for SV40 small-t antigen in human cell transformation. Virology **290**:192–198.

94. **Reich NC**, **Sarnow P**, **Duprey E**, **Levine AJ**. 1983. Monoclonal antibodies which recognize native and denatured forms of the adenovirus DNA-binding protein. Virology **128**:480–484.

95. **Nevels M**, **Tauber B**, **Kremmer E**, **Spruss T**, **Wolf H**, **Dobner T**. 1999. Transforming potential of the adenovirus type 5 E4orf3 protein. Journal of virology **73**:1591–1600.

96. **Sarnow P**, **Sullivan CA**, **Levine AJ**. 1982. A monoclonal antibody detecting the adenovirus type 5-E1b-58Kd tumor antigen: characterization of the E1b-58Kd tumor antigen in adenovirus-infected and -transformed cells. Virology **120**:510–517.

97. **Gräble M**, **Hearing P**. 1990. Adenovirus type 5 packaging domain is composed of a repeated element that is functionally redundant. Journal of virology **64**:2047–2056.

98. **Hearing P**, **Shenk T**. 1983. Functional analysis of the nucleotide sequence surrounding the cap site for adenovirus type 5 region E1A messenger RNAs. Journal of molecular biology, 1983rd ed. **167**:809–822.

99. **Jones N**, **Shenk T**. 1979. An adenovirus type 5 early gene function regulates expression of other early viral genes. Proc Natl Acad Sci U S A, 1979 ed. **76**:3665–3669.

100. **Chartier C**, **Degryse E**, **Gantzer M**, **Dieterle A**, **Pavirani A**, **Mehtali M**. 1996. Efficient generation of recombinant adenovirus vectors by homologous recombination in Escherichia coli. Journal of virology, 1996 ed. **70**:4805–4810.

101. **Pfaffl MW**. 2001. A new mathematical model for relative quantification in real-time RT-PCR. Nucleic acids research **29**:e45.

102. **Zheng Y**, **Hearing P**. 2014. The use of chromatin immunoprecipitation (ChIP) to study the binding of viral proteins to the adenovirus genome in vivo. Methods Mol Biol **1089**:79–87.

103. **Tavalai N**, **Papior P**, **Rechter S**, **Stamminger T**. 2008. Nuclear domain 10 components promyelocytic leukemia protein and hDaxx independently

contribute to an intrinsic antiviral defense against human cytomegalovirus infection. Journal of virology, 2007 ed. **82**:126–137.

104. **Adler M**, **Tavalai N**, **Muller R**, **Stamminger T**. 2011. Human cytomegalovirus immediate-early gene expression is restricted by the nuclear domain 10 component Sp100. The Journal of general virology, 2011 ed. **92**:1532–1538.

105. **Glass M**, **Everett RD**. 2012. Components of PML Nuclear Bodies (ND10) act cooperatively to repress herpesvirus infection. Journal of virology.

106. **Anderson KP**, **Fennie EH**. 1987. Adenovirus early region 1A modulation of interferon antiviral activity. Journal of virology, 1987 ed. **61**:787–795.

107. **Kitajewski J**, **Schneider RJ**, **Safer B**, **Munemitsu SM**, **Samuel CE**, **Thimmappaya B**, **Shenk T**. 1986. Adenovirus VAI RNA antagonizes the antiviral action of interferon by preventing activation of the interferon-induced eIF-2 alpha kinase. Cell, 1986 ed. **45**:195–200.

108. **Look DC**, **Roswit WT**, **Frick AG**, **Gris-Alevy Y**, **Dickhaus DM**, **Walter MJ**, **Holtzman MJ**. 1998. Direct suppression of Stat1 function during adenoviral infection. Immunity, 1999 ed. **9**:871–880.

109. **Kalvakolanu DV**, **Bandyopadhyay SK**, **Harter ML**, **Sen GC**. 1991. Inhibition of interferon-inducible gene expression by adenovirus E1A proteins: block in transcriptional complex formation. Proc Natl Acad Sci U S A, 1991st ed. **88**:7459–7463.

110. **Gutch MJ**, **Reich NC**. 1991. Repression of the interferon signal transduction pathway by the adenovirus E1A oncogene. Proc Natl Acad Sci U S A, 1991st ed. **88**:7913–7917.

111. **Ackrill AM**, **Foster GR**, **Laxton CD**, **Flavell DM**, **Stark GR**, **Kerr IM**. 1991. Inhibition of the cellular response to interferons by products of the adenovirus type 5 E1A oncogene. Nucleic acids research, 1991st ed. **19**:4387–4393.

112. **Reich N**, **Pine R**, **Levy D**, **Darnell JEJ**. 1988. Transcription of interferon-stimulated genes is induced by adenovirus particles but is suppressed by E1A gene products. Journal of virology, 1988 ed. **62**:114–119.

113. **Fonseca GJ**, **Thillainadesan G**, **Yousef AF**, **Ablack JN**, **Mossman KL**, **Torchia J**, **Mymryk JS**. 2012. Adenovirus evasion of interferon-mediated innate immunity by direct antagonism of a cellular histone posttranslational modification. Cell Host Microbe **11**:597–606.

114. **Lau L**, **Gray EE**, **Brunette RL**, **Stetson DB**. 2015. DNA tumor virus oncogenes antagonize the cGAS-STING DNA sensing pathway. Science.

115. **Chahal JS**, **Qi J**, **Flint SJ**. 2012. The Human Adenovirus Type 5 E1B 55 kDa Protein Obstructs Inhibition of Viral Replication by Type I Interferon in Normal Human Cells. PLoS Pathog, 2012 ed. **8**:e1002853.

116. **Chahal JS**, **Gallagher C**, **DeHart CJ**, **Flint SJ**. 2013. The repression domain of the E1B 55-kilodalton protein participates in countering interferon-induced inhibition of adenovirus replication. Journal of virology **87**:4432–4444.

117. **Geoffroy MC**, **Chelbi-Alix MK**. 2011. Role of promyelocytic leukemia protein in host antiviral defense. Journal of interferon & cytokine research : the official journal of the International Society for Interferon and Cytokine Research, 2011 ed. **31**:145–158.

118. **Toth K**, **Lee SR**, **Ying B**, **Spencer JF**, **Tollefson AE**, **Sagartz JE**, **Kong I-K**, **Wang Z**, **Wold WSM**. 2015. STAT2 Knockout Syrian Hamsters Support Enhanced Replication and Pathogenicity of Human Adenovirus, Revealing an Important Role of Type I Interferon Response in Viral Control. PLoS Pathog **11**:e1005084.

119. **Bernardi R**, **Pandolfi PP**. 2007. Structure, dynamics and functions of promyelocytic leukaemia nuclear bodies. Nature reviews. Molecular cell biology, 2007 ed. **8**:1006–1016.

120. **Everett RD**, **Chelbi-Alix MK**. 2007. PML and PML nuclear bodies: implications in antiviral defence. Biochimie, 2007 ed. **89**:819–830.

121. **Hwang J**, **Kalejta RF**. 2007. Proteasome-dependent, ubiquitin-independent degradation of Daxx by the viral pp71 protein in human cytomegalovirus-infected cells. Virology, 2007 ed. **367**:334–338.

122. **Wilkinson GW**, **Kelly C**, **Sinclair JH**, **Rickards C**. 1998. Disruption of PML-associated nuclear bodies mediated by the human cytomegalovirus major immediate early gene product. The Journal of general virology, 1998 ed. **79 (Pt 5)**:1233–1245.

123. **Saffert RT**, **Kalejta RF**. 2006. Inactivating a cellular intrinsic immune defense mediated by Daxx is the mechanism through which the human cytomegalovirus pp71 protein stimulates viral immediate-early gene expression. Journal of virology, 2006 ed. **80**:3863–3871.

124. **Korioth F**, **Maul GG**, **Plachter B**, **Stamminger T**, **Frey J**. 1996. The nuclear domain 10 (ND10) is disrupted by the human cytomegalovirus gene product IE1. Experimental cell research, 1996 ed. **229**:155–158.

125. **Muller S**, **Dejean A**. 1999. Viral immediate-early proteins abrogate the modification by SUMO-1 of PML and Sp100 proteins, correlating with nuclear body disruption. Journal of virology **73**:5137–5143.

126. **Berscheminski J**, **Wimmer P**, **Brun J**, **Ip WH**, **Groitl P**, **Horlacher T**, **Jaffray E**, **Hay RT**, **Dobner T**, **Schreiner S**. 2014. Sp100 isoform-specific regulation of human adenovirus 5 gene expression. Journal of virology **88**:6076–6092.

127. **Berk AJ**. 2005. Recent lessons in gene expression, cell cycle control, and cell biology from adenovirus. Oncogene **24**:7673–7685.

128. **Radko S**, **Koleva M**, **James KMD**, **Jung R**, **Mymryk JS**, **Pelka P**. 2014. Adenovirus E1A targets the DREF nuclear factor to regulate virus gene expression, DNA replication, and growth. Journal of virology **88**:13469–13481.

129. **Whyte P**, **Williamson NM**, **Harlow E**. 1989. Cellular targets for transformation by the adenovirus E1A proteins. Cell **56**:67–75.

130. **Dick FA**, **Rubin SM**. 2013. Molecular mechanisms underlying RB protein function. Nature reviews. Molecular cell biology **14**:297–306.

131. **Knudsen ES**, **Knudsen KE**. 2008. Tailoring to RB: tumour suppressor status and therapeutic response. Nat Rev Cancer **8**:714–724.

132. **Harbour JW**, **Dean DC**. 2000. The Rb/E2F pathway: expanding roles and emerging paradigms. Genes Dev **14**:2393–2409.

133. **Hearing P**, **Shenk T**. 1986. The adenovirus type 5 E1A enhancer contains two functionally distinct domains: one is specific for E1A and the other modulates all early units in cis. Cell, 1983rd ed. **33**:695–703.

134. **Bolwig GM**, **Bruder JT**, **Hearing P**. 1992. Different binding site requirements for binding and activation for the bipartite enhancer factor EF-1A. Nucleic acids research, 1992nd ed. **20**:6555–6564.

135. **Bruder JT**, **Hearing P**. 1989. Nuclear factor EF-1A binds to the adenovirus E1A core enhancer element and to other transcriptional control regions. Molecular and cellular biology, 1989 ed. **9**:5143–5153.

136. **Bruder JT**, **Hearing P**. 1991. Cooperative binding of EF-1A to the E1A enhancer region mediates synergistic effects on E1A transcription during adenovirus infection. Journal of virology, 1991st ed. **65**:5084–5087.

137. **Kovesdi I**, **Reichel R**, **Nevins JR**. 1986. Identification of a cellular transcription factor involved in E1A trans-activation. Cell, 1986 ed. **45**:219–228.

138. **Kovesdi I**, **Reichel R**, **Nevins JR**. 1987. Role of an adenovirus E2 promoter binding factor in E1A-mediated coordinate gene control. Proc Natl Acad Sci U S A **84**:2180–2184.

139. **Rosmarin AG**, **Resendes KK**, **Yang Z**, **McMillan JN**, **Fleming SL**. 2004. GA-binding protein transcription factor: a review of GABP as an integrator of intracellular signaling and protein-protein interactions. Blood Cells Mol. Dis. **32**:143–154.

140. **LaMarco K**, **Thompson CC**, **Byers BP**, **Walton EM**, **McKnight SL**. 1991. Identification of Ets- and notch-related subunits in GA binding protein. Science, 1991st ed. **253**:789–792.

141. **Chinenov Y**, **Schmidt T**, **Yang XY**, **Martin ME**. 1998. Identification of redox-sensitive cysteines in GA-binding protein-alpha that regulate DNA binding and heterodimerization. The Journal of biological chemistry **273**:6203–6209.

142. **Wu H**, **Xiao Y**, **Zhang S**, **Ji S**, **Wei L**, **Fan F**, **Geng J**, **Tian J**, **Sun X**, **Qin F**, **Jin C**, **Lin J**, **Yin Z-Y**, **Zhang T**, **Luo L**, **Li Y**, **Song S**, **Lin S-C**, **Deng X**, **Camargo F**, **Avruch J**, **Chen L**, **Zhou D**. 2013. The Ets transcription factor GABP is a component of the hippo pathway essential for growth and antioxidant defense. Cell Rep **3**:1663–1677.

143. **Sawa C**, **Goto M**, **Suzuki F**, **Watanabe H**, **Sawada J**, **Handa H**. 1996. Functional domains of transcription factor hGABP beta1/E4TF1-53 required for nuclear localization and transcription activation. Nucleic acids research, 1996 ed. **24**:4954–4961.

144. **Jones C**, **Lee KA**. 1991. E1A-mediated activation of the adenovirus E4 promoter can occur independently of the cellular transcription factor E4F. Molecular and cellular biology **11**:4297–4305.

145. **Nishikawa N**, **Izumi M**, **Yokoi M**, **Miyazawa H**, **Hanaoka F**. 2001. E2F regulates growth-dependent transcription of genes encoding both catalytic and regulatory subunits of mouse primase. Genes Cells **6**:57–70.

146. **Izumi M**, **Yokoi M**, **Nishikawa NS**, **Miyazawa H**, **Sugino A**, **Yamagishi M**, **Yamaguchi M**, **Matsukage A**, **Yatagai F**, **Hanaoka F**. 2000. Transcription of the catalytic 180-kDa subunit gene of mouse DNA polymerase alpha is controlled by E2F, an Ets-related transcription factor, and Sp1. Biochimica et biophysica acta, 2000 ed. **1492**:341–352.

147. **Hauck L**, **Kaba RG**, **Lipp M**, **Dietz R**, **Harsdorf von R**. 2002. Regulation of E2F1-dependent gene transcription and apoptosis by the ETS-related transcription factor GABPgamma1. Molecular and cellular biology **22**:2147–2158.

148. **Freimuth PI**, **Ginsberg HS**. 1986. Codon insertion mutants of the adenovirus terminal protein. Proc Natl Acad Sci U S A **83**:7816–7820.

149. **Miralles VJ**, **Cortes P**, **Stone N**, **Reinberg D**. 1989. The adenovirus inverted terminal repeat functions as an enhancer in a cell-free system. The Journal of biological chemistry **264**:10763–10772.

150. **Ross PJ**, **Kennedy MA**, **Christou C**, **Risco Quiroz M**, **Poulin KL**, **Parks RJ**. 2011. Assembly of helper-dependent adenovirus DNA into chromatin promotes efficient gene expression. Journal of virology, 2011 ed. **85**:3950–3958.

151. **Johnson JS**, **Osheim YN**, **Xue Y**, **Emanuel MR**, **Lewis PW**, **Bankovich A**, **Beyer AL**, **Engel DA**. 2004. Adenovirus protein VII condenses DNA, represses transcription, and associates with transcriptional activator E1A. Journal of virology, 2004 ed. **78**:6459–6468.

152. **Fang TC**, **Schaefer U**, **Mecklenbrauker I**, **Stienen A**, **Dewell S**, **Chen MS**, **Rioja I**, **Parravicini V**, **Prinjha RK**, **Chandwani R**, **MacDonald MR**, **Lee K**, **Rice CM**, **Tarakhovsky A**. 2012. Histone H3 lysine 9 di-methylation as an epigenetic signature of the interferon response. J Exp Med **209**:661–669.

153. **Strahl BD**, **Allis CD**. 2000. The language of covalent histone modifications. Nature **403**:41–45.

154. **Hake SB**, **Allis CD**. 2006. Histone H3 variants and their potential role in indexing mammalian genomes: the "H3 barcode hypothesis". Proc Natl Acad Sci U S A **103**:6428–6435.

155. **Goldberg AD**, **Banaszynski LA**, **Noh KM**, **Lewis PW**, **Elsaesser SJ**, **Stadler S**, **Dewell S**, **Law M**, **Guo X**, **Li X**, **Wen D**, **Chapgier A**, **DeKelver RC**, **Miller JC**, **Lee YL**, **Boydston EA**, **Holmes MC**, **Gregory PD**, **Greally JM**, **Rafii S**, **Yang C**, **Scambler PJ**, **Garrick D**, **Gibbons RJ**, **Higgs DR**, **Cristea IM**, **Urnov FD**, **Zheng D**, **Allis CD**. 2010. Distinct factors control histone variant H3.3 localization at specific genomic regions. Cell, 2010 ed. **140**:678–691.

156. **Tagami H**, **Ray-Gallet D**, **Almouzni G**, **Nakatani Y**. 2004. Histone H3.1 and H3.3 complexes mediate nucleosome assembly pathways dependent or independent of DNA synthesis. Cell **116**:51–61.

157. **Ahmad K**, **Henikoff S**. 2002. The histone variant H3.3 marks active chromatin by replication-independent nucleosome assembly. Molecular cell, 2002nd ed. **9**:1191–1200.

158. **Evans JD**, **Hearing P**. 2003. Distinct roles of the Adenovirus E4 ORF3 protein in viral DNA replication and inhibition of genome concatenation. Journal of virology, 2003rd ed. **77**:5295–5304.

159. **Boutell C**, **Cuchet-Lourenço D**, **Vanni E**, **Orr A**, **Glass M**, **McFarlane S**, **Everett RD**. 2011. A viral ubiquitin ligase has substrate preferential SUMO targeted ubiquitin ligase activity that counteracts intrinsic antiviral defence. PLoS Pathog **7**:e1002245.

160. **Tavalai N**, **Adler M**, **Scherer M**, **Riedl Y**, **Stamminger T**. 2011. Evidence for a dual antiviral role of the major nuclear domain 10 component Sp100 during the immediate-early and late phases of the human cytomegalovirus replication cycle. Journal of virology, 2011 ed. **85**:9447–9458.

161. **Diner BA**, **Lum KK**, **Cristea IM**. 2015. The Emerging Role of Nuclear Viral DNA Sensors. The Journal of biological chemistry **290**:26412–26421.

162. **Giberson AN**, **Davidson AR**, **Parks RJ**. 2012. Chromatin structure of adenovirus DNA throughout infection. Nucleic acids research **40**:2369–2376.

163. **Bertoli C**, **Skotheim JM**, **de Bruin RAM**. 2013. Control of cell cycle transcription during G1 and S phases. Nature reviews. Molecular cell biology **14**:518–528.

164. **Hanahan D**, **Weinberg RA**. 2000. The hallmarks of cancer. Cell **100**:57–70.

165. **O'Connor RJ**, **Schaley JE**, **Feeney G**, **Hearing P**. 2001. The p107 tumor suppressor induces stable E2F DNA binding to repress target promoters. Oncogene **20**:1882–1891.

166. **O'Connor RJ**, **Hearing P**. 2000. The E4-6/7 protein functionally compensates for the loss of E1A expression in adenovirus infection. Journal of virology **74**:5819–5824.

167. **Hardy S**, **Engel DA**, **Shenk T**. 1989. An adenovirus early region 4 gene product is required for induction of the infection-specific form of cellular E2F activity. Genes Dev, 1989 ed. **3**:1062–1074.

168. **Huang MM**, **Hearing P**. 1989. The adenovirus early region 4 open reading frame 6/7 protein regulates the DNA binding activity of the cellular transcription factor, E2F, through a direct complex. Genes Dev **3**:1699–1710.

169. **Obert S**, **O'Connor RJ**, **Schmid S**, **Hearing P**. 1994. The adenovirus E4-6/7 protein transactivates the E2 promoter by inducing dimerization of a heteromeric E2F complex. Molecular and cellular biology **14**:1333–1346.

170. **Raychaudhuri P**, **Bagchi S**, **Neill SD**, **Nevins JR**. 1990. Activation of the E2F transcription factor in adenovirus-infected cells involves E1A-dependent stimulation of DNA-binding activity and induction of cooperative binding mediated by an E4 gene product. Journal of virology **64**:2702–2710.

171. **Matsuse T**, **Hayashi S**, **Kuwano K**, **Keunecke H**, **Jefferies WA**, **Hogg JC**. 1992. Latent adenoviral infection in the pathogenesis of chronic airways obstruction. Am. Rev. Respir. Dis. **146**:177–184.

172. **Alkhalaf MA**, **Guiver M**, **Cooper RJ**. 2013. Prevalence and quantitation of adenovirus DNA from human tonsil and adenoid tissues. J. Med. Virol. **85**:1947–1954.

173. **Zhang Y**, **Huang W**, **Ornelles DA**, **Gooding LR**. 2010. Modeling adenovirus latency in human lymphocyte cell lines. Journal of virology **84**:8799–8810.

174. **Markel D**, **Lam E**, **Harste G**, **Darr S**, **Ramke M**, **Heim A**. 2014. Type dependent patterns of human adenovirus persistence in human T-lymphocyte cell lines. J. Med. Virol. **86**:785–794.

175. **Ehret GB**, **Reichenbach P**, **Schindler U**, **Horvath CM**, **Fritz S**, **Nabholz M**, **Bucher P**. 2001. DNA binding specificity of different STAT proteins. Comparison of in vitro specificity with natural target sites. The Journal of biological chemistry **276**:6675–6688.

176. **Chen H**, **Sun H**, **You F**, **Sun W**, **Zhou X**, **Chen L**, **Yang J**, **Wang Y**, **Tang H**, **Guan Y**, **Xia W**, **Gu J**, **Ishikawa H**, **Gutman D**, **Barber G**, **Qin Z**, **Jiang Z**. 2011. Activation of STAT6 by STING Is Critical for Antiviral Innate Immunity. Cell, 2011 ed. **147**:436–446.

177. **Gupta S**, **Jiang M**, **Pernis AB**. 1999. IFN-alpha activates Stat6 and leads to the formation of Stat2:Stat6 complexes in B cells. J. Immunol. **163**:3834–3841.

178. **Huang Z**, **Xin J**, **Coleman J**, **Huang H**. 2005. IFN-gamma suppresses STAT6 phosphorylation by inhibiting its recruitment to the IL-4 receptor. J. Immunol.

174:1332–1337.

179. **Dickson MA**. 2014. Molecular pathways: CDK4 inhibitors for cancer therapy. Clin. Cancer Res. **20**:3379–3383.

180. **Kiladjian J-J**, **Mesa RA**, **Hoffman R**. 2011. The renaissance of interferon therapy for the treatment of myeloid malignancies. Blood **117**:4706–4715.

181. **Kominsky S**, **Johnson HM**, **Bryan G**, **Tanabe T**, **Hobeika AC**, **Subramaniam PS**, **Torres B**. 1998. IFNgamma inhibition of cell growth in glioblastomas correlates with increased levels of the cyclin dependent kinase inhibitor p21WAF1/CIP1. Oncogene **17**:2973–2979.

182. **Sangfelt O**, **Erickson S**, **Einhorn S**, **Grandér D**. 1997. Induction of Cip/Kip and Ink4 cyclin dependent kinase inhibitors by interferon-alpha in hematopoietic cell lines. Oncogene **14**:415–423.

183. **Sangfelt O**, **Erickson S**, **Castro J**, **Heiden T**, **Gustafsson A**, **Einhorn S**, **Grandér D**. 1999. Molecular mechanisms underlying interferon-alpha-induced G0/G1 arrest: CKI-mediated regulation of G1 Cdk-complexes and activation of pocket proteins. Oncogene **18**:2798–2810.

184. **Hertel L**, **Rolle S**, **De Andrea M**, **Azzimonti B**, **Osello R**, **Gribaudo G**, **Gariglio M**, **Landolfo S**. 2000. The retinoblastoma protein is an essential mediator that links the interferon-inducible 204 gene to cell-cycle regulation. Oncogene **19**:3598–3608.

185. **Kwak JC**, **Ongusaha PP**, **Ouchi T**, **Lee SW**. 2003. IFI16 as a negative regulator in the regulation of p53 and p21(Waf1). The Journal of biological chemistry **278**:40899–40904.

186. **Xin H**, **Curry J**, **Johnstone RW**, **Nickoloff BJ**, **Choubey D**. 2003. Role of IFI 16, a member of the interferon-inducible p200-protein family, in prostate epithelial cellular senescence. Oncogene **22**:4831–4840.

187. **Garnett CT**, **Erdman D**, **Xu W**, **Gooding LR**. 2002. Prevalence and quantitation of species C adenovirus DNA in human mucosal lymphocytes. Journal of virology **76**:10608–10616.

188. **Garnett CT**, **Talekar G**, **Mahr JA**, **Huang W**, **Zhang Y**, **Ornelles DA**, **Gooding LR**. 2009. Latent species C adenoviruses in human tonsil tissues. Journal of virology **83**:2417–2428.

189. **Kirn D**. 2001. Clinical research results with dl1520 (Onyx-015), a replication-selective adenovirus for the treatment of cancer: what have we learned? Gene Ther. **8**:89–98.

190. **Johnson L**, **Shen A**, **Boyle L**, **Kunich J**, **Pandey K**, **Lemmon M**, **Hermiston T**, **Giedlin M**, **McCormick F**, **Fattaey A**. 2002. Selectively replicating adenoviruses targeting deregulated E2F activity are potent, systemic antitumor agents. Cancer Cell **1**:325–337.

191. **Majem M**, **Cascallo M**, **Bayo-Puxan N**, **Mesia R**, **Germa JR**, **Alemany R**. 2006. Control of E1A under an E2F-1 promoter insulated with the myotonic dystrophy locus insulator reduces the toxicity of oncolytic adenovirus Ad-Delta24RGD. Cancer Gene Ther **13**:696–705.

192. **Alonso MM**, **Cascallo M**, **Gomez-Manzano C**, **Jiang H**, **Bekele BN**, **Perez-Gimenez A**, **Lang FF**, **Piao Y**, **Alemany R**, **Fueyo J**. 2007. ICOVIR-5 Shows E2F1 Addiction and Potent Antiglioma Effect In vivo. Cancer Res **67**:8255–8263.

193. **Choubey D**, **Li SJ**, **Datta B**, **Gutterman JU**, **Lengyel P**. 1996. Inhibition of E2F-mediated transcription by p202. The EMBO journal **15**:5668–5678.

194. **Choubey D**, **Gutterman JU**. 1997. Inhibition of E2F-4/DP-1-stimulated transcription by p202. Oncogene **15**:291–301.

195. **Mallette FA**, **Goumard S**, **Gaumont-Leclerc M-F**, **Moiseeva O**, **Ferbeyre G**. 2004. Human fibroblasts require the Rb family of tumor suppressors, but not p53, for PML-induced senescence. Oncogene **23**:91–99.

196. **Vernier M**, **Bourdeau V**, **Gaumont-Leclerc M-F**, **Moiseeva O**, **Bégin V**, **Saad F**, **Mes-Masson A-M**, **Ferbeyre G**. 2011. Regulation of E2Fs and senescence by PML nuclear bodies. Genes Dev **25**:41–50.

197. **Vernier M**, **Ferbeyre G**. 2014. Complete senescence: RB and PML share the task. Cell Cycle **13**:696.

198. **Sadasivam S**, **DeCaprio JA**. 2013. The DREAM complex: master coordinator of cell cycle-dependent gene expression. Nat Rev Cancer **13**:585–595.

199. **Litovchick L**, **Florens LA**, **Swanson SK**, **Washburn MP**, **DeCaprio JA**. 2011. DYRK1A protein kinase promotes quiescence and senescence through DREAM complex assembly. Genes Dev **25**:801–813.

200. **Zhang Z**, **Smith MM**, **Mymryk JS**. 2001. Interaction of the E1A oncoprotein with Yak1p, a novel regulator of yeast pseudohyphal differentiation, and related mammalian kinases. Mol Biol Cell **12**:699–710.

201. **Wang S**, **Nath N**, **Minden A**, **Chellappan S**. 1999. Regulation of Rb and E2F by signal transduction cascades: divergent effects of JNK1 and p38 kinases. The EMBO journal **18**:1559–1570.

202. **Déjardin J**, **Kingston RE**. 2009. Purification of Proteins Associated with Specific Genomic Loci. Cell **136**:175–186.

203. **Pourfarzad F**, **Aghajanirefah A**, **de Boer E**, **Have Ten S**, **Bryn van Dijk T**, **Kheradmandkia S**, **Stadhouders R**, **Thongjuea S**, **Soler E**, **Gillemans N**, **Lindern von M**, **Demmers J**, **Philipsen S**, **Grosveld F**. 2013. Locus-specific proteomics by TChP: targeted chromatin purification. Cell Rep **4**:589–600.

204. **Schoggins JW**, **Wilson SJ**, **Panis M**, **Murphy MY**, **Jones CT**, **Bieniasz P**, **Rice CM**. 2011. A diverse range of gene products are effectors of the type I

interferon antiviral response. Nature **472**:481–485.

205. **Sourvinos G**, **Everett RD**. 2002. Visualization of parental HSV-1 genomes and replication compartments in association with ND10 in live infected cells. The EMBO journal, 2002nd ed. **21**:4989–4997.

206. **Everett RD**, **Murray J**. 2005. ND10 components relocate to sites associated with herpes simplex virus type 1 nucleoprotein complexes during virus infection. Journal of virology, 2005 ed. **79**:5078–5089.

207. **Everett RD**, **Rechter S**, **Papior P**, **Tavalai N**, **Stamminger T**, **Orr A**. 2006. PML contributes to a cellular mechanism of repression of herpes simplex virus type 1 infection that is inactivated by ICP0. Journal of virology, 2006 ed. **80**:7995–8005.

208. **Tavalai N**, **Papior P**, **Rechter S**, **Leis M**, **Stamminger T**. 2006. Evidence for a role of the cellular ND10 protein PML in mediating intrinsic immunity against human cytomegalovirus infections. Journal of virology, 2006 ed. **80**:8006–8018.

209. **Everett RD**, **Murray J**, **Orr A**, **Preston CM**. 2007. Herpes simplex virus type 1 genomes are associated with ND10 nuclear substructures in quiescently infected human fibroblasts. Journal of virology, 2007 ed. **81**:10991–11004.

210. **Schreiner S**, **Wimmer P**, **Sirma H**, **Everett RD**, **Blanchette P**, **Groitl P**, **Dobner T**. 2010. Proteasome-dependent degradation of Daxx by the viral E1B-55K protein in human adenovirus-infected cells. Journal of virology, 2010 ed. **84**:7029–7038.

211. **Negorev DG**, **Vladimirova OV**, **Maul GG**. 2009. Differential functions of interferon-upregulated Sp100 isoforms: herpes simplex virus type 1 promoter-based immediate-early gene suppression and PML protection from ICP0-mediated degradation. Journal of virology **83**:5168–5180.

212. **Lukashchuk V**, **Everett RD**. 2010. Regulation of ICP0-null mutant herpes simplex virus type 1 infection by ND10 components ATRX and hDaxx. Journal of virology **84**:4026–4040.

213. **Cuchet D**, **Sykes A**, **Nicolas A**, **Orr A**, **Murray J**, **Sirma H**, **Heeren J**, **Bartelt A**, **Everett RD**. 2011. PML isoforms I and II participate in PML-dependent restriction of HSV-1 replication. Journal of cell science, 2010 ed. **124**:280–291.

214. **Cuchet-Lourenco D**, **Boutell C**, **Lukashchuk V**, **Grant K**, **Sykes A**, **Murray J**, **Orr A**, **Everett RD**. 2011. SUMO Pathway Dependent Recruitment of Cellular Repressors to Herpes Simplex Virus Type 1 Genomes. PLoS Pathog, 2011 ed. **7**:e1002123.

215. **Hwang J**, **Kalejta RF**. 2011. In vivo analysis of protein sumoylation induced by a viral protein: Detection of HCMV pp71-induced Daxx sumoylation. Methods, 2011 ed. **55**:160–165.

216. **Kim Y-E**, **Lee J-H**, **Kim ET**, **Shin HJ**, **Gu SY**, **Seol HS**, **Ling PD**, **Lee CH**, **Ahn J-H**. 2011. Human cytomegalovirus infection causes degradation of Sp100

proteins that suppress viral gene expression. Journal of virology **85**:11928–11937.

217. **Cuchet-Lourenço D**, **Vanni E**, **Glass M**, **Orr A**, **Everett RD**. 2012. Herpes simplex virus 1 ubiquitin ligase ICP0 interacts with PML isoform I and induces its SUMO-independent degradation. Journal of virology **86**:11209–11222.

218. **Rux JJ**, **Burnett RM**. 2004. Adenovirus structure. Hum Gene Ther **15**:1167–1176.

219. **San Martín C**, **Burnett RM**. 2003. Structural studies on adenoviruses. Curr Top Microbiol Immunol **272**:57–94.

220. **Sourvinos G**, **Tavalai N**, **Berndt A**, **Spandidos DA**, **Stamminger T**. 2007. Recruitment of human cytomegalovirus immediate-early 2 protein onto parental viral genomes in association with ND10 in live-infected cells. Journal of virology, 2007 ed. **81**:10123–10136.

221. **Shaner NC**, **Steinbach PA**, **Tsien RY**. 2005. A guide to choosing fluorescent proteins. Nat Methods, 2005 ed. **2**:905–909.

222. **Schiedner G**, **Hertel S**, **Kochanek S**. 2000. Efficient transformation of primary human amniocytes by E1 functions of Ad5: generation of new cell lines for adenoviral vector production. Hum Gene Ther **11**:2105–2116.

223. **Thimmappaya B**, **Weinberger C**, **Schneider RJ**, **Shenk T**. 1982. Adenovirus VAI RNA is required for efficient translation of viral mRNAs at late times after infection. Cell, 1982nd ed. **31**:543–551.

224. **Gooding LR**, **Ranheim TS**, **Tollefson AE**, **Aquino L**, **Duerksen-Hughes P**, **Horton TM**, **Wold WS**. 1991. The 10,400- and 14,500-dalton proteins encoded by region E3 of adenovirus function together to protect many but not all mouse cell lines against lysis by tumor necrosis factor. Journal of virology **65**:4114–4123.

225. **Yu J**, **Xiao J**, **Ren X**, **Lao K**, **Xie XS**. 2006. Probing gene expression in live cells, one protein molecule at a time. Science, 2006 ed. **311**:1600–1603.

226. **Yang W**, **Gelles J**, **Musser SM**. 2004. Imaging of single-molecule translocation through nuclear pore complexes. Proc Natl Acad Sci U S A **101**:12887–12892.

Appendix

Upon entering the host cell, adenovirus will encounter multiple cellular sensing molecules triggering cellular defensive responses, such as an IFN response and a DNA damage response. However, the dynamic interactions between the Ad genome and these sensing molecules, as well as inhibitory factors, are largely unclear. This prompted us to develop a proper method to label the Ad genome by fluorescent probes to enable the monitoring of virus-host interactions, especially PML nuclear bodies (PML-NB), in live cells in real time.

The interplay between herpesviruses and PML-NBs has been well characterized (103-105, 124, 160, 205-217). For instance, HSV-1 immediate early protein ICP4 is a viral transcriptional activator, and it strongly associates with viral genomes and is frequently used as the marker for the site of viral DNA. Thus, fluorescent protein tagged ICP4 has been widely used for the study of the interaction between HSV-1 genome and PML NBs (205). For Ad, the immediate early protein E1A is also a transcriptional regulator and it is indispensable for activation of Ad gene expression. However, E1A does not directly bind with Ad genome; it regulates viral protein expression by modulating activities of cellular transcriptional factors (99). Moreover, E1A exhibits a diffuse nuclear localization pattern. Thus, it cannot be used for detection of the Ad genome. Furthermore, early proteins cannot be used to monitor the events before early gene expression occurs. It is ideal to label the viral proteins that are associated with the Ad genome within the virus particle and deliver such proteins into the nucleus along with the Ad genome. As discussed in chapter 1, Ad protein VII is one of the major core proteins. It is known there are approximated 800-1,000 copies of VII associated with the viral genome within the virion (218, 219). Protein VII stays bound to the parent Ad

genome until the transcription of E1A gene occurs (151). Thus, Ad core protein VII is ideally suited as a marker of the Ad genome during the early stages of infection. In order to study the immediate early events of Ad infection, we aimed to develop a strategy to visualize in live cells both the virus genome and PML-NBs simultaneously.

A.1 Visualizing PML NBs in HDF-TERT Cells

It is well established that fluorescent protein-tagged Sp100 protein can be utilized for visualization of PML-NBs in live cells (220). Lentiviral vector pLenti/V5-mCherrySp100 was kindly provided by Dr. Roger Stamminger. This plasmid expresses Sp100A (Sp100 isoform A) fused with red fluorescent protein, mCherry, at its N-terminus. It was also used as the backbone for the construction of an eGFP-tagged Sp100 vector. The eGFP coding sequence was generated by PCR amplification using primers eGFP-Sp100-SpeI and eGFP-Sp100-2-2 together with plasmid pEGFP-C1 (Clontech) as the template. In parallel, the Sp100 coding sequence was amplified with primers eGFP-Sp100-3 and eGFP-Sp100-MluI together with pLenti/V5-mCherrySp100 as the template. mCherry and eGFP share the identical 5' and 3' sequence, and eGFP-Sp100-2-2 and eGFP-Sp100-3 are complementary with each other. EGFP-Sp100 fusion gene was generated by overlapping PCR and inserted into the pLenti/V5-mCherrySp100 via SpeI and MluI (Figure A-1A and A-1B). Lentivirus stocks were generated by cotransfection of 293FT cells with packaging vectors, pLP1, pLP2, and pLP-VSVG, in combination with the respective Sp100-expression vectors. Low passage HDF-TERT cells were transduced with undiluted lentivirus stock overnight. Stably-transduced pools of cell populations were selected using 1 µg/ml blasticidin. HDF-TERT cells were also transduced with a low concentration of lentiviruses and multiple blasticidin-resistant single cell colonies were expanded. The expression levels of mCherry/eGFP-tagged Sp100 were examined by western blot (Figure A-1C and A-1D) using antibodies against

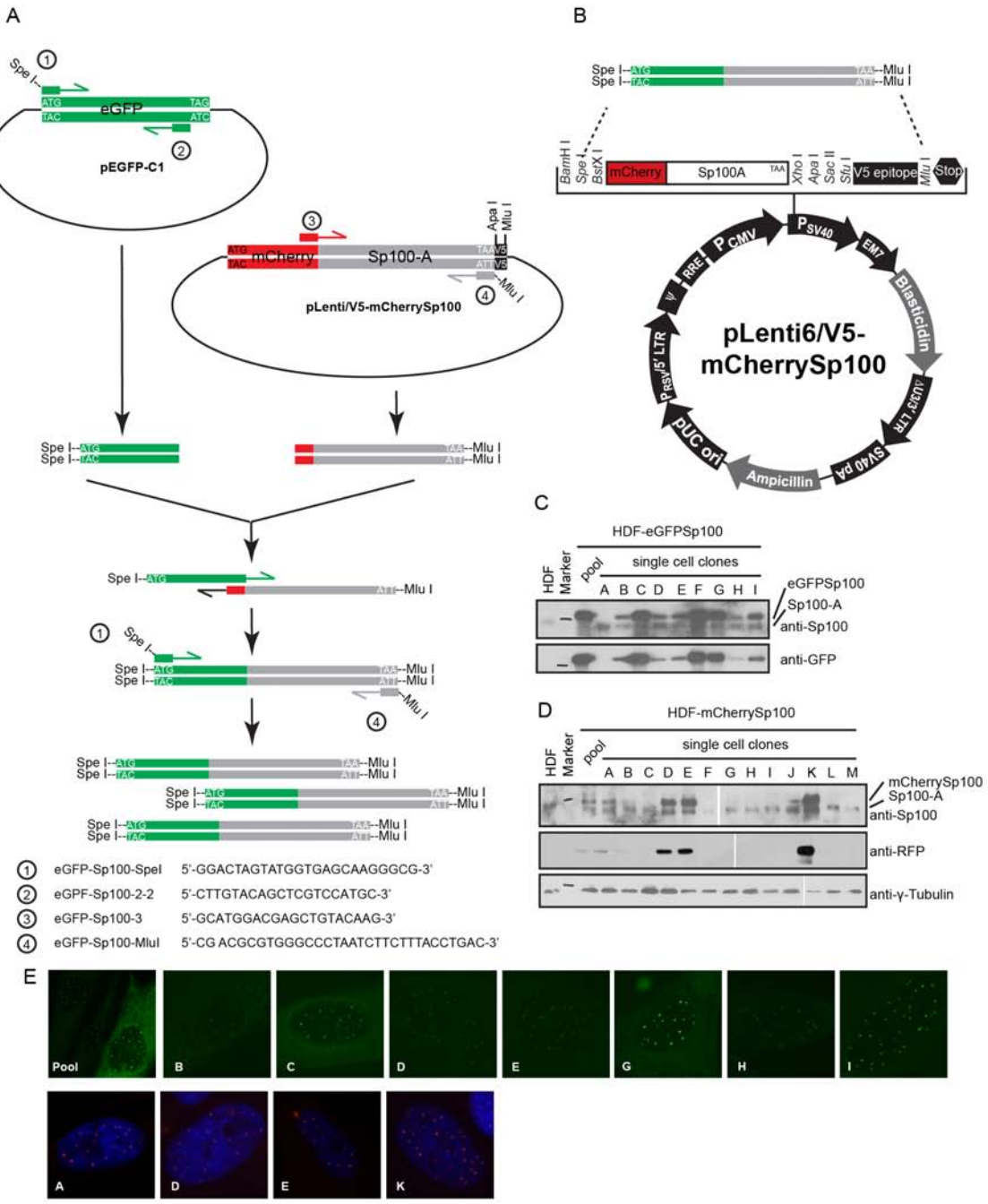

Figure A-1. Generation of HDF-TERT cells stably-expressing mCherry-Sp100 or eGFP-Sp100 fusion protein.
(A) Overlapping PCR to generate the coding sequence of eGFP-Sp100 fusion protein.
(B) Maps of pLenti/V5-mCherry-Sp100 and -eGFP-Sp100.
(C and D) Screening of mCherrySp100/eGFPSp100-expressing HDF-TERT cells by western blot.
(E) Autofluorescent images of mCherry-Sp100/eGFP-Sp100-expressing HDF-TERT cells. Top panel is HDF-eGFP-Sp100 cells. Bottom panel is HDF-mCherry-Sp100 cells

Sp100, GFP, and RFP. mCherry-Sp100 and eGFP-Sp100 fusion proteins formed distinct foci in the nucleus, presumably localized to PML-NBs (Figure A-1E). The fluorescent intensity of mCherry-Sp100 and eGFP-Sp100 foci were correlated with their expression levels as determined by western blot.

A.2 Tagging Ad pVII protein with a Fluorescent Protein

Dr. Kasey Karen attempted to generate a pVII-EYFP virus whose pVII gene was replaced by a C-terminal tagged pVII-EYFP fusion gene in its natural position in the L2 region (unpublished result). However, this recombinant virus was unable to grow in cell culture for an unknown reason. She also noticed that EYFP fluorescence became less intense after 2 hour (unpublished data). This is probably because EYFP is very sensitive to acidic pH, losing ~50% of its fluorescence at pH 6.5 (221). Ad enters the cell through receptor-mediated endocytosis and EYFP could be quenched in the acidified endosome. The other possibility is EYFP has an intermediate photostability and it might loss fluorescent caused by photobleaching (221). Taking together, EYFP protein is not suitable for detection of pVII using live cell imaging. I decided to use fluorescent protein mCherry to tag protein pVII for the following reasons: 1) It is a monomer, while EYFP is a weak dimer. mCherry is more likely to be encapsidated due to its smaller size; 2) It is one of the most photostable fluorescent proteins, ideal for detection for an extended period of time; and, 3) It has a pKa lower than 4.5, suggesting it is very resistant to acidic pH conditions.

The Ad virion has a very compact structure. Addition of a mCherry tag (27 kDa) to pVII (~20 kDa) might be too large to fit into virion. Therefore, I planned to construct a virus that lacks the E1A gene and instead expresses pVII-mCherry under the control of either the CMV promoter or the Ad major late promoter (MLP). The wild-type pVII gene is kept at its natural location. Thus, pVII-mCherry and WT pVII would compete for the

encapsidation into the virion. The fluorescence intensity within the virion, therefore, was expected to be lower due to the presence of WT pVII protein. However, visualization should still be feasible since each Ad genome is associated with more than 800 copies of the pVII protein. Early region 3 (E3) was further deleted to theoretically gain more space within the virion to improve the packaging efficiency of pVII-mCherry.

The pAd-CMV plasmid is a transfer vector that contains the left-end of the Ad5 genome. The E1A coding region (Ad nt 454-3329) is replaced by a CMV promoter (Figure A-3A). With the vector pNL3C(HI), the E1A coding sequence (Ad nt 350-1575) is replaced by MLP-TPL (Figure A-3A). Overlapping PCR was employed (Fig. A-2) to generate a C-terminal tagged pVII-mCherry fusion protein. The 594 bp of the coding sequences of the pVII gene (without the stop codon TAG) was amplified with a forward primer that added a BamHI site at the 5' end and a reverse primer that added several bp of the 5' sequence that is complementary to the mCherry gene to the 3'end. The mCherry gene was then amplified with a few base pairs of pVII sequence at its 5' end and the BglII site at the 3' end following the stop codon. The second step involved combining the pVII and mCherry fragments at 1:1 molar ratio in a PCR reaction without primers. The 3' end of the pVII fragment was complementary with the 5' end of the mCherry fragment, and was then elongated. At the last step, the pVII-mCherry fusion fragment was further amplified by PCR using the forward primer of the pVII gene and the reverse primer of the mCherry gene. The pVII-mCherry fusion fragment was inserted into pAd-CMV via a BamHI site by the ligation of compatible cohesive ends, and it was inserted into the pNL3C(HI) vector via BamHI and BglII sites.

The resulting plasmids, pAd-CMV-pVII-mCherry and pNL3C(HI)-pVII-mCherry, were linearized with EcoRI and cotransfected into N52Cre cells, an E1A complementing cell line gifted by Dr. G. Schiedner and Dr. S. Kochanek, University of Ulm, Germany (222), along with the right end fragment of *dl*327, carrying a 1.9 kb deletion in the E3 region

(223). Recombinant viruses AdΔE1/E3-CMV-pVII-mCherry and AdΔE1/E3-MLP/TPL-pVII-mCherry (referred as CMV-7mC and MLP-7mC) successfully grew and were used to infect A549 cells to examine fluorescence properties. However, there was no red fluorescence signal detected at 2 hr post-infection (data not shown). Detection of the pVII protein by immunofluorescence assay using an antibody against pVII suggested that the CMV-7mC and MLP-7mC viruses have normal infectivities compared with WT Ad5. The levels of VII and VII-mCherry proteins in purified virions and in whole cell extracts from infected N52Cre cells were evaluated by western blot. VII-mCherry protein was present in infected N52Cre cells. However, there was no or greatly diminished levels of the fusion protein detected in MLP-7mC and CMV-7mC virions, respectively (Figure A-3B). This result suggests that the VII-mCherry protein was not properly packaged into virions, perhaps due to a size constraint, or the C-terminal mCherry protein prevents pVII-DNA interaction. If the problem is due to a packaging constraint, then additional deletion of the Ad genome may create more space for encapsidation. We attempted to generate a backbone virus that carries the deletion of both E3 and E4 regions. For this virus, an E4 deletion was planned to be introduced into the transfer vectors pTG-ΔB-*dl*327 and pTG-ΔB-*dl*7001 by homologous recombination using *dl*366 (2.3 kb deletion in E4 region). pTG-ΔB-*dl*327 contains the *dl*327 deletion (1.9 kb deletion in E3 region) and pTG-ΔB-*dl*7001 contains the *dl*7001 deletion (3 kb deletion in E3 region; (224)). Unfortunately, the sequences of *dl*327 and *dl*7001 were different from WT Ad5 and I was unable to find a restriction site that was suitable for this strategy. Considering the packaging issue of the large pVII-mCherry fusion protein, we decided to label VII protein with smaller tag.

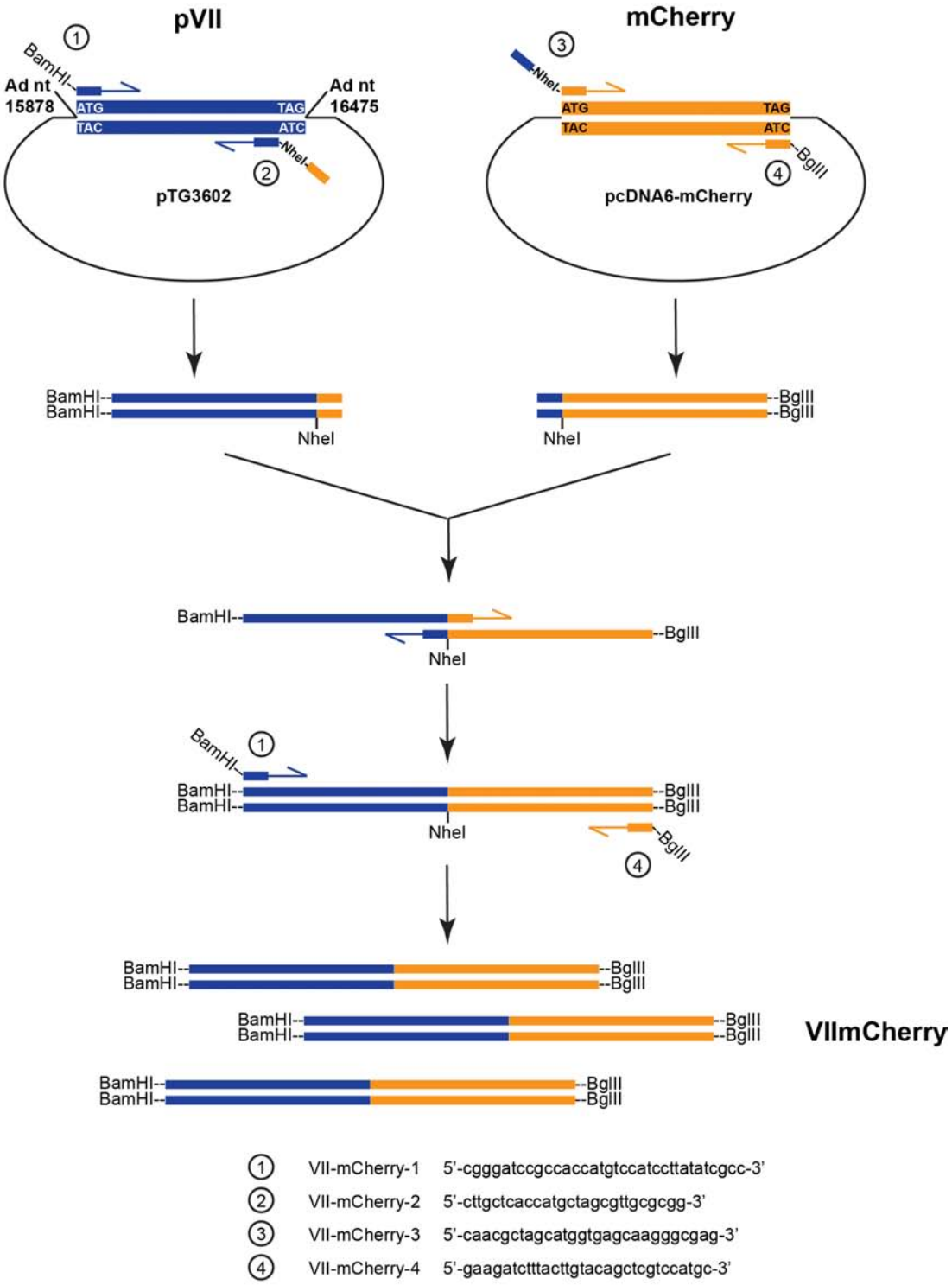

Figure A-2. Overlapping PCR to generate pVII-mCherry fusion protein.

A.3 Tagging pVII Protein with Tetracysteine Motif

Biarsenical labeling reagents FIAsH (green) and ReAsH (red) are non-fluorescent when they are free, but they become fluorescent when binding to the tetracysteine (TC) motif, Cys-Cys-Pro-Gly-Cys-Cys. Since a TC tag is only six-amino acids in length, it may have reduced interference with the function of the pVII protein and allow packaging of a TC-tagged pVII protein.

The transfer plasmid of pBS-pVII-NheI was used to introducing TC tag at the C-terminus of pVII. It contains the Ad sequence between 10809 and 19703, and the stop codon of the pVII gene was replaced by an NheI site through site-directed mutagenesis (Dr. Kasey Karen, unpublished results). The oligonucleotides encoding the optimal TC tag N-FLNCCPGCCMEP-C, were synthesized, annealed, and inserted into the 3' end of the pVII gene via the NheI site. The resulting plasmid, pBS-pVII-TC was linearized by double digestion of BspE1 and NdeI, and then recombined with pTG3602 digested with FseI and PmeI (Figure A-4A). The recombinant virus, named as Ad5 pVII-TC, has the identical sequence of WT Ad5, except with a peptide of 12 amino acids inserted at the C-terminus of pVII in its natural genomic location (Figure A-4D). Ad5-pVII-TC virus growth rate was comparable to *dl*309 (WT Ad5). To ensure the fusion protein was packaged, a western blot was performed using 10^9 virus particles of Ad5 pVII-TC, *dl*309 virions were used for comparison. Based on the molecular weight of pVII-TC, the C-terminal tagged pVII-TC was packaged and its N-terminus was properly processed (cleaved) by the Ad protease (Figure A-4E).

Before we attempted to label Ad5-pVII-TC virus with ReAsH, pilot experiments were performed to evaluate the accessibility of the pVII C-terminal TC tag. A549 cells were infected with Ad5-pVII-TC at 100 virus particles/cell. At 24 hr post-infection, ReAsH signal was detected following 15 min of incubation, and the fluorescent intensity was increased as incubation time increased (Figure A-5A). The infected cells were also

exposed to various low pH buffers for 30 min. There was no noticeable loss of red fluorescence, suggesting that the biarsenical labeling reagent is resistant to an acid environment (Fig. A-5B). We first attempted to label pVII-TC protein with ReAsH *in vitro*. Purified Ad5-pVII-TC virions were passed through a filter column to remove CsCl, followed by the incubation with ReAsH at room temperature for 1 hr. Then excess ReAsH was removed by passing the sample through filter columns twice. A549 cells were infected with this virus, but there were no red foci (i.e., labeled VII-TC) detected at 2 hr post-infection. Next, we tried to incorporate ReAsH into virions as the ligand of pVII-TC during the late phase of infection *in vivo*. pVII protein expression can be detected as early as 12 hr post-infection (Figure A-5C). Ad5-pVII-TC-infected cells were incubated with ReAsH for 1 hr at 12 hr post-infection, followed by another two rounds of ReAsH incubation at 18 and 22 hr post-infection. Unfortunately, when A549 cells were infected with this virus, diffuse red signals were observed (Figure A-5D). Lastly, we tried to simultaneously label pVII-TC protein with ReAsH during the early phase of infection. For this purpose, A549 cells were infected with Ad5-pVII-TC for 1 hr, and then ReAsH was added to the culture and incubated with cells for another 1 hr prior to fixation. The result was still disappointing since no labeled VII-TC was evident. We conclude that the C-terminal TC tag is masked when VII protein is associated with the viral genome.

We moved on to test an N-terminal tagged VII protein. The plasmid pET28-12293/22341 contains the Ad5 sequences between nt 12293 and 22341. A TC tag was engineered to be positioned immediately downstream of the proteolytic cleavage site in pVII (Figure A-4D). The resulting plasmid pET28-ITC-pVII (internal TC tag, ITC) was linearized with BspHI, and then recombined with pTG3602. The virus, Ad5 ITC-pVII, was successfully propagated. Western blot confirmed that the internal TC tag did not interfere with proteolytic cleavage of pVII (Figure A-4D). The same labeling strategies as

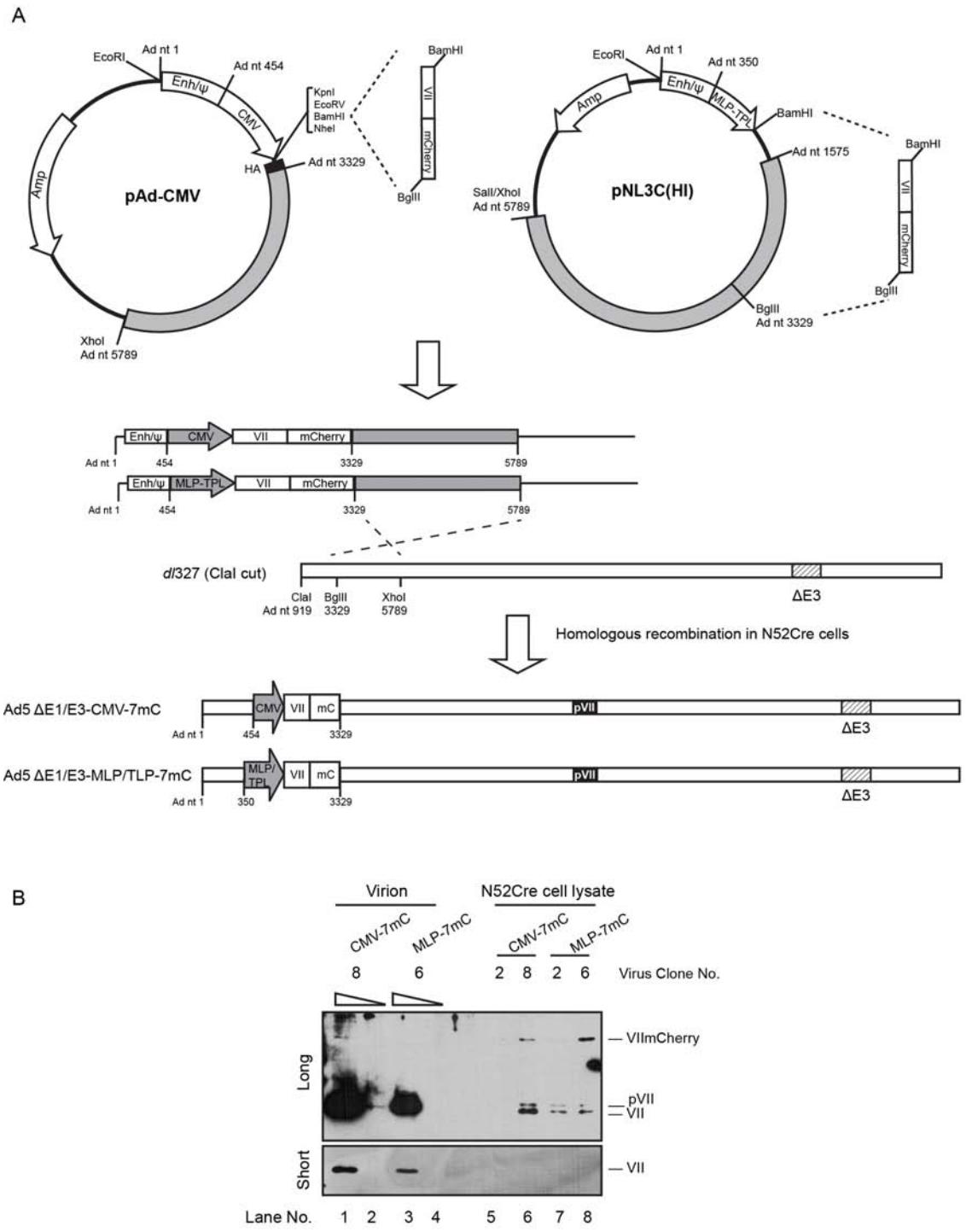

Figure A-3. mCherry-tagged recombinant virus.
(A) Construction of Ad5 ΔE1/E3-CMV-pVIImCherry and ΔE1/E3-MLP/TPL-pVIImCherry.
(B) Western blot to detect pVII/VII protein in the virion of CMV-7mc (lane 1, 2) and MLP-7mC (lane 3, 4), or cell extract from CMV-7mC (lane 5, 6) and MLP-7mC (lane 7, 8) infected N52Cre cells

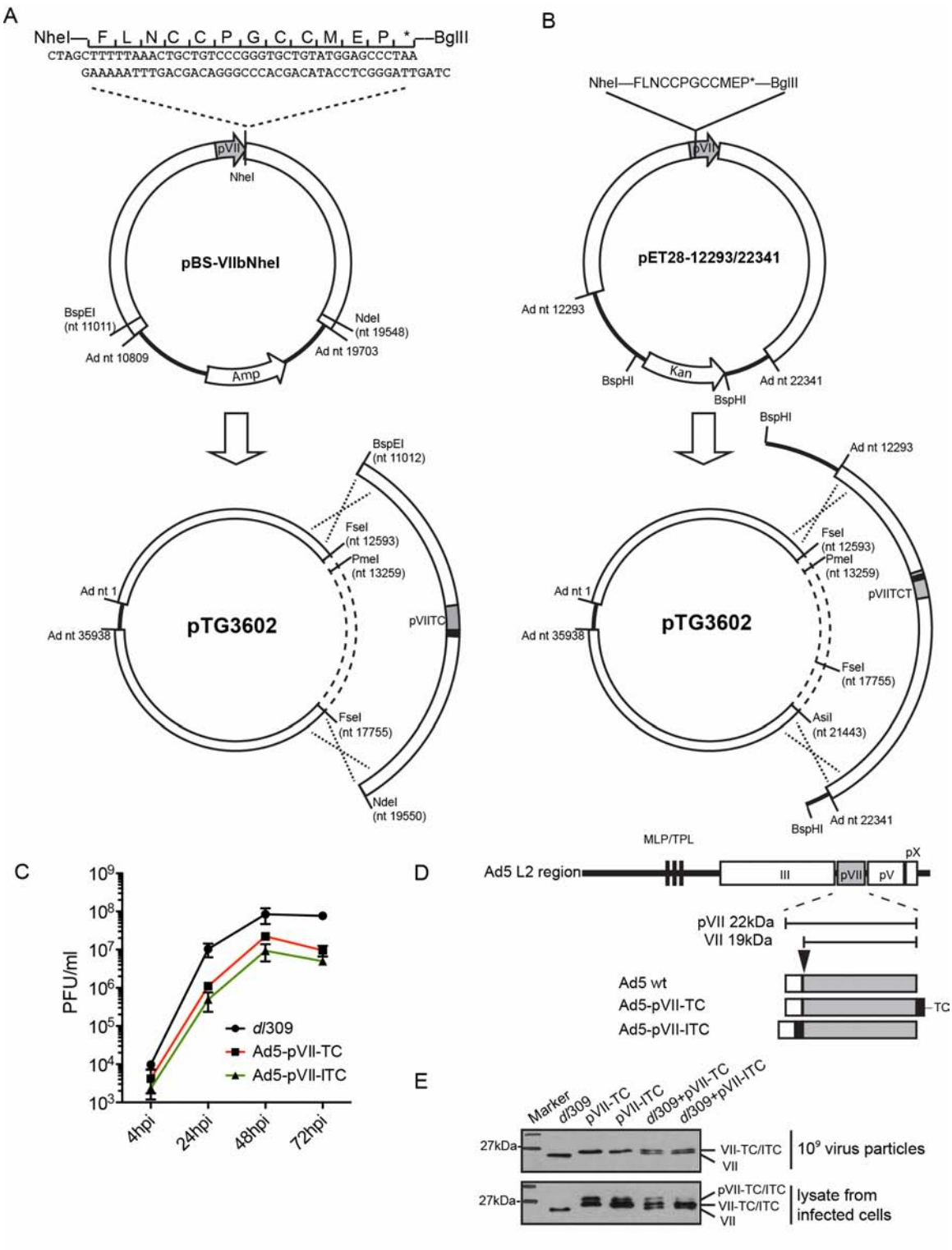

Figure A-4. Recombinant viruses of Ad5-pVII-TC and Ad5-pVII-ITC.
(A and B) Construction stratagies of Ad5-pVII-TC (A) and Ad5-pVII-ITC (B).
(C) Growth curves of Ad5-pVII-TC and Ad5-pVII-ITC.
(D) Organization of Ad L2 region of Ad wt, Ad5-pVII-TC and Ad5-pVII-ITC.
(E) Detection of VII-TC and VII-ITC fusion protein in virus lysate and purified virions.

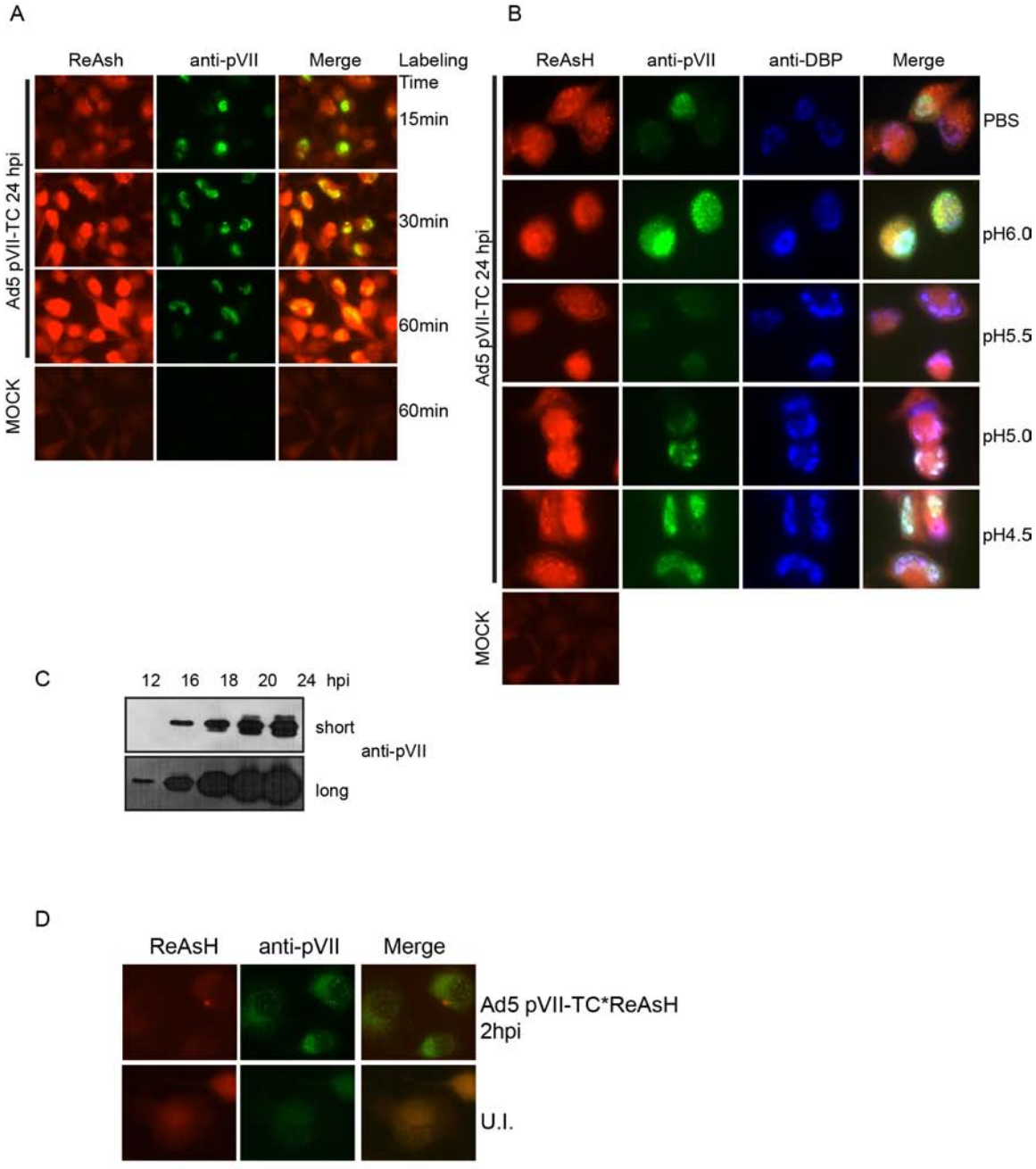

Figure A-5. Detection of VII-TC protein with biarsenic dye ofReAsH.
(A) Detection of pVII-TC by ReAsH during late stage of Ad infection.
(B) Acid resistant property of ReAsH.
(C) Expression of pVII/VII of Ad5-pVII-TC virus inN52Cre cells.
(D) Detection of Ad5-pVII-TC labeled with ReAsH in vitro.

described above were explored to detect ITC-VII fluorescence, but still no positive foci were observed during the early stage of Ad infection *in vivo*.

A.4 Tagging Ad Preterminal Protein with a Fluorescent Protein

Besides protein VII, terminal protein (TP) is also associated with the Ad genome. Preterminal protein (pTP) is an early viral gene expressed prior to viral replication. Newly synthesized pTP proteins bind to inverted terminal repeats (ITRs) at both ends of Ad genome, and serve as protein primers for viral DNA replication. pTP is covalently linked to the 5' end of the Ad genome. At the end of the Ad life cycle, pTP, along with the Ad genome, is packaged into progeny virions. pTP is cleaved by the Ad protease multiple times at N-terminal half, yielding intermediate TP (iTP) and mature TP (TP). The covalent linkage between TP protein and the Ad genome make it ideal for the monitoring the parent viral genome throughout the entire Ad infection.

Since there are only two copies of TP per Ad genome, detection of fluorescent protein at the single molecule level is challenging. tdTomato protein is the tandem dimer of Tomato proteins. It is the brightest fluorescent protein and equally photostable to mCherry, which make it the best option for tagging TP protein in live cells.

First, we wanted to test whether tdTomato-tagged pTP is functional for Ad replication. A pcDNA-pTP-tdTomato plasmid was constructed by sequential, in-frame insertion of the coding sequences of pTP and tdTomato via HindIII/EcoRI and EcoRI/XbaI respectively (Figure A-4A). A549 cells were transfected with pTP, pTP-tdTomato, or empty vector. Twenty-four hr later, cells were infected with 100 virus particles/cell of Ad-ΔTP-GFP, a pTP null mutant virus. Virus replication was determined by an immunofluorescence assay at 24 hr post-infection. As shown in Figure A-6B, there was no DBP expression and formation of viral replication centers in empty vector transfected cells. When cells expressed pTP or pTP-tdTomato proteins, Ad-ΔTP-GFP

virus replication was rescued. This suggested that C-terminal tagged pTP is functional to prime Ad replication. Next, I generated 293- and N52Cre-derived pTP-tdTomato-expressing cell lines. Individual antibiotic-resistant cell colonies were expanded and screening for pTP-tdTomato expression (Figure A-6D). 293-pTP-tdTomato-5 and N52Cre-pTP-tdTomato-21 were used in the following experiments, because Ad formed normal size plaques with both cell lines. In 293-pTP-tdTomato-5 cells, Ad-ΔTP-GFP had a particle:plaque forming unit (P/PFU) ratio of 22:1, which is very similar to that of WT Ad5 *dl*309 (~17:1)(Figure A-5E). Ad-ΔTP-GFP virus produced in pTP-tdTomato cells was named as Ad-ΔTP/TP-tdTomato.

To ensure tdTomato-tagged TP exists inside of progeny virions, western blot was performed using purified virions. This requires the removal of CsCl, digestion of viral genome with nuclease and a minimum of 2 X 10^{10} virus particles. To fulfill this, 15 plates of 293-pTP-tdTomato cells were infected with Ad-ΔTP-GFP virus at 100 virus particles/cell. Progeny viruses were purified by two rounds of CsCl equilibrium centrifugation. Virions were dialyzed against three changes of 1 liter of TE buffer (10 mM TRIS, pH 8.0, 1 mM EDTA) for 1 hr at room temperature using a "dialysis button". After dialysis, virions were recovered and the concentration was determined by measuring optical density at 260 nm. Next, virions were disrupted by incubation at 60°C for 1 hr. To release TP from the Ad genome, benzonase was added to 1,250 U/ml followed by incubation at 37 °C for 30 min. Proteins from ~2 X 10^{10}-10^{11} virus particles were resolved on SDS-PAGE and blotted with an antibody against for RFP to detect tdTomato. As shown in Figure A-6F, two unique bands were observed in Ad-ΔTP/TP-tdTomato virus, but not WT Ad5. They are predicted as iTP-tdTomato and TP-tdTomato according to their molecular weights. All of this evidence indicated that pTP-tdTomato can support Ad replication and be packaged into the virion. Unfortunately, the tdTomato fluorescent signal from Ad-ΔTP/TP-tdTomato virus was very weak and the number of red foci

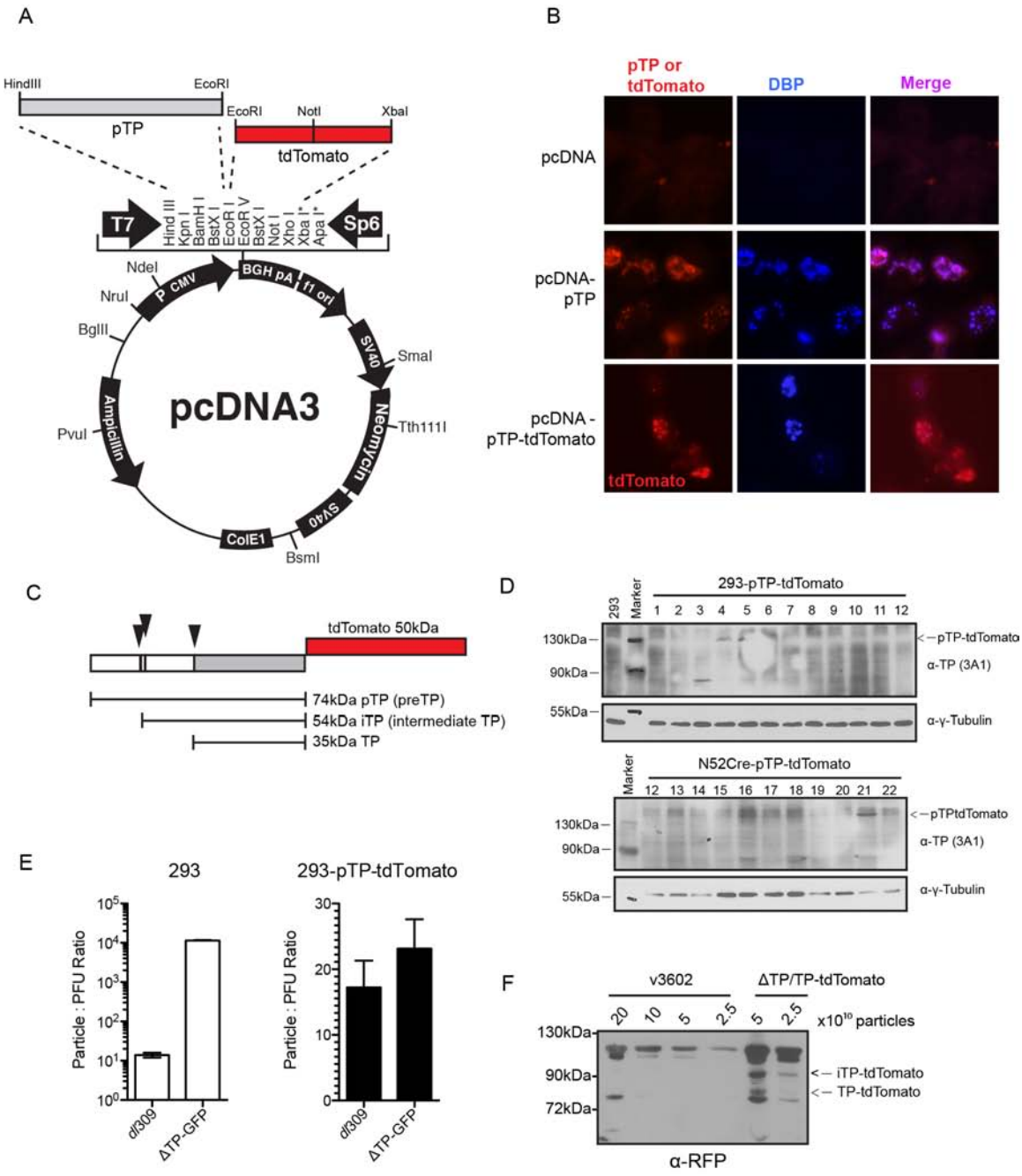

Figure A-6. Generation of pTP-tdTomato-tagged virus.
(A) Contruction of pTP-tdTomato expression vector
(B) Transient expression of pTP or pTP-tdTomato protein rescured the replication of ΔTP-GFP virus.
(C) Schematic view of proteolytic cleavage sites of pTP.
(D) Screening of 293- and N52Cre-derived pTP-tdTomato expression cell lines by western blot.
(E) Determination of particle:PFU ratios of dl309 and ΔTP-GFP in 293 and 293-pTPtdTomato cell lines.
(F) Detection of TPtdTomato protein in the recombinant virus ΔTP-GFP propergated in pTP-tdTomato complementing cell lines.

observed was significantly lower than expected. We could not conclude if the red foci observed by fluorescence microscopy were from tdTomato or background noise.

Although detection of two molecules of tdTomato is inconclusive in our hands, detection of a single copy of YFP-tagged protein in live cells has been concurred (225, 226). It required more sophisticated microscopy that could be customized for both the CCD camera and optical path in order to improve the signal to noise ratio, as well as sophisticated data processing after imaging capture. All of these techniques are beyond our technical capability. We could seek a collaboration to continue this project in the future. If the detection of tdTomato in live cells succeeded, we could continue to generate a recombinant Ad carrying a C-terminal tdTomato-tagged pTP gene.

A.5 Direct Visualization of the Ad Genome

EdU (5-ethynyl-2'-deoxyuridine), a thymidine analogue, can be incorporated into DNA during DNA synthesis and detected by Click-iT reaction. Dr. Kasey Karen successfully detected *dl*355/*in*ORF3 viral DNA during the early phase of infection utilizing Click-iT EdU technology (28). I attempted to label and detect WT Ad5 *dl*309 through the same strategy. But the vendor changed the format of the Click-iT Edu Alexa Fluor 488 Imaging Kit. The new kit resulted in a very high background. This project was abandoned due to inability to reduce nonspecific background.

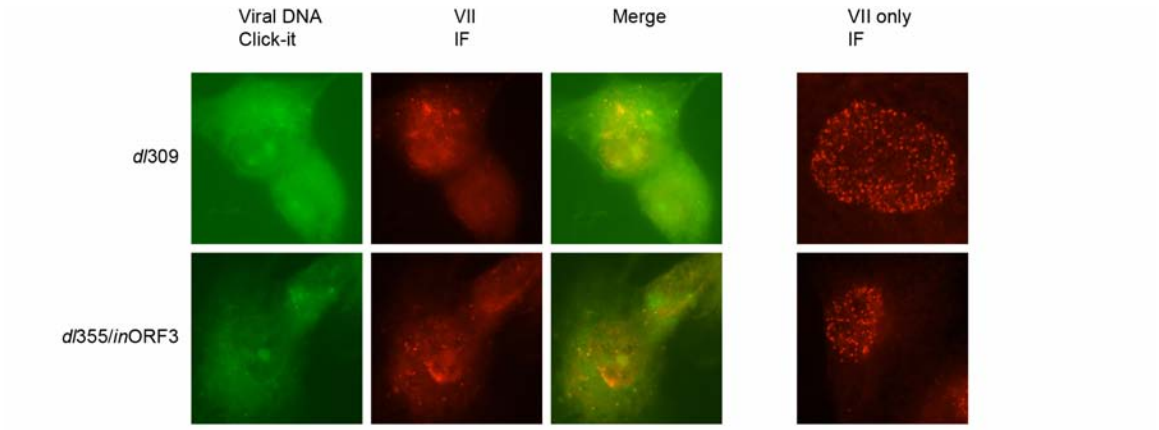

Figure A-7. Detection of Edu labeled adenovirus by Click-it reaction.
A549 cells were seeded on cover slips, and infected with Edu-labeled *dl*309 or *dl*355/*in*ORF3 at 500 virus particles/cell. At 5 hpi, cells were fixed and subjected to Click-it dection, followed by the detection of VII protein by immunofluorescence assay. To ensure the infectivity, control samples directly proceded to immunofluorescence assay for VII (right panel).